IAEA RADIATION TECHNOLOGY REPORTS No. 1

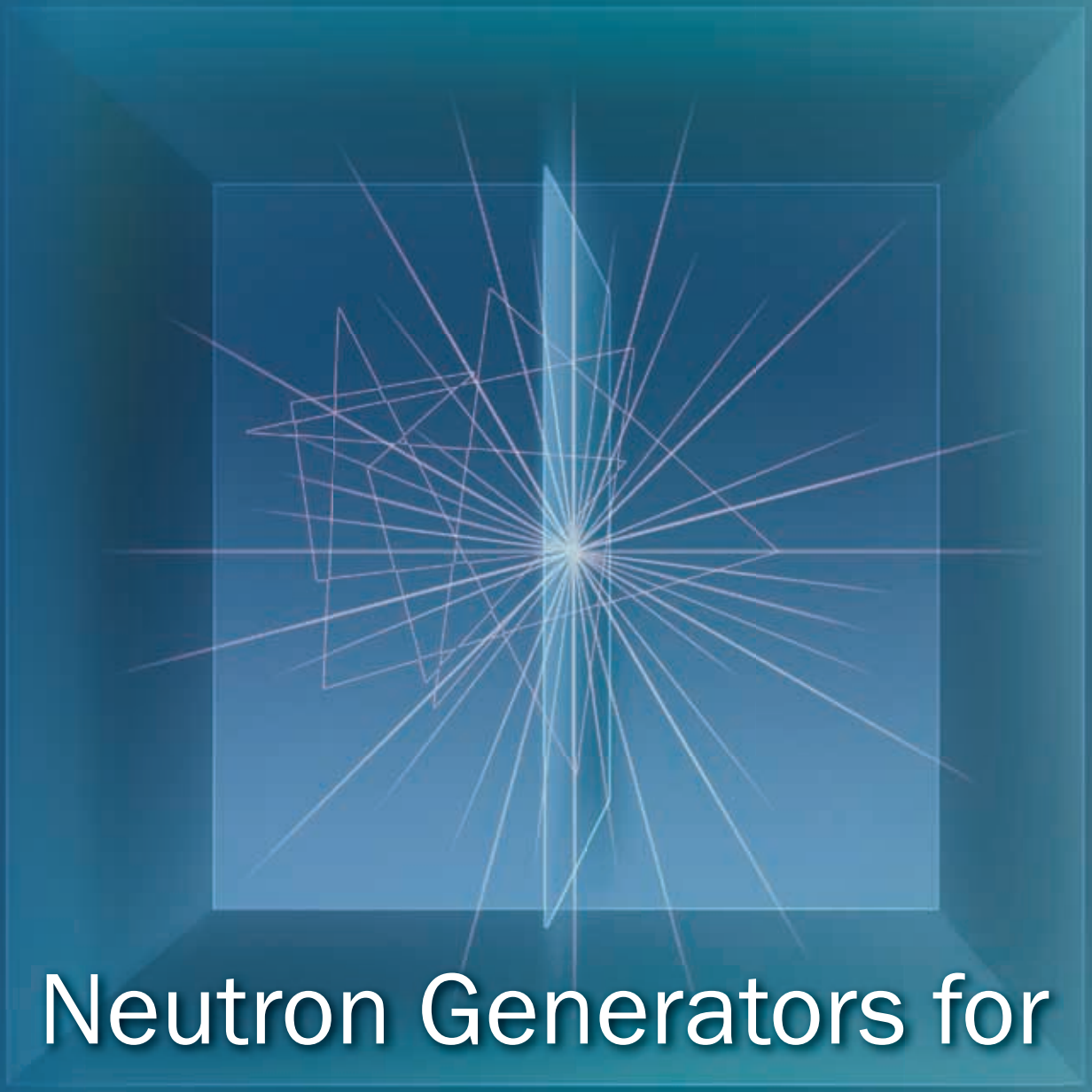

Neutron Generators for Analytical Purposes

IAEA
International Atomic Energy Agency

NEUTRON GENERATORS FOR ANALYTICAL PURPOSES

The following States are Members of the International Atomic Energy Agency:

AFGHANISTAN
ALBANIA
ALGERIA
ANGOLA
ARGENTINA
ARMENIA
AUSTRALIA
AUSTRIA
AZERBAIJAN
BAHRAIN
BANGLADESH
BELARUS
BELGIUM
BELIZE
BENIN
BOLIVIA
BOSNIA AND HERZEGOVINA
BOTSWANA
BRAZIL
BULGARIA
BURKINA FASO
BURUNDI
CAMBODIA
CAMEROON
CANADA
CENTRAL AFRICAN REPUBLIC
CHAD
CHILE
CHINA
COLOMBIA
CONGO
COSTA RICA
CÔTE D'IVOIRE
CROATIA
CUBA
CYPRUS
CZECH REPUBLIC
DEMOCRATIC REPUBLIC OF THE CONGO
DENMARK
DOMINICA
DOMINICAN REPUBLIC
ECUADOR
EGYPT
EL SALVADOR
ERITREA
ESTONIA
ETHIOPIA
FINLAND
FRANCE
GABON
GEORGIA
GERMANY
GHANA
GREECE
GUATEMALA
HAITI
HOLY SEE
HONDURAS
HUNGARY
ICELAND
INDIA
INDONESIA
IRAN, ISLAMIC REPUBLIC OF
IRAQ
IRELAND
ISRAEL
ITALY
JAMAICA
JAPAN
JORDAN
KAZAKHSTAN
KENYA
KOREA, REPUBLIC OF
KUWAIT
KYRGYZSTAN
LAO PEOPLE'S DEMOCRATIC REPUBLIC
LATVIA
LEBANON
LESOTHO
LIBERIA
LIBYA
LIECHTENSTEIN
LITHUANIA
LUXEMBOURG
MADAGASCAR
MALAWI
MALAYSIA
MALI
MALTA
MARSHALL ISLANDS
MAURITANIA
MAURITIUS
MEXICO
MONACO
MONGOLIA
MONTENEGRO
MOROCCO
MOZAMBIQUE
MYANMAR
NAMIBIA
NEPAL
NETHERLANDS
NEW ZEALAND
NICARAGUA
NIGER
NIGERIA
NORWAY
OMAN
PAKISTAN
PALAU
PANAMA
PARAGUAY
PERU
PHILIPPINES
POLAND
PORTUGAL
QATAR
REPUBLIC OF MOLDOVA
ROMANIA
RUSSIAN FEDERATION
SAUDI ARABIA
SENEGAL
SERBIA
SEYCHELLES
SIERRA LEONE
SINGAPORE
SLOVAKIA
SLOVENIA
SOUTH AFRICA
SPAIN
SRI LANKA
SUDAN
SWEDEN
SWITZERLAND
SYRIAN ARAB REPUBLIC
TAJIKISTAN
THAILAND
THE FORMER YUGOSLAV REPUBLIC OF MACEDONIA
TUNISIA
TURKEY
UGANDA
UKRAINE
UNITED ARAB EMIRATES
UNITED KINGDOM OF GREAT BRITAIN AND NORTHERN IRELAND
UNITED REPUBLIC OF TANZANIA
UNITED STATES OF AMERICA
URUGUAY
UZBEKISTAN
VENEZUELA
VIETNAM
YEMEN
ZAMBIA
ZIMBABWE

The Agency's Statute was approved on 23 October 1956 by the Conference on the Statute of the IAEA held at United Nations Headquarters, New York; it entered into force on 29 July 1957. The Headquarters of the Agency are situated in Vienna. Its principal objective is "to accelerate and enlarge the contribution of atomic energy to peace,

IAEA Radiation Technology Reports Series No. 1

NEUTRON GENERATORS FOR ANALYTICAL PURPOSES

INTERNATIONAL ATOMIC ENERGY AGENCY
VIENNA, 2012

For further information on this publication, please contact:

Physics Section
International Atomic Energy Agency
Vienna International Centre
PO Box 100
1400 Vienna, Austria
email: Official.Mail@iaea.org

IAEA Library Cataloguing in Publication Data

Neutron generators for analytical purposes. – Vienna :
International Atomic Energy Agency, 2012.
p. ; 30 cm. – (IAEA radiation technology reports series, ISSN 2225-8833 ; no. 1)
STI/PUB/1535
ISBN 978-92-0-125110-7
Includes bibliographical references.

1. Neutron sources. 2. Nuclear activation analysis.
3. Radiography. I. International Atomic Energy Agency
II. Series.

IAEAL 12-00724

FOREWORD

The IAEA's project on strengthening capabilities for detection of explosives and illicit materials and for compositional analysis helps Member States to find appropriate applications of specific nuclear techniques. Neutron based techniques are excellent tools for characterization of a very broad range of materials. The same technique with different analytical power can be applied for detection of elements in extremely low quantities in illicit materials hidden in large volume, or be utilized as qualitative and quantitative multi-element analysis of major, minor and trace elements in samples from almost every conceivable field of scientific or technical interest.

Prompt gamma neutron activation analysis (PGNAA) has been used for prospecting of minerals, for process control in the cement industry and in coal fired power plants, for the detection of explosives at airports and for demining of land, for in vivo measurement of various elements in animal and human bodies, for the determination of hydrogen in metals, and various elements in biological and environmental materials. The equipment needed for PGNAA is virtually identical to conventional neutron activation analysis (NAA). Thus, all research facilities where INAA is carried out could potentially install PGNAA if a beam line from a research reactor or any other neutron source is made available for the irradiation of samples. New generations of neutron generators (NGs) are available and offer increased possibilities for any NAA applications especially towards in situ measurement.

The capability of assaying elemental compositions of complex objects non-destructively using fast neutron probes has been demonstrated in a number of scenarios over the past decade. In a broader sense of the term 'radiography', one can state that such devices are capable of producing elemental images of medium to large sized objects (even in three dimensions) with adequate spatial resolution for other specific applications such as screening air cargo or unattended luggage, as well as quality control in the textile industry.

Current developments of new and powerful NGs make them attractive as cost effective alternatives to isotopic neutron sources for irradiation purposes. In particular, new DD NGs (Deuterium-Deuterium Neutron Generators) seem to overcome the constraints of deuterium/tritium technology with respect to tritium handling and the limited lifetime of sealed tubes. The use of NGs for irradiation of samples for analytical purposes has been explored in the past, and thus the use of these devices for teaching purposes is feasible and might also be attractive for some industrial and research applications.

Following the publication by the IAEA of Isotopic Neutron Sources for Neutron Activation Analysis (IAEA-TECDOC-465) in 1988 and Use of Accelerator Based Neutron Sources (IAEA-TECDOC-1153) in 2000, it was felt that an updated report should be published on the Use of Neutron Generators for Analytical Purposes with the emphasis on describing the new generation of generators and evaluating their value for NAA and PGNAA in a special design study. This publication is the result of extensive work carried out by the participants of an IAEA coordinated research project on 'New Applications of PGNAA' (2003–2005) and inputs from Technical Meetings on 'Neutron Generators for Analytical Purposes' (2007) and 'Fast-Neutron Resonance Radiography Applications' (2009).

The IAEA officer responsible for this publication was F. Mulhauser, of the Division of Physical and Chemical Sciences.

EDITORIAL NOTE

The use of particular designations of countries or territories does not imply any judgement by the publisher, the IAEA, as to the legal status of such countries or territories, of their authorities and institutions or of the delimitation of their boundaries.

The mention of names of specific companies or products (whether or not indicated as registered) does not imply any intention to infringe proprietary rights, nor should it be construed as an endorsement or recommendation on the part of the IAEA.

CONTENTS

CHAPTER 1
INTRODUCTION

1.1. Nuclear analytical techniques

Neutron Activation Analysis (NAA) and Prompt Gamma Neutron Activation Analysis (PGNAA) are proven methods of elemental analyses traditionally performed at nuclear research reactors. With NAA, samples are irradiated with highly thermalized neutrons inside the reactor and then taken to a low background counting area where the induced radioactive decay products are analysed. NAA can be used to measure the concentrations of many elements, often with very high (<ng/g) sensitivity, but is not sensitive for about one third of the elements where no radioactive product can be produced. PGNAA utilizes a neutron beam, external to the reactor, to irradiate a sample, which then emits prompt γ rays with energies and cross-sections characteristic of all elements. With PGNAA, sensitivities to <0.1 mg of any element, except Helium, can be achieved. Both NAA and PGNAA offer the distinct advantage that many elements in a small sample can be simultaneously and accurately analysed. Traditionally, NAA and PGNAA have been limited to research reactor laboratories which are not always conveniently accessible to scientists around the world. There are currently about 382 research reactors of which only 27 in developing countries. Few nuclear research reactors are being built today, and many are facing decommissioning in the near future. Without alternatives to reactor based NAA and PGNAA, these analytical techniques will become increasingly unavailable in many parts of the world. Beside it should be noticed the increasing development of PGNAA industrial application particularly in the mining industries. These systems use low flux ($<10^8$ neutrons/s) neutron sources.

1.2. Alternatives to research reactors

Development of alternative neutron sources for the application of PGNAA and NAA would greatly expand the availability of these techniques. Neutrons have been produced with radioactive sources using (α,n) reactions and spontaneous fission sources (^{252}Cf) with limited success. These sources are typically limited to a total intensity of 10^7 n/s, far less than that in a reactor. Radioactive sources capable of producing high neutron flux contain hazardous quantities of radiation requiring many safety considerations. In addition, these sources produce an intense γ ray background that makes PGNAA nearly impossible. Neutrons can also be produced by nuclear reactions with accelerators (e.g. LINAC, cyclotrons, Van de Graaff based accelerators) with large yields, up to 10^{13} n/s, but at substantial cost and complexity of operation.

Neutrons can be produced with neutron generators (NG) by the deuterium–deuterium (DD) (at 2.5 MeV) or deuterium–tritium (DT) (at 14 MeV) reactions (see Eqs (2.3) & (2.4), next chapter). NGs are available since many years and commercial DT generators produce $>10^9$ n/s. Unlike radioactive sources, NGs contain no radioactivity (except those based on the DT reaction) making them inherently safe when turned off. Once the generator is shut off, no radiation is produced. However, DT NGs must be sealed because of their tritium content. A limiting factor of these generators consists in the tritium target erosion which makes their typical lifetime of the order of few thousand hours with continually decreasing neutron flux. DD NGs are also available commercially but, because of the lower reaction cross-section, their neutron output is only 1% of the equivalent DT generators. They are also sealed systems requiring regular replacement of the deuterium.

1.3. New developments in neutron generators

Recently, a new generation of NG has been developed in different laboratories that overcome many of the deficiencies of early ones. In particular at Lawrence Berkeley National Laboratory (LBNL/USA) compact NGs have been designed to produce up to at least 10^{11} n/s. The open design allows the continuous regeneration of the target so that these generators should be able to operate indefinitely at maximum neutron fluency. These generators can be continually pulsed on a very short time scale (<1 μs) allowing applications that could not be envisioned for most nuclear reactors. A tabletop NG suitable for PGNAA and NAA analysis, with moderator and shielding, has been conceptually designed and presented in this report. Neutron fluxes, calculated with the General Monte Carlo N-Particle Transport Code (MCNP), are in excess of 10^8 neutrons $\cdot$ cm^{-2} $\cdot$ s^{-1} for NAA in this design. Apart from particular applications using 2.5 MeV neutrons for irradiation at these thermalized fluxes many traditional NAA elemental analyses can be performed, and by pulsing the NG very short half-lives <1 ms can be exploited. The neutron flux for PGNAA with a favourable, low background detector arrangement is calculated as $>10^6$ neutrons $\cdot$ cm^{-2} $\cdot$ s^{-1}, which is comparable to guided thermal neutron flux at reactor based PGNAA facilities. Increasing detector efficiency by implementing multidetector or HPGe clover detectors systems can provide sensitivities comparable to those at reactors.

Many additional NG designs with lower fluxes have been devised for specialized applications, and costs of a complete PGNAA/NAA system should run <300k$, well within reach of many laboratories. Coaxial NG target designs provide the maximum neutron flux, axial designs allow sample positioning within <1 cm from the generator, and low flux NGs can be used for teaching and handheld operation. Even the largest NG can be installed for bench top applications or in vehicles for transportable operation. The new generation of high performance, inherently safe NG can provide research quality facilities anywhere in the world at low cost without concern for nuclear proliferation. It is also worthwhile mentioning new developments of DT NGs in the field of Associated Particle Imaging (API) technology. This technology uses the associated particle, helium nuclei, properties to add spatial resolution by time of flight and neutron trajectory computation to conventional PGNAA.

This document describes, among others, the design of a versatile NAA irradiator as the results of MCNP calculations with the optimum configuration for neutron moderation and radiation shielding for NAA/PGNAA. The analytical capabilities of this system are described with examples of recent progress at a variety of facilities. The results of an intercomparison of standard cement material with PGNAA analyses at various facilities are included.

1.4. Applications of neutron generators

NGs can effectively be used for elemental analysis with NAA and PGNAA. They are also effective for analysis of hidden materials by neutron radiography. Traditional NGs have been shown to be effective for applications including borehole logging, homeland security, nuclear medicine and the on-line analysis of aluminium, coal and cement. Potential applications in land mine detection, cargo screening, archaeology, and isotope production have been proposed. The availability of a new generation of low cost NGs offers the opportunity for professional and technical training at universities, research institutes for physicists, chemists, nuclear engineers, biologists, radiologists and health physicists. Useful guidelines for developing NG based research laboratories are provided in this report.

CHAPTER 2
THE HISTORICAL DEVELOPMENT OF NEUTRON GENERATORS

2.1. Introduction

In 1920, Rutherford postulated that there were neutral, massive particles in the nucleus of atoms. James Chadwick, a colleague of Rutherford, discovered the neutron in 1932. He bombarded a beryllium target with alpha particles producing neutrons that recoiled into a block of paraffin. Chadwick's apparatus, the first NG, is described in Fig. 1.

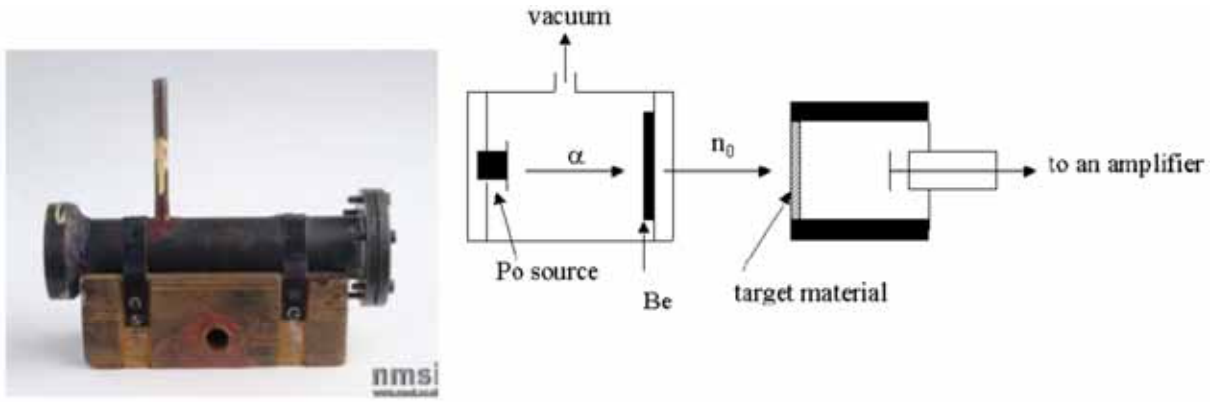

FIG. 1. Detector used by James Chadwick to discover the neutron. Inside the detector, particles from a radioactive source hit a beryllium target. The reaction $^{9}Be + a \rightarrow {}^{12}C + n$ *produced neutrons that were detected when they knocked protons of paraffin wax.*

By measuring protons emerging from the paraffin with a Geiger counter, Chadwick inferred that the neutron had a mass comparable to that of the proton. Soon Enrico Fermi recognized that neutrons could be used to produce radioactive nuclides sent off Emilio Segre to "get all of the elements in Mendeleev's table". Together they bombarded over sixty elements discovering, for example, a 1–2 day activity from bombarding gold. Fermi was awarded the 1938 Nobel Prize for this work. George de Hevesy helped Fermi obtain samples of rare earths, and he too became interested in activating these materials. His assistant Hilde Levi irradiated dysprosium with neutrons producing a large amount of radioactivity that decayed with time [1]. This episode triggered the realization that the half-lives and magnitudes of induced activities could be used to identify and quantify trace elements and led to the invention of NAA.

2.2. Neutron production reactions

Large fluxes of neutrons are produced by the fission of ^{235}U at nuclear reactors. These can be thermalized for use in applications such as NAA, and thermal or cold neutron beams can be produced for PGNAA. Neutrons can also be produced by charged particle induced reactions like those used by Fermi and Hevesy. The neutron flux produced in reactions is much lower, but NGs are more widely available than reactors, and produce a wide variety of neutron energies. They are much easier to operate than reactors and can be shut down completely when not in use.

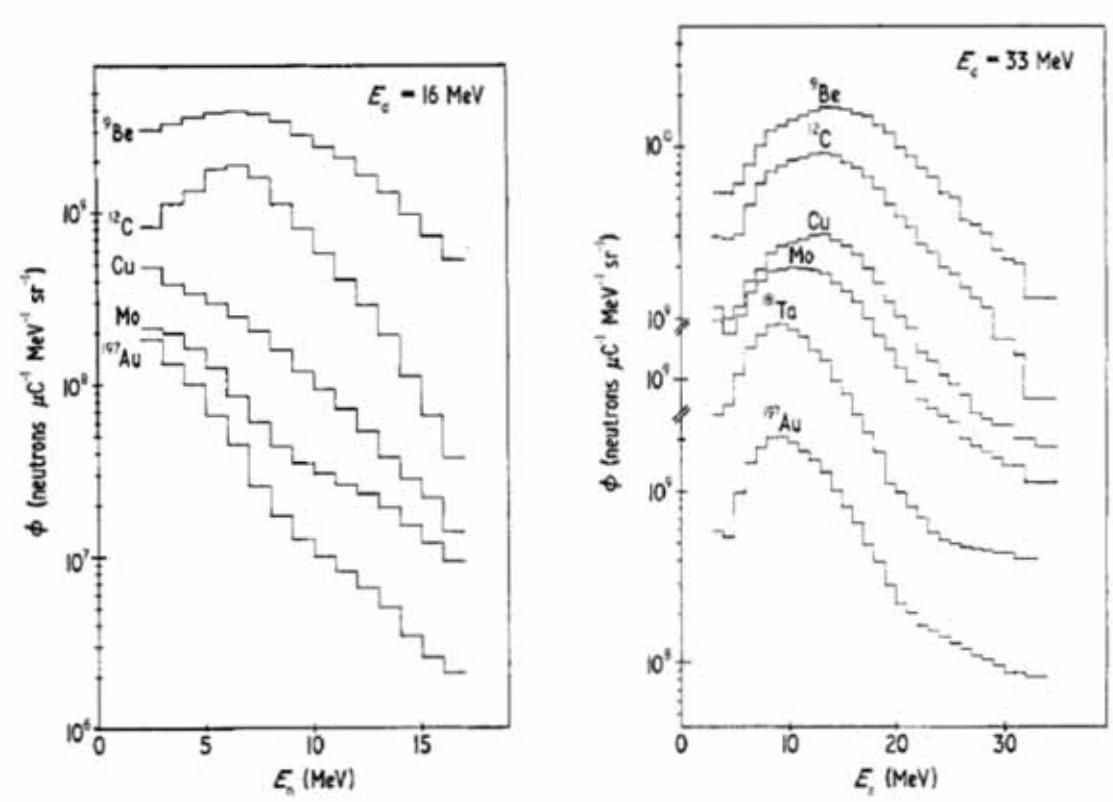

FIG. 2. Neutron energy spectra produced in the (d, n) reaction on thick targets with 16 and 33 MeV deuteron beams [2].

TABLE 1. REACTIONS FOR PRODUCING NEUTRONS

Reaction	Threshold Incident Particle Energy (MeV)	Q Value (MeV)	Threshold Neutron Energy (MeV)
^{3}H(d,n)^{3}He	0	+3.266	2.448
^{3}H(p,n)^{3}He	1.019	–0.764	0.0639
^{3}H(d,n)^{4}He	0	+17.586	14.064
^{9}Be(α,n)^{12}C	0	+5.708	5.266
^{12}C(d,n)^{13}N	0.328	–0.281	0.0034
^{13}C(α,n)^{16}O	0	+2.201	2.07
^{7}Li(p,n)^{7}Be	1.882	–1.646	0.0299

A summary of commonly used neutron production reactions is given in TABLE 1. The total yield F of neutrons produced in a nuclear reaction is given by

$$F = N\sigma\phi \tag{2.1}$$

where F is the neutron yield per second, N is the number of target nuclei per square centimetre of target, σ is the reaction cross-section in cm^2 and ϕ is the incident particle rate per second. The incident particle rate can be expressed in terms of beam current by

$$\phi = 6.25 \cdot \frac{I}{C} \times 10^{18} \tag{2.2}$$

I is the beam current in amperes and C is the charge of the particle in Coulomb. Thick target yields for various (d,n) reactions are shown in FIG. 2 and the thick target yield for ^{9}Be(α,n) is shown in FIG. 3.

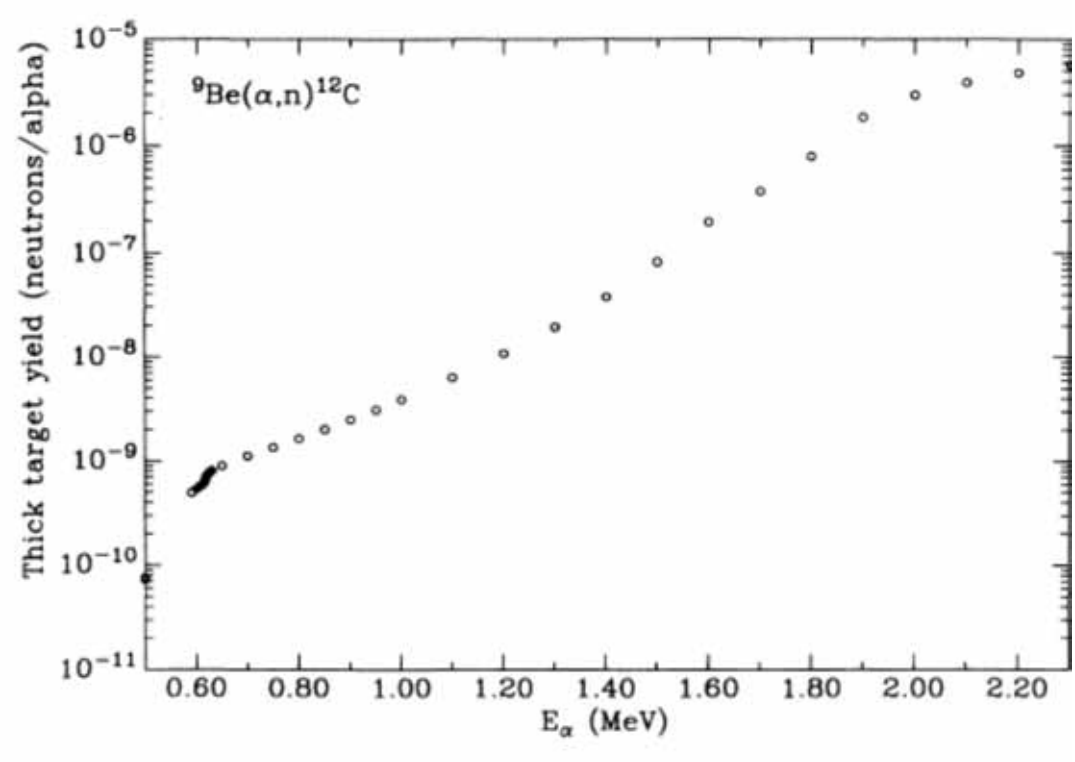

FIG. 3. Thick target yields for $^{9}Be(\alpha,n)^{12}C$ [3].

Two nuclear reactions used for producing fast neutrons with low voltage accelerators, commonly referred to as NG, are DD

$$^{2}H + ^{2}H \rightarrow ^{3}He + ^{1}n + 3.266\,MeV \tag{2.3}$$

and DT

$$^{2}H + ^{3}H \rightarrow ^{4}He + ^{1}n + 17.586\,MeV \tag{2.4}$$

The neutron yield for the DD and DT reactions is given in Fig. 4. For thin targets the neutron energy also varies with laboratory angles as shown for DD in Fig. 5 and for DT in Fig. 6.

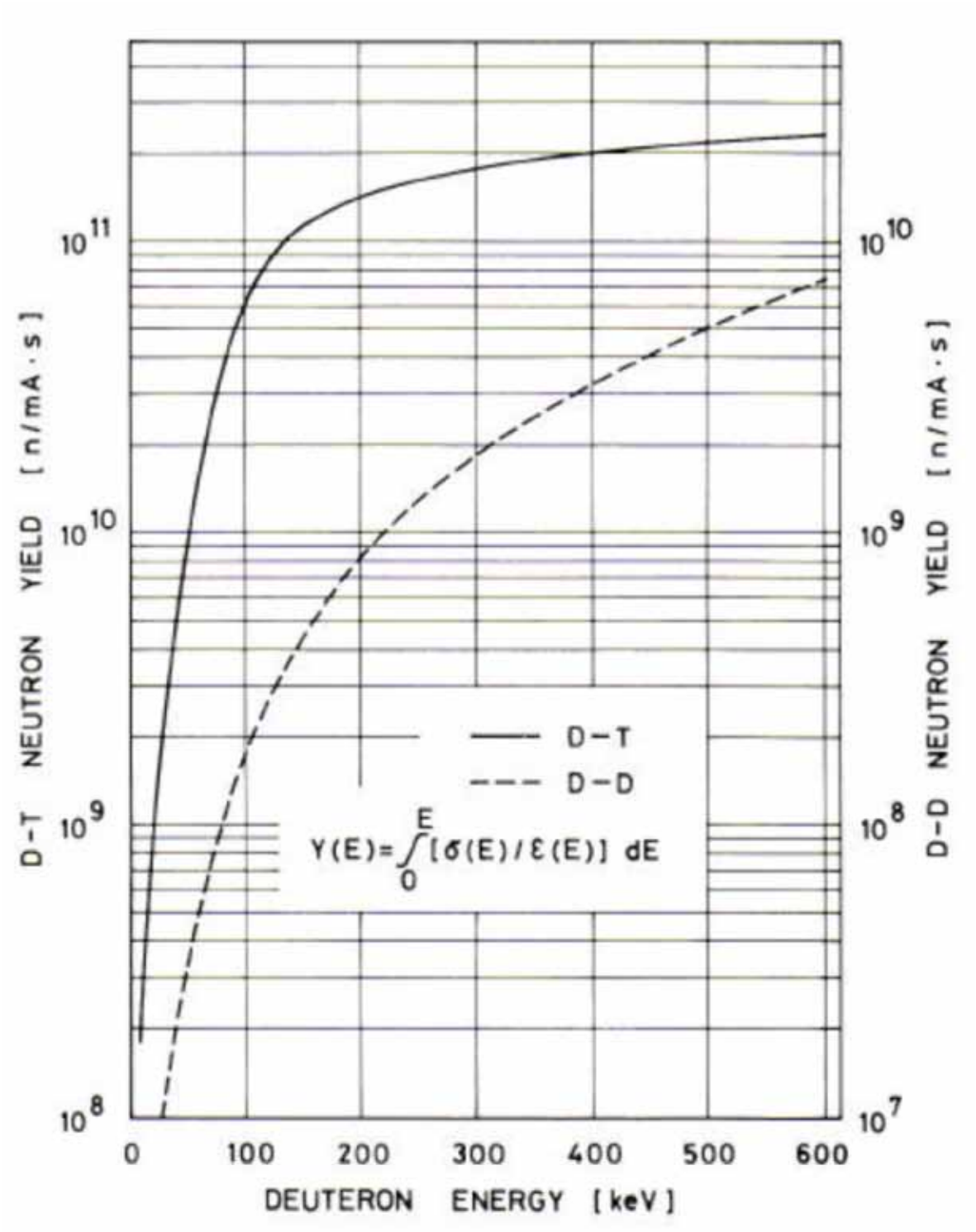

FIG. 4. Neutron yield for DD and DT reactions as a function of deuteron energy.

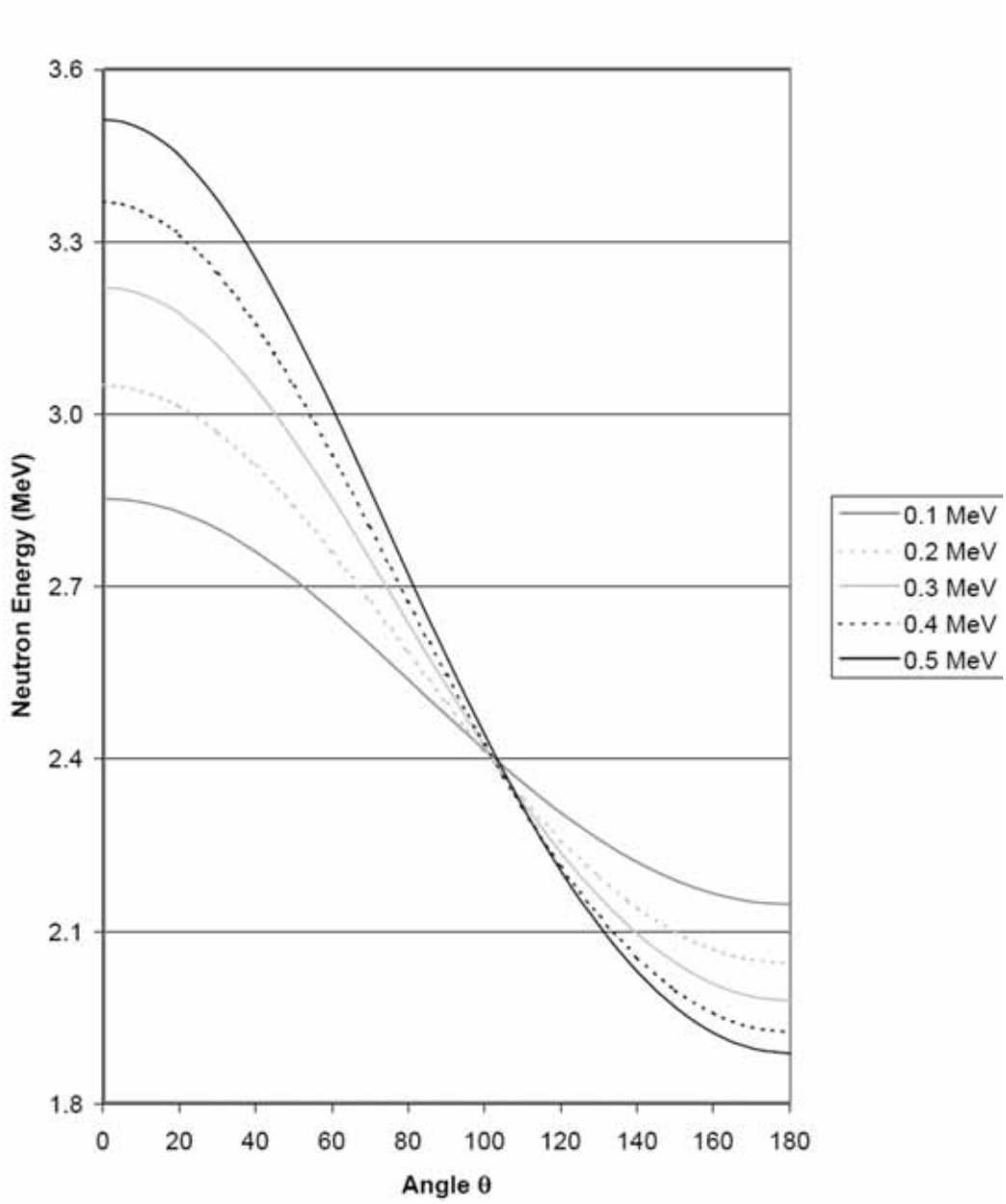

FIG. 5. DD neutron energy angular distribution as a function of deuteron energy.

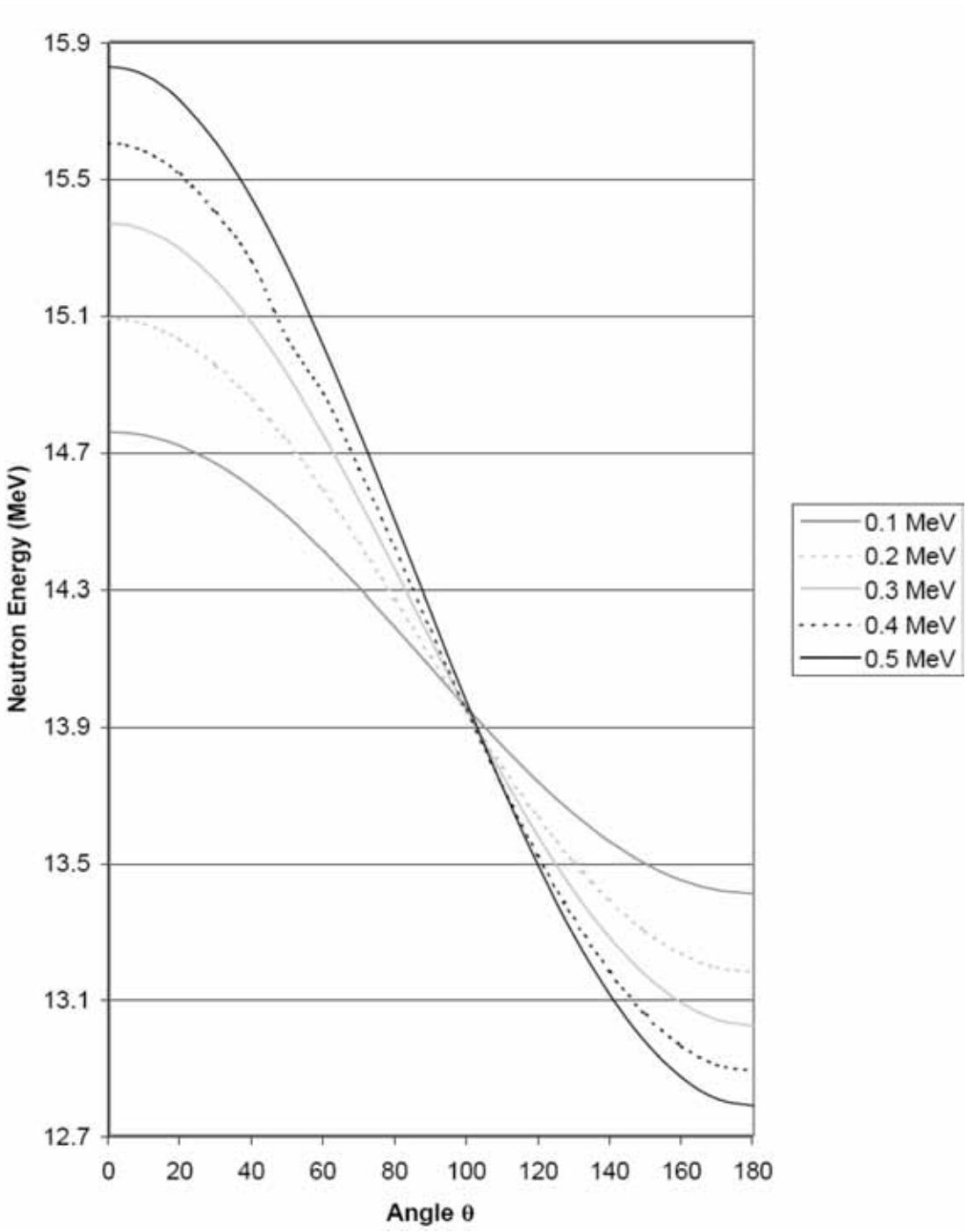

FIG. 6. DT neutron energy angular distribution as a function of deuteron energy.

CHAPTER 3
ANALYTICAL APPLICATIONS OF FAST NEUTRONS

3.1. Neutron sources

Neutrons, not being stable particles, have to be released from nuclei. Most nuclear reactions, used for neutron generation, require high energy particles and produce fast neutrons, i.e. neutrons with energies of several MeV. The most important reactions are listed below:

(1) $\gamma + {}^{9}Be \rightarrow 2\ {}^{4}He + n - 1.67$ MeV
(2) ${}^{9}Be + \alpha \rightarrow {}^{12}C + n + 5.91$ MeV
(3) ${}^{2}H + {}^{2}H \rightarrow {}^{3}He + n + 3.29$ MeV (neutron energy about 2.4 MeV)
(4) ${}^{3}H + {}^{2}H \rightarrow {}^{4}He + n + 17.6$ MeV (neutron energy about 14.1 MeV)
(5) ${}^{3}H + {}^{1}H \rightarrow {}^{3}He + n - 0.763$ MeV

(Other, less important reactions are: ${}^{7}Li(p,n){}^{7}Be$, ${}^{9}Be(d,n){}^{10}B$, ${}^{7}Li(d,n){}^{8}Be$, ${}^{51}V(p,n){}^{51}Cr$.)

The first two reactions are used in radioisotopic neutron sources, where gamma and alpha radiation are obtained from other radioactive nuclides. The most commonly used photoneutron source exploits reaction (1) with the ^{124}Sb nuclide with a half-life of 60 days, whose 1692 keV gamma radiation kicks out the loosely bound neutron from a ^{9}Be nucleus with an energy of 26±1.5 eV, i.e., it exceptionally produces relatively low energy, epithermal neutrons. Alpha particles emitted by the nuclides ^{210}Po, ^{239}Pu, and ^{241}Am are used most frequently to implement reaction (2). Po–Be, Pu–Be and Am–Be sources emit 10–12 MeV neutrons. The spontaneous fission of ^{252}Cf also provides a widely used isotopic fast neutron source.

Reactions (3) and (4) are used in NGs. Both of them are exothermic, thus requiring relatively low energy particle beams (100–500 kV). The DT reaction has a resonance at about 100 keV with the cross-section of 5 barns, while the DD reaction has its weaker resonance at about 2 MeV (about 0.1 barn) [4]. Both of them have reasonable cross-sections at low energies, however the cross-section of reaction (4) is much higher than that of reaction (3), which results in a yield of about two orders of magnitude higher around 100 keV for the DT reaction. Because of their higher fluence mainly DT NGs were manufactured in past decades. However reaction (3) together with (5) is used to produce a beam of monochromatic neutrons to study inelastic neutron scattering of fast neutrons.

3.2. Nuclear reactions used in activation analysis

3.2.1. Radiative neutron capture, (n,γ) reaction

The most important reaction in PGNAA and NAA is the (n,γ) reaction. Whenever a nucleus absorbs a neutron, a compound nucleus is formed whose excitation energy equals the binding energy plus the kinetic energy of the neutron. When irradiating with slow neutrons (i.e. when the kinetic energy is in the meV range), the capture state has a well defined energy value, which practically equals the neutron binding energy. The decay of the compound nucleus happens within 10^{-16} s. The nucleus reaches its ground state, typically in 10^{-12}–10^{-9} s, by emitting 2–4 γ rays in a cascade. Γ rays are called prompt, if their decay times following the capture, appear much faster than the resolving time of the detection system, which typically is in the range of 10 ns to 10 μs. Prompt gamma radiation is characteristic, i.e., the energy values of the γ rays identify the nuclide, and their intensities are proportional to the number of atoms.

Thus they can be used for elemental analysis. If the ground state of the daughter nucleus is stable, the process ends here.

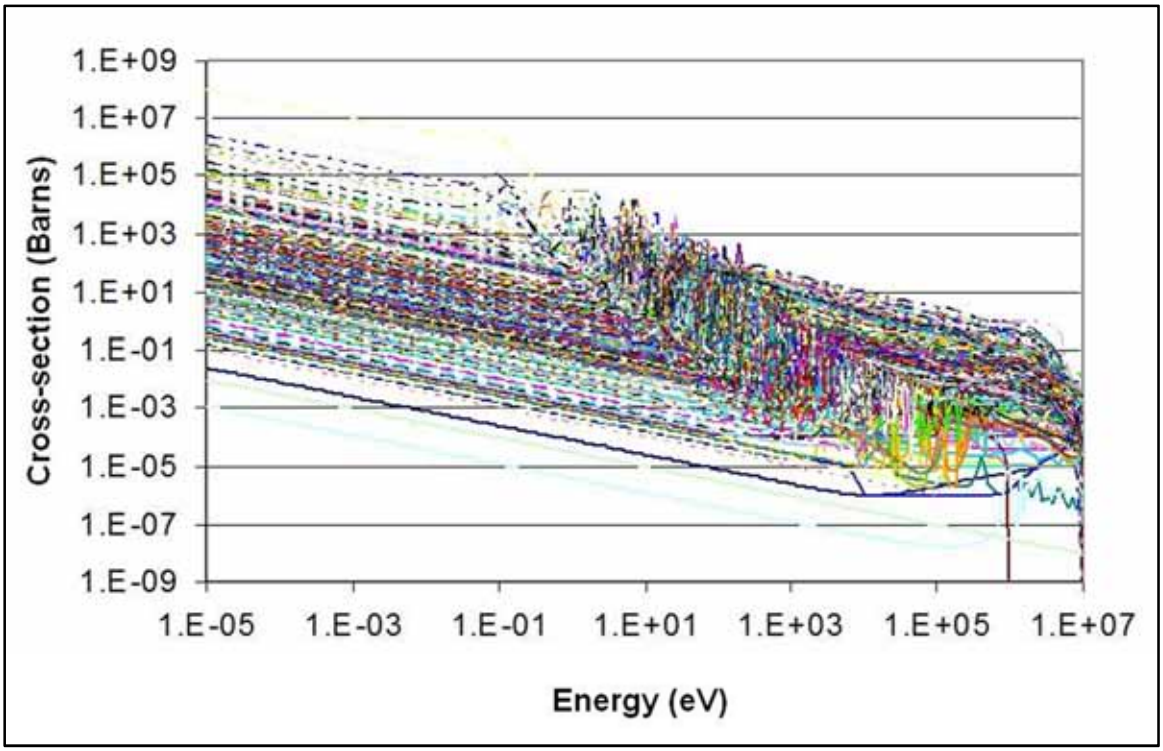

FIG. 7. Neutron capture cross-sections of the stable nuclides.

When the ground state reached after the de-excitation is not stable, radioactive decay radiation (typically β decays and electron capture followed by γ rays) with a given half-life will take place. The detection of the delayed gamma radiation produced in this way is the basis of the traditional NAA, but several nuclides can be analysed in PGNAA using their prompt decay radiation too. Prompt gamma cascades may be delayed by metastable levels. The gamma transitions from metastable levels are called isomeric transitions.

The capture cross-section is highly dependent on the neutron energy. For slow neutrons the most important energy dependence is the so called 1/*v* law, i.e., the cross-section is inversely proportional to the velocity of the neutrons. Its validity has been demonstrated down to 10^{-6} eV [5]. Fig. 7 shows the general tendency of the capture cross-section for stable nuclides.

In the thermal energy region (around 0.025 eV) some capture cross-section may be as high as several ten thousand barns (e.g. for ^{113}Cd, ^{149}Sm), while some others may be 6–8 orders of magnitude lower. In general, capture cross-sections decrease by 4–5 orders of magnitude from thermal to fast region.

3.2.2. Inelastic scattering of fast neutrons, (n,n'γ) reaction

The inelastic scattering of neutrons or (n,n'γ) reaction takes place if the neutron energy is above the energy of the first excited state of the scattering nucleus, i.e. it is a threshold reaction. The energy of the neutron will be reduced by the excitation energy, and the same

amount of energy will be released by the scattering nucleus in form of characteristic prompt gamma radiation. This radiation can also be used for chemical analysis. This reaction is particularly used for carbon and oxygen measurement.

The inelastic neutron scattering or (n,n') cross-section, σ_{inel} has an energy dependence close to the threshold of $\sigma_{\text{inel}} \propto \sqrt{(E_n - E_{\text{level}})}$ [6, 8]. It reaches its maximum a few hundred keV above the threshold. The cross-section value at the maximum is a few tenths of barns for most nuclides. From the maximum value it decreases exponentially due to the increase in the number of competing levels. The sum of the individual inelastic cross-sections for all the levels increases to a maximum at a few MeV above the threshold [8]. The total inelastic cross-section has a value of a few barns around its maximum. This inelastic scattering reaction is the basis of the API systems.

3.2.3. Nuclear reactions with fast neutrons

Energetic fast neutrons may produce other particle emission in materials. These include (n,pγ), (n,Xnγ), where X = 1, 2, … or (n,αγ) reactions which are mostly threshold or endothermic reactions. In other words, they can happen only above a given energy, characteristic of the target material. The daughter nuclei may be radioactive. These reactions are usually regarded as a first order noise in traditional NAA since they produce different nuclei that may interfere with capture reactions used for the identification of the elements. However, when using fast neutron only, these reactions identify nuclides unambiguously.

The fast neutron reaction channels open at about a few MeV [7, 8]. Albeit these are threshold reactions their energy dependence is quite similar to that described in the previous paragraph. As a rule of thumb one can say that below the binding energy per nucleon, inelastic scattering is typical, while above fast neutron reactions tend to dominate.

Summarizing, nuclear reactions of neutrons can be used for identification of target nuclides (elements). The capture of thermal neutrons is of the highest probability of all possible reactions. The thermalization is very efficient in nuclear reactors, as it is needed to maintain the chain reaction, but may be inefficient in using other neutron sources, like isotopic sources or generators. Thermalization broadens the energy range of neutrons emerging from the source thus enabling different reactions. While in the case of generators, almost monochromatic neutrons can be applied for chemical analysis directly. Because of the large variation of thermal capture cross-sections along the nuclides table, NAA and PGNAA exhibit largely variable sensitivities for different elements. Most elements can be excited using inelastic neutron scattering, and they will have similar sensitivities.

3.3. 14 MeV neutron activation analysis

14 MeV NAA is capable of determining many light elements that cannot be analyzed using classical NAA. One of the most important applications of this technique is the determination of oxygen using the reaction $^{16}O(n,p)^{16}N$. ^{16}N decays with a half-life of 7.13 s, and emits exceptionally high energy gamma photons with the energies of 6.13 MeV, and 7.12 MeV. The following elements are routinely determined using 14 MeV NAA: F, Mg, Al, Si, Cu, Fe, P and Zn. The most important reactions are listed in TABLE 2, [4, 9]. Sensitivity data are taken from Ref. [4] in the unit of decay per second per gram, i.e. it gives the activity per unit target mass after 1 hour of irradiation assuming a fast neutron flux of 10^9 $cm^{-2}s^{-1}$.

The detection limits are calculated to be 0.1–1 mg for the above elements, when using a generator with an output of 10^{11} s^{-1} [4]. As it can be seen from TABLE 2, there are interference problems even in this short list of elements in case the spectroscopic analysis is performed with scintillator detectors. Close-lying energies (e.g. Br and Ag from the above cases) can be resolved using HPGe detectors. Since most half-lives of the detected nuclides are relatively short, the cyclic activation technique was introduced to improve the sensitivities. A cyclic activation analysis facility with 14 MeV neutrons was established at the end of 1980s at GKSS Research Center, Geesthacht. 39 nuclides were reported to have half-lives between 0.3 and 30 s that can be measured in up to 30 cycles [10]. One of the major problems in cyclic 14 MeV NAA is the correction for the effective neutron flux, which may vary from cycle to cycle [11].

TABLE 2. MOST IMPORTANT REACTION USED FOR ANALYSIS USING 14 MeV NEUTRONS

Element	Reaction	Half-life	Gammas (MeV)	Sensitivity (10^6 decay · s^{-1} · g^{-1})
B	$^{11}B(n,p)^{11}Be$	13.8 s	2.125	15
O	$^{16}O(n,p)^{16}N$	7.13 s	6.13, 7.12	1.3
N	$^{14}N(n,2n)^{13}N$	9.97 min	0.511 (ann.)	15
Al	$^{27}Al(n,p)^{27}Mg$	9.46 min	0.844	1.6
Si	$^{28}Si(n,p)^{28}Al$	2.25 min	1.78	4.5
P	$^{31}P(n,\alpha)^{28}Al$	2.25 min	1.78	2.3
Cu	$^{63}Cu(n,2n)^{62}Cu$	9.74 min	0.511 (ann.)	3.6
Br	$^{79}Zr(n,2n)^{78}Br$	6.5 min	0.614	3.7
Ag	$^{109}Ag(n,2n)^{108}Ag$	2.37 min	0.633	2.3
Ba	$^{138}Ba(n,2n)^{137}Ba$	2.55 min	0.662	3.7

X rays emitted by nuclides decaying in electron capture can also be used for elemental analysis (e.g. Tb, Er, Ta, Re, Os, U). Since X rays may also be generated in other ways, an interference correction is necessary. Because of the low energy of X rays, self-absorption needs to be corrected for when possible.

The most important application of 14 MeV NAA has always been the determination of oxygen. An American Society for Testing and Materials (ASTM) standard method also appeared for the determination of “Oxygen content Using a 14-MeV Neutron Activation and Direct Counting Technique” (ASTM Standard E385-90, [12]). The standard method contains the discussion of interferences, neutron fluence monitoring, calibration and standardization.

The oxygen content of steel during the production phase is a widespread application. The average time for a complete analysis is in the order of about 30 s, the two high energy lines are counted using NaI(Tl) crystals. Because of the relatively large metal mass the detection

limit is as low as 5 ppm or, when using no container, even lower. Other important applications in metallurgy are the determination of Si, P and Mg in cast iron [4].

Pollutants and minor elements have been determined in organic chemicals. Various elements have been determined in biological samples, from major components (O, N) to minor elements (F, Na, Mg, Al, Si, P, S, Cl, K, Ca, Ti, Fe). In the elemental analysis of proteins and amino acids for N, O, S and P it was found that in a small sample of 10 mg the analysis could be performed with a precision of 5% [4].

Pulsed 14-MeV neutron beams were proposed for in vivo whole body analysis of H, C, N, O, Cl, P and Ca [13]. Both, prompt and delayed gammas could be used for this purpose. Actual measurements were reported in Ref. [14]. In vivo measurements were performed by other groups for the determination of Ca, Na, Cl, N and P in human body. Five minutes irradiation time and 15 minutes counting time resulted in a ±4% precision in a repeated measurement of the same patient. The radiation dose was about 1 mrad (10 μSv) [15]. Ca/F ratios of bones or F content of human teeth were also measured in vitro. Other applications: determination of N fertilizer in plants, selection of seed corn with high protein content based on the amount of nitrogen.

Lunar and meteoritic samples were analyzed for the abundance of O, Si, Al, Mg, Ca, Ti, and Fe. The rocks collected by Apollo 11 and condrite meteorites could be classified based on the analysis. Another important field of application of 14-MeV NAA is the analysis of geologic samples. Practically all major components of typical minerals can be measured with this technique.

On-line analyzers are installed now worldwide for the analysis of raw material on conveyor belts. These instruments are used for several purposes to regulate an enrichment process (nickel, copper ores), to regulate raw materials composition (adding additives like lime, sand, iron in a cement manufacturing process), to adjust parameters in mills, crushers or furnaces (coal combustion) or to measure material qualities intrading. They are mostly used in cemeteries (measurement of Al, Si, Ca, Fe) and coal plants (C, O, S, and other thermal properties). New developments already use a system which contains a moderator, and the composition is determined from prompt gammas after thermal neutron capture and also from inelastic scattering.

Applications to the oil industry include borehole logging. Probes containing a small NG and gamma spectrometer are commercially available. Some also contain epithermal and thermal neutron detectors for the detection of uranium. The method is extremely sensitive for the detection of hydrogenous layers (e.g. oil) because of the thermalization by the olefins neutrons generating capture gamma (n,γ) radiation.

14-MeV NGs are also applied in nuclear safeguards. Fissile material can be identified using e.g. the delayed neutrons, or certain prompt and delayed gammas from fission products. The API method has been used for the detection of explosives [16].

Thanks to a relatively new development 14-MeV NGs can be used for imaging using the API. A position sensitive detector has to be built in the sealed tube to detect space resolved alpha particles produced by the fusion reaction. Based on the analysis of the elapsed time between the detection of the alpha particle and the detection of prompt gammas from inelastic scattering a space resolved counting from the sample can be performed. The method has been used for the detection of explosives [16]. Commercial productions are available in the scope

of many projects, the SENNA system by APSTEC Russia [17] and ULIS system by SODERN France [18].

Oxygen content of ores and rocks were determined using cyclic activation analysis e.g. by Ila [19]. The relative accuracy proved to be better than 1%. The determination of oxygen in uranium is disturbed by the high energy gammas from the fission products [20]. N and P were simultaneously determined in human tissue [21] using coincidence counting for the detection of annihilation photon from ^{13}N. N content of seed grains, N and P content of biological samples and polymers have been studied by Ehmann [11].

14 MeV NAA as a non-destructive method proved to be extremely useful for the investigation of archaeological artefacts, or coins. Si content of geological samples can also be determined using this technique. Usually a second counting is needed to wait until ^{16}N from the oxygen decays away [11]. James [22] identifies the oxygen determination, borehole logging using transportable pulsed generators and on-line analyzers as some of the most important applications.

14-MeV neutron using pulsed fast thermal neutron analysis (PFTNA), detecting the gammas with a BGO or other scintillator have recently been used for the determination of H, C and O in coal. The reliability of the results was improved using different mathematical tools [23], [24]; industrial coal analyzers are now available (e.g. Thermo Scientific, SODERN). A rapid method for the determination of gold in sand, concrete and rock samples has been developed by a Romanian group [25, 26]. A pulsed generator has been used for the determination of Hg, Cd and Pb in liquid radioactive waste in 200-l drums using the prompt gamma radiation from the capture of thermalized neutrons in the liquid [27]. The protein content of food was determined by a Nigerian group analyzing N. The results agreed well with those obtained by the standard Kjeldahl method [28]. Heavy metal content was determined with different methods including 14-MeV NAA in air pollution biomonitors in Morocco [29, 30]. N, O and Si content of fossil fuels [31], Al and Si content of alumino silicate ores [32] and protein content of grains [33] was determined using fast neutron activation analysis (FNAA) in Nigeria. N, Cl and O content of polymers were determined by an Indian group [34]. P and Ca content of bones were measured by a Brazilian group using 14-MeV neutrons generated by a Van de Graaff accelerator [35]. Fe, Cr, Ni, Si and Mo content of steels were determined by a Libyan group [36].

Oxygen content of coal standard reference materials was determined at the National Institute of Standards and Technology (NIST). The method was accurate enough to determine relative changes of about 5% [37]. A method was developed to determine ^{129}I using thermal and 14-MeV NAA, as an alternative to X ray spectrometry or inductively coupled plasma mass spectroscopy (ICP-MS) [38].

Pulsed elemental analysis with neutrons (PELAN) is performed with a portable system for the detection of explosives based on their significantly different H, C, N and O contents. The gammas induced by the 14-MeV neutron pulses are detected by a BGO, and are acquired in three time windows: fast, thermal and decay events. The signal to noise ratio was optimized to reach better sensitivities [39]. The optimization of the lengths time windows was investigated by Gozani et al. [40]. Cross-section measurements were performed on very short half-life nuclides (20 μs–1 s) using a SODERN sealed tube generator with tunable pulse length. Gamma lines were measured by an HPGe detector. Isomeric states were studied by cyclic activation method [41]. The industrial application of long life SODERN neutron tubes was also investigated [42]. Pulse pile up and deadtime correction methods were developed for

cyclic activation analysis in Algeria [43]. The API was proposed for the whole body measurement of protein, fat and water. 20–40 kg meat samples were scanned, and C, N and O was measured [44].

3.4. Overview of possible applications with neutron generators

Applications of analytical methods using fast neutrons produced with NGs can be found in almost every conceivable field of scientific inquiry. This is true in large part to a series of unique characteristics which separate the method from most others. While it is correctly identified as a method of "chemical analysis" because of the information it can generate, it is based on nuclear rather than atomic or molecular properties. This, at the outset, avoids the issue of chemical state in which the analyte exists in the sample, which is a common source of uncertainty in traditional analytical methods. In addition, simplicity of design and inherent safety of operation makes it an attractive alternative to its more powerful cousin, reactor based instrumental neutron activation analysis (INAA), for those analytical problems for which it is appropriate.

Perhaps the predominant characteristics which promote its uniqueness, which are shared by INAA, is the commonly touted non-destructive nature, multi-element capability, ease of sample preparation and freedom from reagent blank and contamination often encountered during sample preparation steps[1]. Also, like INAA, many sample matrices are rather transparent to the incident radiation probe, the neutron, as well as to the gammas emitted from the reaction product which are used to generate the analytical signal. In the case of analysis using NGs, however, the non-destructive characteristic is enhanced due to the generally lower fluxes and lower specific activities produced in isotopes with shorter half-lives likely to be produced. The small size and transportability lends the method as well to application to field measurements and implementation in site laboratories where conventional analytical instruments are unlikely to be usable.

In this section, we attempt to survey some known existing analytical applications of NG and suggest potential applications. Our discussion is organized by general field of study. We make no attempt nor claim to have exhausted the full list of applications; rather the purpose is to provide the potential user with sufficient information to allow a more informed decision concerning the potential utilization of these devices. In addition to the paragraphs below, TABLE 3 provides a brief outline of our discussion.

[1] The IAEA issued many publications (TECDOCs, Special Report Series and Technical Report Series) in which the principles, characteristics and applications of nuclear analytical techniques have been outlined. Examples are IAEA-TECDOC-459 (1988), 1215 (2001), 1121 (1999) and IAEA Special report series STI/PUB/1181 (2004) and Technical Report Series No. 416 (2003).

TABLE 3. SELECTED FIELDS OF APPLICATION OF NG

Field	Category	Energy Required	Existing Applications
Security	Explosives detection	14 MeV	Cargo/luggage inspection, Suspicious objects C,O,N
	Chemical weapon detection	14 MeV, metals might be possible with 2.5 MeV	N, P, CW inspections
	Contraband detection	14 MeV	Narcotics, C,O,N
Safeguards	Nuclear material detection	2.5 MeV	Fission product nuclides
Art and Archaeology	Artefacts	2.5 MeV, 14 MeV thermalized	Major components
	Archaeological objects	2.5 MeV, 14 MeV thermalized	Major components
Industrial	on-line analyzers	2.5 MeV, 14 MeV	Cement process monitoring Coal and mining industries Ca, Si, Fe, Al
	metal cleanliness	14 MeV	Oxygen in Mg, Al, Steel
	raw materials	2.5 MeV, thermalized and not thermalized	Purity, contaminants
	Al based catalysts	14 MeV	F
	Energy production	thermalized	H in fuel cell technology
Research	Cross-section 2.5 MeV reactions	2.5 MeV	

TABLE 3. SELECTED FIELDS OF APPLICATION OF NG (cont.)

Field	Category	Energy Required	Existing Applications
Educational	NAA training	2.5 MeV, 14 MeV	
	Nuclear parameter training	2.5 MeV, 14 MeV	
	Inelastic neutron scattering		
	Imaging, Radiography		
Medical	body screening	pulsed 14 MeV	C, O, N, Ca, Na, Cl, P
Nutrition	protein content of food	14 MeV	N
	animal fodder	2.5 MeV, thermalized	Trace elements
Environmental	Recycled material	2.5 MeV thermalized	Cd, Hg, Br, Cl
	Waste material	2.5 MeV thermalized	
	Radiography	2.5 MeV	Water content of plants (in vivo)
	Pesticides	2.5 MeV	Halogens (Br, Cl)
		14 MeV	Halogens (F)
Geological	on-line analyzers		Ash value of coal, Si, Al, C, H, Fe, Ca, S, calorific value
	exploration		Downhole inspection/oil, H

TABLE 3. SELECTED FIELDS OF APPLICATION OF NG (cont.)

Field	Category	Energy Required	Existing Applications
	Boron determination	2.5 MeV thermalized	B
	U and Th measurement	2.5 MeV	DNC

3.5. Materials analysis

Since the overall topic of this communication deals with the use of NGs specifically for analytical purposes, one would correctly presume that applications in all of the fields of study could be described as materials analysis. This section with that name therefore is largely reserved to a few applications of generic interest which encompasses essentially all scientific fields.

3.5.1. Elemental analysis

In the early 1960s a great deal of activity was underway in the development and application of NAA in general, and particularly in the use of NG based NAA. One has only to peruse the early transaction documents for the Modern Trends in Activation Analysis series [45–47] to see that a large portion of the papers concerned either fast neutrons or generator produced thermalized neutrons. In 1973 John Wiley and Sons published, as volume 39 in their "Series of Monographs on Analytical Chemistry and its Applications," a text on "Activation Analysis with Neutron Generators" by Nargolwalla and Przybylowicz [48]. This highly regarded treatise continues to provide detailed basic information for today's activation analysis practitioner; with most of us having an often used and well-thumbed copy readily available on our desktop. The text provides thorough discussions of NG of the day, shielding considerations, radiation hazards, production reactions, sample preparation, systematic analytical errors and every other aspect of protocols for generator based analysis. In addition, over half of the book (about 350 pages) is devoted to specific discussions of generator based analysis, element by element. For each element, the conditions for analysis, the reactions available for utilization from 14 MeV, 3 MeV and thermalized neutrons, activation curves, decay curves and interferences are dealt with in detail. Experimental sensitivities are even presented for 14 MeV and thermal activation analysis with a NG, again based on the generators available in the early 1970s. The salient point here is that our current attempt to evaluate the potential for use of generators for analytical purposes is far from ground breaking. In fact, this early work, which is based on work performed in the heyday of NG use, already provides this definitively. Rather, our work is an attempt to reiterate the potential of the method and to point out additional applications, both currently in place and proposed.

3.5.2. Fast neutron activation analysis for oxygen

No doubt the most routinely useful and enduring application of NGs as an analytical tool is for the fast (14 MeV) neutron activation analysis for oxygen. Again, we cannot assign a discussion of this highly developed method to any particular field of scientific study, because it has found commonplace usage in many of them. It has long been recognized that the determination of oxygen using the $^{16}O(n,p)^{16}N$ reaction provides a quick and accurate measurement that is otherwise difficult to obtain [49–51]. The high energy γ rays emitted

from the reaction product are rather unique and therefore their counting is readily used as the analytical signal by discriminating against lower energy lines. Self-absorption effects are also reduced therefore widely varying matrices can be studied with often insignificant variation in gamma attenuation. Contributions to the apparent oxygen content from the few potential interferences can be readily determined and corrected if necessary. The threshold value for the (n,p) reaction is 9.6 MeV [48] so neither 3 MeV nor thermalized neutrons can be used to induce the reaction.

The longevity the technique has experienced is due at least in part to the fact that no competing method has been developed and is readily automated with computer control [52]. Geochemical analyses including compositional measurements of coal and coal products have historically reported oxygen concentration by difference (subtracting concentrations of all other major elements from 100%) or by stoichiometry. Combustion methods are generally less sensitive and much more time consuming.

Current applications for FNAA of oxygen include chemical process intermediates, light metal cleanliness in the automotive industry, petroleum based fuel research, battery components, weld inspection and plastics. Submissions to facilities which offer generator based neutron activation analysis are dominated by requests for oxygen determinations.

3.5.3. Major/minor element measurements

In addition to oxygen, several other components present at major (percent levels) and minor (tenths of percent levels) concentrations are readily determined using generators in many matrices. Commonly determined elements using fast neutron induced reactions include: silicon $^{28}Si(n,p)^{28}Al$, nitrogen $^{14}N(n,2n)^{13}N$, aluminium $^{27}Al(n,p)^{27}Mg$, fluorine $^{19}F(n,2n)^{18}F$, phosphorus $^{31}P(n, 2n)^{30}P$ and perhaps iron $^{56}Fe(n,p)^{56}Mn$. In addition, thermalized neutrons are used in capture reactions to measure magnesium, manganese and others if present in sufficient quantities. Samples returned from lunar exploration in the 1970s were routinely measured for major/minor components using generator based NAA [53].

3.6. Online analyzers

FIG. 8. Commercial Cross-Belt Analyzer, using the PGNAA technique for the cement industry.

More than 400 on-line analyzers are operating in cement factories to monitor the composition of the raw material on the conveyor belts. They are commercially available from several manufacturers. A typical analyzer (sometimes called continuous neutron analyzers) is built up from a 14-MeV NG, a moderator (e.g. polyethylene), the belt with the material on it, and the detectors (typically scintillators) above it. A large housing accommodates the instrument, which serves as a shielding against the radiation. 20 s measurements are made and the spectra are collected by an MCA card in a computer. The spectra are compared to those of pure materials (SiO_2, Al_2O_3, $CaCO_3$ and Fe_2O_3), and the composition is determined from linear combination of the library spectra. The great advantage of this method is that the irradiation averages about 90% of the raw material, while conventional sampling covers about 10^{-4}%. Most recent facilities prefer NGs because they can be switched off. There are a few requirements: the conveyor belt must be free of chlorine and iron, the loading usually should be kept between a minimum and a maximum level. The unit has to be cleaned from dust regularly. The reproducibility of the measurements proved to be proper for the quality control of the production. The experts find the on-line analyzers indispensable tools for raw material production in cement factories [54] (see FIG. 8 and FIG. 9).

FIG. 9. SODERN Neutron analyser on a cement plant conveyor belt – Allmedingen, Germany (Schwenk Courtesy).

Another type of on-line analyzer has also been developed. This one analyzes coal as it moves through a coal chute for continuous control of coal quality in power plants. O and C is measured based on the fast neutron reaction. Neutrons are thermalized by the large volume of

carbon, thus prompt gammas from thermal neutron capture in H, S and Cl can also be measured. Delayed gammas from radioactive isotopes (such as ^{24}Na) are also collected. These three types of spectra (gammas from fast neutron reaction, prompt gammas from the capture of slowed down neutrons and decay gammas) are collected in three separate spectra using appropriate time windows. For the gamma detection a BGO scintillator and digital electronics is used. The prototype, installed on a trailer, was tried out using 8 loads of different coal samples with a mass of 600 kg each. The compositions were then compared to those from averages of several small samples taken from the load, and analyzed in chemical laboratories. The agreement was good [55].

3.7. Security

The application of NGs to security operations has been intensively studied and at least provisionally implemented over the last decades. Detection of explosive material, illegal drugs, chemical and nuclear weapons are all potentially possible using generator produced neutrons.

FIG. 10. The SODERN ULIS (Unattended Luggage Inspection System) system for inspection of suspicious object.

Interrogation of luggage or cargo containers for hidden explosives or illegal drugs is an area of extreme interest. In addition, monitoring and identification of high explosive weapons sometimes buried or underwater, is an application which requires non-intrusive methods development. Several approaches have been developed in which the oxygen, nitrogen and carbon concentrations and ratios are correlated to known ratios in explosive material as well as contraband [56, 60]. Thermal neutron analysis (TNA) uses thermal neutrons as the analytical probe, so the method can make use of isotopic sources, as well as 14 or 2.5 MeV generators. This can also be done using a pulsed generator (PTNA) which allows for the measurement of both prompt capture and decay gammas. This is sometimes combined with fast neutron analysis (FNA) which adds the capability of using inelastic scattering and other particle emitting reactions as well. FNA requires neutron energies of >6.5 MeV so only the DT generators are applicable. Several other variations of these methods are possible including pulsed fast neutron analysis (PFNA), API and specialized detection methods like time of flight and gamma resonance attenuation. The generator characteristics required for these

methods are variable and technique dependant, but in general there are applications for both 2.5 and 14 MeV NGs. While a great deal of development has occurred in the application of these generators to security operations such as airport locations and sea ports, rather few implementations are actually in use. This is an area of great potential utilization. APSTEC in Russia [17] and SODERN [18] have developed portable systems using API the typical capability of detection is one kilogram in one minute at 90 % probability of detection (see FIG. 10 and FIG. 11).

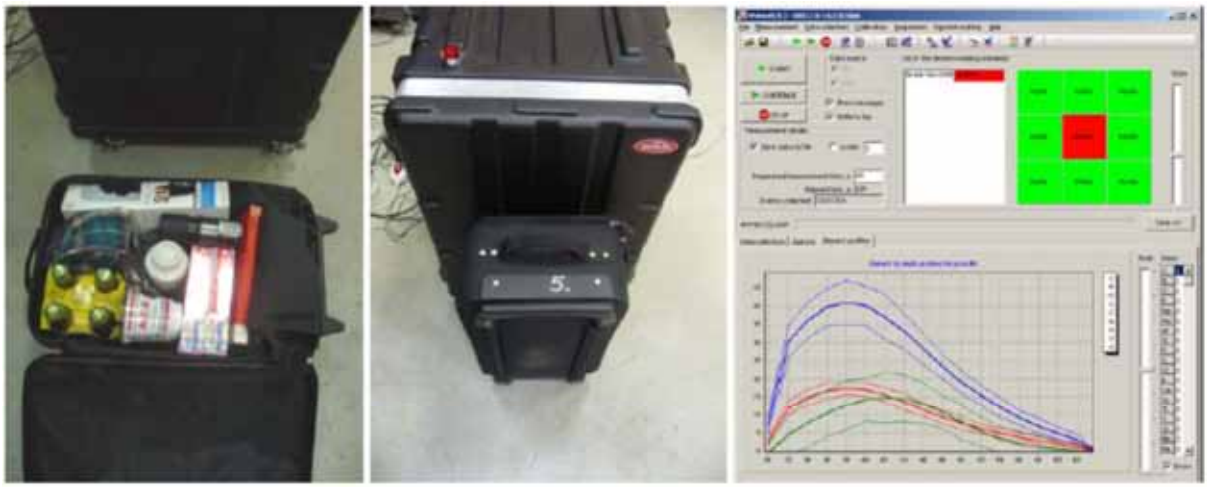

FIG. 11. Automatic detection of explosives' imitators in a suitcase by SENNA IV device. The samples in suitcase are shown on the left. The middle photo is the inspection geometry. The right screenshot represents the result automatically obtained by the device. The blue, red, and green lines represent respectively the concentrations of O, C, and N with respect to the depth of the measured sample.

Chemical weapon detection methodology is closely related to those discussed above. Inspection of recovered munitions which are likely to be without markings and monitoring for buried mines are areas of concern [61]. Elements of interest, depending on the weapon, include chlorine (primarily in old generation weapons), phosphorus (in new generation weapons), fluorine, nitrogen oxygen and hydrogen. High neutron energies are generally required for elements other than C, H and O. Prompt gamma activation analysis using isotopic sources is possible but, since all delayed as well as prompt gammas will be superimposed in the spectrum, sensitivity is poor. A pulsed fast neutron analysis system allows the separation of these spectra, but requires the use of a pulsed 14 MeV system.

3.8. Safeguards

Homeland security in today's world now depends on our ability to monitor our borders for the potential trafficking of special nuclear material. In addition, there is a need for sophisticated methods to locate hidden caches of nuclear material in locations being monitored to avoid the proliferation of nuclear weapon technology. Since most materials of interest are radioactive, passive measures are effective but suffer from the possibility of the material being easily hidden and long measurement times. Shielding readily reduces or eliminates characteristic radioactive emissions. The use of active neutron probes to induce fission reactions which result in delayed neutron emission or gammas from fission product decay has a distinct advantage. Most NG systems being studied for use in such a system are based on the DT

reaction [62]. However, since thermalization of the neutrons for increased reaction probability is required, DD generators should be applicable as well.

3.9. Art and archaeology

Art objects and archaeological artefacts are highly valuable samples, which are typically not permitted to investigate with destructive techniques. PGNAA and the use of inelastic neutron scattering (INSECT method) can be advantageously applied for the analysis of these precious objects, as they are non-destructive, and also because of the great penetration depth of both, the activating and the radiation. Because of the weak attenuation of high energy neutrons and gamma radiation these methods are not sensitive to the shape of the sample, or any packing, even covering soil or rust. The samples need no preparation before measurement, which might be of high importance in case of these objects. The result of the analysis will be an average of the irradiated volume, thus the neutrons “see inside” the sample.

3.10. Industrial applications

As mentioned in previous chapters, NGs are widely used in on-line analyzers of raw materials transported on conveyor belts, especially in cement factories [55, 55]. They all use thermalized neutrons, and are based on the detection of prompt gamma spectra by scintillator detectors. The 14-MeV NG could be replaced with the high flux DD generators as well. The real advantage however would be to use the 2.5-MeV neutrons for direct activation, i.e. without using any moderator. The inelastic scattering reaction, i.e. the INSECT method, as proposed by Yates [63], is capable of analysing all major components with the exception of light elements ($Z<10$). The analytical sensitivities for all the available elements are similar. Thus this method is an ideal tool for the analysis of major and minor components, and can be applied in the analysis of minerals, or any other materials with similar compositions (glass, cement or even for the pollutant analysis of coal).

Since hydrogen energy is forecasted as a realistic alternative for fossil fuel, a continuous research on storage and improvement of fuel cells can be expected. Prompt gamma neutron activation analysis is a well-established technique for in situ determination of hydrogen content and behaviour, and is generally seen as an important independent technique to e.g. gas analysis techniques. In combination with the large sample analysis approach, entire fuel cells may be analysed making the technique unique in its kind. NGs can provide adequate neutron fluence rates for prompt gamma analysis, competitive to those that can be obtained with nuclear research reactors. As such, industry may set-up its in-house PGNAA system for hydrogen determination.

3.11. Research

The reactions, induced by 14-MeV, as well as their spectroscopic data are well known since the 70s and 80s [4]. These 14-MeV neutron reaction cross-sections have also been compiled into the JEF databases [64, 65] and their updates, which have two fixed points in their cross-section curves, one at the thermal energy, and the other one at 14 MeV. Even the interfering reactions have been studied thoroughly [48]. However, a similar research could not have been performed for the reactions with 2.5 MeV neutrons because of the relatively poor performance of the earlier versions of DD NGs. The previously mentioned handbook tried to collect all the available information of the relevant analytical data on 2.5 MeV NG, but their accuracy and reliability is far from enough from the analytical needs.

The new generation of high flux 2.5-MeV NG opens a new field for basic research: with their help the cross-section with 2.5-MeV neutrons can be measured in a systematic way for all the elements. The accurate measurement of these nuclear data could serve a double purpose: on the one hand a third important point would appear in the cross-section curve, which would be of high importance in nuclear physics. On the other hand the accurate spectroscopic dataset could serve as a basis for chemical analysis, too.

3.12. Education

A NG is an excellent tool for the training of young scientists in various aspects of neutron generation and diagnostics and a wide spectrum of modern technologies, such as those related to ion sources, particle acceleration techniques, beam handling and diagnostics, magnet technology, vacuum techniques, detector technology, nuclear electronics, data acquisition as well as processing techniques. The new low cost, small scale NG facilities, suitable for a university or an industrial setting, provide a testing ground of instrumentation destined for use at a larger facility, improve awareness of the use of neutron probes in a wide range of applications and offer a training opportunity for future neutron physicists.

A well-developed training program using NGs will provide a more diverse portfolio of projects that might permit to attract innovative scientists, including those with multidisciplinary outlooks, establish the nuclear culture and support fundamental and applied research in the fields of neutron physics, isotope production and industrial applications.

The courses and practical training for the students should be organized, to a large extent, for preparing specialists in neutron physics both for the laboratory and for work in neutron centres. Lectures and experiments can be divided in four main categories:

(1) NG principles:

- design
- instrumentation
    - vacuum system
    - cooling system
    - high voltage supply
    - RF systems
- optimization
    - production
    - energy distribution

(2) Neutron Physics

- neutron transport calculations
- neutron spectrum characterization
- irradiation facility design

(3) Health Physics

- shielding
- dosimetry

- radiation protection concepts for the protection of workers involved in the use of NGs
- moderator design and optimization

(4) Applications

- principles of isotope production
- principles of activation analysis (RNAA, INAA, PGNAA, FNAA)
- principles of associated particle techniques
- principles of neutron radiography
- measurement of induced radioactivity
- measurement of gamma and neutron self-shielding

The above mentioned subjects are indicative and do not pretend being complete.

3.13. Medical and nutrition

In medical sciences DT NGs are being used for in vivo determination of the total body levels of the main elements e.g. calcium, nitrogen, carbon, oxygen, potassium, chlorine, sodium, phosphorus and hydrogen. The total body levels are routinely used for the diagnosis and therapeutic monitoring of diseases of the skeletal system or diseases involving nutrition.

3.14. Environmental and geological

The limited sensitivity of NG based activation analysis (if compared to reactor based NAA and other analytical techniques) sets the boundaries for applications in environmental research with a small group of elements like the determination of the total amount of the halogens in solid materials. NG based NAA has little to offer for environmental studies focused on elements of interest such as Hg, Cd, As, Cu unless these elements are dominantly present, e.g. in industrial waste streams.

Related materials such as recycled material (metals, plastics or mixtures thereof), waste rock piles, mine tailings, etc. are often inhomogeneous, raising difficulties in homogenization and/or subsampling. The analysis of large samples (a few kilograms) to determine the major element concentrations can be a solution to this problem. In the early 1990's, the laboratory for INAA in Delft developed an approach and facilities for reactor irradiation of large samples [66, 69]. The experience of this laboratory with large sample analysis can be projected on the situation with NGs. However some adjustments are needed concerning the design of the irradiation facility and the correction of longitudinal and axial fluence gradients. The large sample approach may also be considered to improve the sensitivity in trace element determinations.

Neutron Radiography is a powerful technique to make non-destructive images of materials containing relatively high amounts of water. The technique can be used in many different research areas. A few of them will be mentioned below. Nakanishi [70] and Yamada [71] applied the technique to image the water distribution in plant material. Neutron radiography is at the present time one of the main techniques able to meet the quality control requirements of explosive devices used in space programs [72], but it can also be used for inspection of oil levels and surface layers.

In geological prospecting, NG based NAA is applied for determining the major components in situ by using well logging devices. This type of work is usually subcontracted to specialized companies. It has been shown [73, 74] that NGs can be used for uranium determination using delayed neutron counting. An overview of the use of NGs in mineral exploration is given in Ref. [75].

3.15. Epithermal neutron activation analysis

Epithermal Neutron Activation Analysis (ENAA) is usually used for the sensitive analysis of elements having large resonance integrals (e.g. Mo, Ni, Au or U) in a matrix of elements with large thermal cross-sections (e.g. Na). When filtering out the thermal component from the neutron spectrum using the usual cadmium cover, the neutrons with the energy above 0.5 eV reach the samples, thus enhancing the sensitivity for some minor or trace elements. (N.B., the proper name should be epicadmium neutron activation analysis.) [9].

It was the activation with epithermal neutrons that drew the attention to the possible application of inelastic neutron scattering in elemental analysis. Mainly short lived isomers were investigated in this way [76, 77]. Alfassi [78] determined the sensitivities for a series of elements in the epithermal and fast neutron spectrum in a 2-MW research reactor. The thermal neutrons were filtered out using a 1 mm thick cadmium cover around the sample. This method proved to be efficient in eliminating a few interferences from typical major components (e.g. Na, Cl, Al).

3.16. Analytical application of inelastic scattering

Inelastic scattering of 14-MeV neutrons from a DT generator was first applied for elemental analysis in geophysics [79], especially for borehole logging [80]. Inelastic scattering of neutrons from a much lower flux DD generator could have been used only in the case of iron determination in iron ores [81].

An analytical technique has been developed at the Van de Graaff laboratory at University of Kentucky based on inelastic scattering of monochromatic fast neutrons [63]. The authors used large volume Ge(Li) detectors for the detection of γ rays instead of the previously used scintillators. The higher resolution of the Ge(Li) detector makes possible the identification of more gamma lines, thus enabling a multi-elemental analysis. However these detectors are much more sensitive to neutrons, which may cause damage in their crystal structure, worsening the resolution of the spectrometer. The neutron source was pulsed in the nanosecond time scale, enabling a time of flight analysis of the signals, thus enabling the discrimination between neutrons and gamma photons. The bombarding energy of the neutrons was varied and adjusted to the actual measurement.

A beam of protons (or deuterons) produced by 6.5 MeV Van de Graaff accelerator were pulsed at a rate of 2 MHz with a pulse width of 10 ns. Mono-energetic neutrons are produced using the $^{3}H(p,n)^{3}He$ reaction providing neutrons with continuously variable energies up to 5 MeV. Higher energy neutrons were generated using the $^{2}H(d,n)^{3}He$ reaction.

The samples were located at a distance of 6.3 cm from the target cell. A 15% relative efficiency Ge(Li) detector was placed about 80 cm from the sample to detect the emitted gamma radiation. The detector was shielded from the direct neutron radiation using a tungsten bar. All measurements were made at an angle of 125° relative to the neutron beam, at this angle the number of scattered neutrons is the lowest. The counts were normalized to the signal

of a neutron monitor. To decrease the background counts in the spectra, the neutron signal was discriminated from the prompt gamma peaks.

Varying the bombarding energy of the neutrons, the selectivity of the method could be modified. With the increasing neutron energy the levels of more and more elements can be excited. The optimum neutron energy was found to be 0.5–1 MeV higher than the first excited state in a given nuclide. The optimum energy for general multi-element purposes was found to be 2.5 MeV, i.e. the energy of the DD generator.

The proposed method is a bulk analysis method. The examined alloy and metal powder samples had masses of about 50 g, and they generated count rates of about 2000 cps in the Ge(Li) detector. Detection limits for a series of elements were also determined for the bombarding energy of 2.5 MeV. They were found to be around 1 g.

Calibration curves were also determined using metal powders containing 1% to 100% Cr and Ni. The count rate vs. metal mass plots was found to be linear, which means that the method is really matrix free even at this large sample masses. The method was validated using metal alloy reference materials.

CHAPTER 4
APPLICATIONS OF PROMPT GAMMA NEUTRON ACTIVATION ANALYSIS USING RADIOISOTOPE NEUTRON SOURCES

4.1. Principles of a prompt gamma neutron activation analysis setup

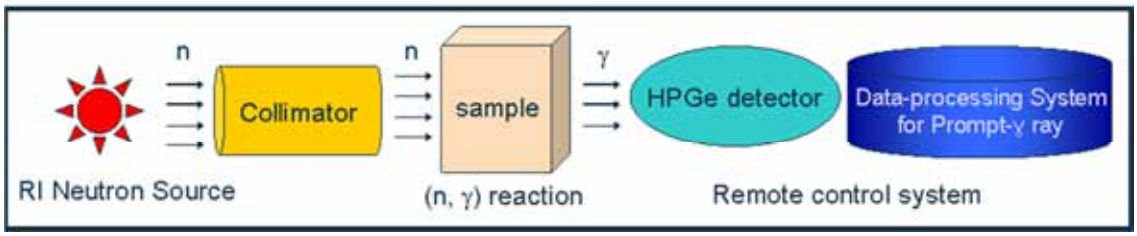

FIG. 12. A schematic setup for a PGNAA system based on a radioisotopic neutron source.

A PGNAA system can be simply assembled by components as shown in Fig. 12. Excited nuclei produced by an irradiation of neutrons emit secondary γ rays, which are characteristic of certain elements. Detector arrays around the inspected object collect the elemental signals that are processed by an electronic data acquisition system [82]. PGNAA is a non-destructive radioanalytical method capable of rapid, in situ and simultaneous analysis for traces and major amounts of various elements. The quantity of the constituent elements is determined by comparison of the γ ray intensities per unit time with the same of known composition calibration standards [83].

4.2. Radioisotopic neutron sources

So far, alpha emitters (^{241}Am or ^{238,239}Pu) embedded in Be and ^{252}Cf are known as radionuclide neutron sources for PGNAA. The former goes through ^{9}Be(α, n) ^{12}C reaction while the other is the spontaneous fission source. For many PGNAA studies, thermal neutrons are used. Therefore, ^{252}Cf source, which has average energy of 2.35 MeV are more popular than Be(α, n) sources, which emits 4.4 MeV neutrons. However, for determination of O and C, higher neutron energy is needed [84].

Californium-252 was immediately realized as a spontaneous source of neutrons after it was discovered in 1952 in thermonuclear test debris, and 40–80 μg of ^{252}Cf for a prototype TNA was used to confirm the presence of mines [85]. ^{252}Cf, with a 2.638 yr half-life can produce up to 10^{11} neutrons s^{-1} in a very small volume [86]. The fast californium neutrons can be moderated to thermal energies by either an external moderator or through moderation on the sample itself. However, thermal neutrons are an approximate categorization according to its energy of 0.003–0.4 eV. ^{252}Cf is normally used as a portable, non-reactor based source of neutrons for lower flux applications, and larger sources of ^{252}Cf can also be used for neutron radiography comparable to the potential of a reactor.

Γ ray spectra can be generally obtained using neutron beams from reactors (including cold neutrons), NGs and radiation sources. In this review, however, the applications of PGNAA using radioisotope neutron source will be discussed.

4.3. Non destructive multi-element analysis using prompt gamma neutron activation analysis

Almost all chemical elements emit characteristic γ rays after neutron capture within 10^{-12} s. The prompt γ rays (2–10 MeV), are detected by high resolution γ ray spectrometers. Qualitative and quantitative analysis can be performed by the position of the characteristic peak and its net count, so over a hundred applications are quoted in chemistry, materials science, geology, archaeology, industry, agriculture, environment, biology, nuclear technology and other fields.

4.3.1. Measurements of coal or oil quality

The group at Science Applications Inc., (SAI), Palo Alto, California, USA obtained spectra from a Pittsburgh #8 coal sample with ^{252}Cf source irradiation. More than ten elements such as C, H, N, S, Al, Si, Ca, Ti, Fe, Na, K and Cl were identified. Hydrogen and iron provide a good response, but carbon does not. However, carbon concentration in coal is high enough to be detected. Determination of the elements in coal or lignite was possible within 15 minutes using 200 μg of ^{252}Cf source with appreciable accuracy [87].

At the beginning, borehole logging was used to determine porosity, density, moisture content, etc. and later, was used with PGNAA for in situ elemental analysis for ore, mineral industries, or oil exploration as an environment friendly technique [88–90].

4.3.2. Environmental pollution studies

PGNAA is very sensitive to toxic elements such as Cd and Hg, which are useful for environmental pollution studies, so it was employed to analyze environmental samples by PGNAA alone or combined with other methods. Neutrons into the soil are thermalized and then captured by soil contaminants and normal soil constituents. Detection of buried materials and determination of the concentration of such materials or contaminants in soil were done by PGNAA using portable, radioisotope based instruments [91].

Liquid sample (500 L) taken from Bahr Elbakar site at Manzala Lake in Egypt was investigated for 7h by PGNAA with a ^{252}Cf isotope neutron source with activity of about 500 MBq. As a result, about 60 γ ray lines were detected and identified [83]. As described in the following, a Neutron Induced Prompt Γ ray Spectrometry (NIPS) facility was set up at the Nuclear Chemistry Research Division, of the Korea Atomic Energy Research Institute (KAERI) too (see Fig. 13).

The neutron production of ^{252}Cf is 2.34×10^6 n · s^{-1} · μg^{-1}. A 5.4 mCi (10.4 μg) ^{252}Cf neutron source was used in the facility. The source is housed in a cylindrical stainless steel drum of 90 cm diameter packed with high density polyethylene blocks. In the middle of the drum there was an elevating device used to raise the neutron source to the top of the drum by pneumatic pressure. The drum was set on a 4 wheel mobile table; stainless steel sheet, and a 5 cm thick layer of lead on the steel sheet covered the top of the drum. The shielding geometry of the storage canister for the ^{252}Cf neutron source was verified by MCNP-4B calculations. The dose rate at several points as well as the container surface was estimated for a storage canister with a ^{252}Cf point source located at the centre of canister of cylindrical shape. The storage canister was made with a 45 cm radius polyethylene cylinder. Additional lead bricks of 5 cm thickness were installed in front of the canister to meet safety regulations, which were proven by theoretical calculation using the MCNP-4B code. The NIPS system facility has been also used as a radio analytical tool for determining the presence and quantity of elements in liquid samples [92].

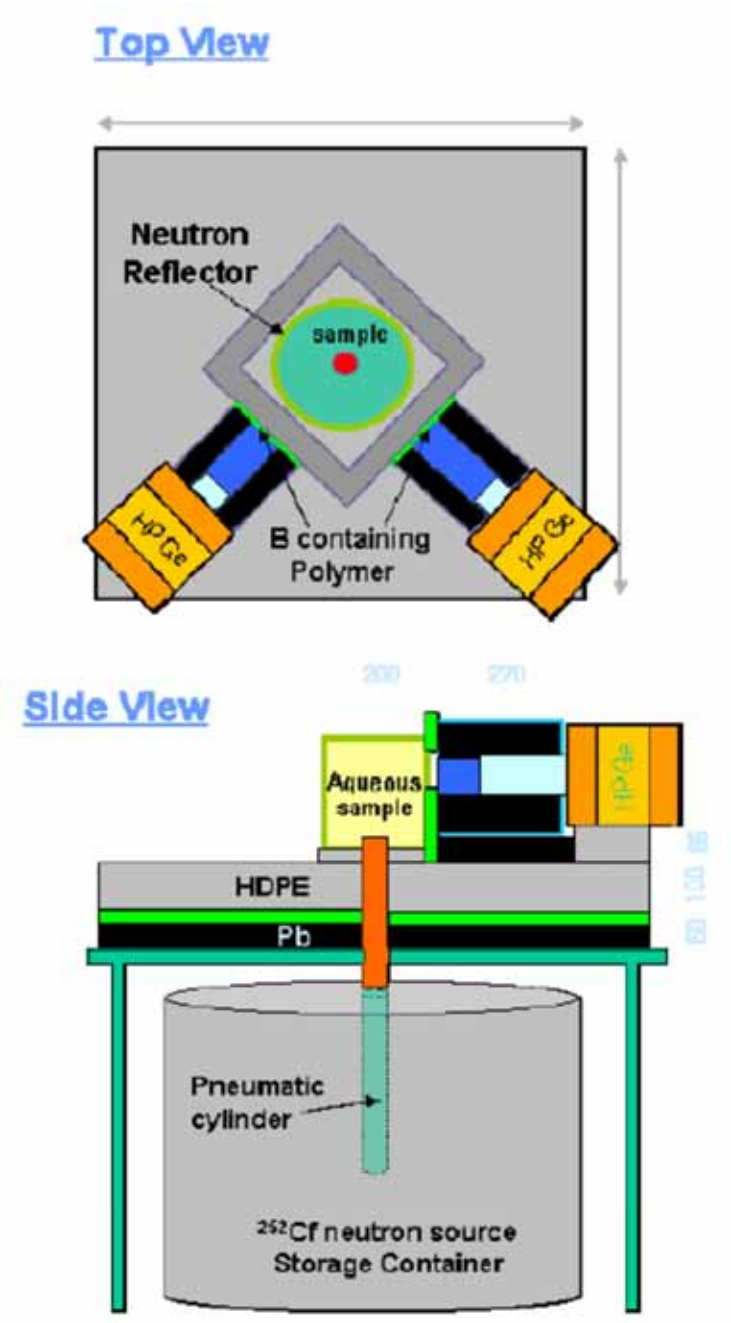

FIG. 13. Schematic diagram of a Neutron Induced Prompt Γ ray Spectrometry (NIPS) facility developed at the Nuclear Chemistry Research Division, of the Korea Atomic Energy Research Institute (KAERI).

From a filter of an aircraft flying across an area of a coal fired power plant fly ash concentrations of 16 elements such as Si (34 w%), Al (20 w%), Fe (3 w%), Ca, Ti, Na, K, and S (all between 0.1 and 2 w%) were determined [93]. Concentrations of Si and Ca in concrete, cement and sand by chemical methods were analyzed and were compared with the Si/Ca concentration obtained from PGNAA using an Am/Be source with activity of 185 GBq (5 Ci). Good agreement between the two methods was obtained thus demonstrating the possibility to use neutron analysis to characterize concrete composition [94, 95].

4.3.3. Detection of chemical weapons, explosive materials and various narcotics

Nitrogen is a major element in explosives, chemical warfare agent (CWA), and various narcotics. Although the concentration of nitrogen is a good indicator of explosives, the combinations of oxygen, hydrogen and carbon should be considered as well. An IAEA Technical Meeting on "Neutron Generators for the Detection of Explosives and Illicit Materials" was held in Vienna from 13–16 June 2005. It was concluded that the use of neutrons is difficult for the first stage screening of illicit drugs, explosives and CWA in the subkilogram mass range in any configurations, mainly due to time and sensitivity constraints. In the 10–100 kg mass range fast neutron and gamma radiography is a very promising technique for illicit materials (drugs, etc.) in air and sea containers

In recent years, considerable effort has been directed toward detecting the elemental compositions of explosives by means of thermal neutron interrogation, which involves exposing baggage to slow neutrons having an energy in the order of 0.025 eV [82, 96, 100]. NIPS facility at KAERI has been also used for PGNAA to distinguish explosives from non-explosive materials [82] by irradiating them continuously with neutrons. The detected 10.83 MeV from nitrogen γ rays can be also tomographically analyzed to screen suspected materials in baggage for airport security [101].

4.3.4. Medical application

Boron determination is difficult by other analytical methods, but high cross-section of boron for producing the 478 keV gamma line of ^{7}Li by neutron irradiation provides non-destructive submicrogram analysis. A PGNAA system has been applied for the boron neutron capture therapy (BNCT) to determine ^{10}B concentration in biological samples. ^{10}B(n, α)^{7}Li reaction is used for BNCT, and the emitted alpha particles play decisive role to cure a tumour cell selectively. Satisfactory results in determining ^{10}B concentrations in human tissues during the BNCT treatments for the brain tumour at many places have been reported [102].

PGNAA for total body nitrogen (TBN) was first applied for in vivo human body composition studies at Birmingham, UK. A patient was exposed to a neutron dose from an isotopic neutron source and the resulting 10.8 MeV γ rays were detected from the ^{14}N(n, γ)^{15}N reaction [103]. The total body hydrogen (TBH) measured at Brookhaven National Laboratory (BNL) with a single ^{238}Pu–Be neutron source (2.8 TBq, 75 Ci), was used as an internal standard [104].

4.3.5. Industrial purpose

A Sino-American Cooperation group developed an on-line thermal Neutron Prompt Gamma Analyzer for the analysis of alumina pulp in the aluminium industry. The neutron prompt gamma on-line element analyzer produces fast, automatic, consecutive, widely representative, and reliable results in real time [105, 106].

CHAPTER 5
DESCRIPTION AND OPERATIONAL REQUIREMENTS OF NEUTRON GENERATORS

5.1. Deuterium–tritium and deuterium–deuterium Penning diode generators

The most widely used and available generators are based on Penning Ion Source technology. This ion source technology has proven itself over the past few decades to be robust in the sense of a given neutron tube being able to run in either continuous mode or pulsed mode. If in pulsed mode, a tube can typically span frequencies ranging from 10 Hz to 20 kHz, with a range of duty cycles between 5% to 95%. These characteristics make the technology suitable to a broad range of applications with modest power needs.

There are two main drawbacks of the Penning ion source technology. The first is achieving less than maximum possible yield at a given accelerating voltage because the majority of ions produced are diatomic, which divides the acceleration energy over two nucleons. The second is a dependence of pulse shape on the duty cycle and pulsing frequency. Commercially available NG based on Penning technology are commonly available in either DT or DD versions. Those with DT range in yield from 10^7 to 10^{10} n/s, while those with DD range from 10^5 to 10^8 n/s.

The basic design of a modern compact Penning diode NG (see FIG. 14) consists of a source to generate positively charged ions and a diode structure to accelerate the ions (usually up to ~110 kV) to a metal hydride target loaded with either deuterium, tritium, or a mixture of the two. A gas control reservoir, attached to the tube and made of a metal hydride material, is used to store the gas. The most common ion source used in NGs is a cold cathode, or Penning ion source, which is a derivative of the Penning trap, used in Penning ion gauges. This simple ion source consists of a hollow cylindrical anode (usually biased 1–2 kV) with cathode plates at each end of the anode, usually at ground potential. An external magnet is arranged to generate a coaxial field of several hundred gauss within the ion source.

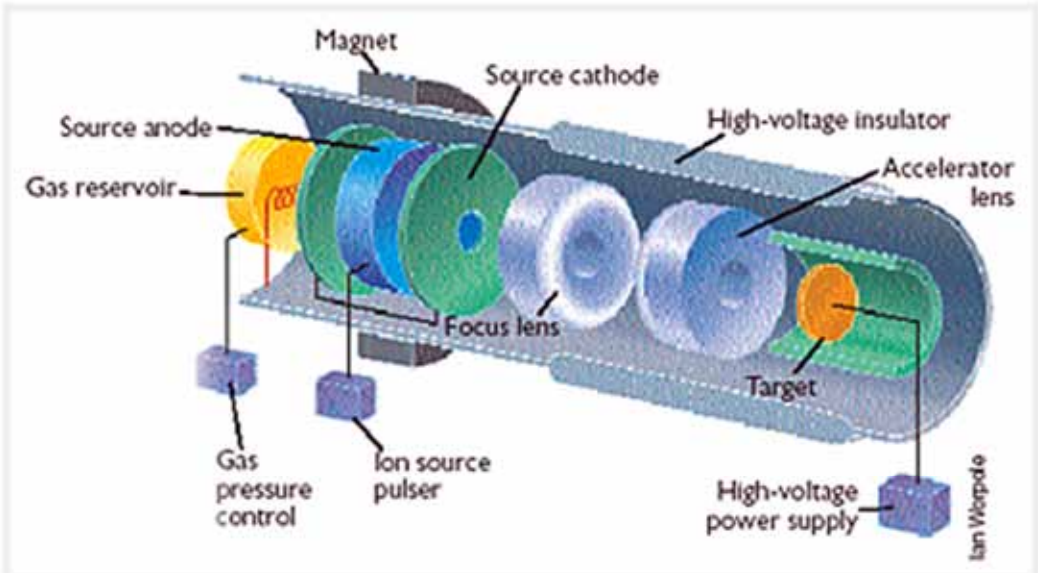

FIG. 14. A schematic illustration of the internal structure of a compact NG.

When deuterium and/or tritium gas is introduced into the anode at a pressure of about 0.1 Pa (10^{-3} Torr), the electric field between the anode and cathodes ionizes the gas. Electron confinement is established in this plasma because of the orientation of the electric and magnetic fields, which forces the electrons to oscillate back and forth between the cathode plates in helical trajectories. Although some low energy electrons are lost and strike the anode, which creates more secondary electrons, most remain trapped and ionize more gas molecules to sustain the plasma. The ions are not similarly trapped, and when they strike the cathodes, they also release secondary electrons, which enter the plasma and help sustain it. Ions, however, can escape the chamber into the acceleration section of the tube through a hole at the centre of one of the cathodes, called the exit cathode.

Construction methods used in building sealed neutron tubes include joining techniques such as welding, metal brazing, ceramic to metal brazing, and glass to metal seals. Materials used in accelerator neutron systems include glass, ceramics, copper, iron, different alloys of stainless steel, and Kovar. Most compact accelerator neutron tubes are loaded with approximately 10^{10} Bq of tritium; for comparison, a typical tritium exit sign used in an airplane or hotel might contain as much as 10^{11} Bq of the isotope.

5.1.1. Sealed source generator applications

Sealed tube NG are in routine use for a number of industrial applications for 40 years. The table below lists basic generator types and applications where they are used. Most of these applications take advantage of the fast neutron spectrum by looking for inelastic γ rays or fast fission γ rays produced by neutrons with more than ~8 MeV of energy. FIG. 15 shows that there is also information available between pulses characteristic of short and longer lived activation products. The number of applications focused on detecting and quantifying the presence of different elements in a variety of materials has grown, providing information for process optimization and control (see TABLE 4).

TABLE 4. APPLICATIONS AND ANALYSIS METHODS USING SEALED TUBE NG

Applications	Analysis Methods	Primary Elements Detected	Type of NG
Explosives Land Mines Chemicals Unexploded Ordnance Drugs Body Composition Minerals Explorations Bulk Materials	Inelastic Scatter Thermal Capture Delayed Activation	O, N, Ca, Si, Al, Mg, H, Fe, S, P, F, Cl, Hg, Cd, Pb, Ba, Th, U, Cr, Tc	Pulsed — Fixed installation — Portable — Subsurface
Transuranic Materials Fissionable Materials	Neutron Die-Away	U, Pu	Pulsed — Fixed installation — Portable — Subsurface
Oil Field Exploration and Exploitation	Neutron Die-Away Inelastic Scatter Delayed Activation	C, O, N, Cl	Pulsed — Subsurface

Usually, NG based systems can provide this information much more quickly than traditional laboratory solutions. Since fast neutrons often have a large effective range in most materials, of several tens of centimetres, neutron analysis of bulk materials also have significant advantages over laboratory techniques where sample collection and preparation is often problematic. For some cases such as nuclear waste assaying or explosives detection the non-contact, non-destructive and remote measurement capability that neutron analysis techniques allow are also advantageous.

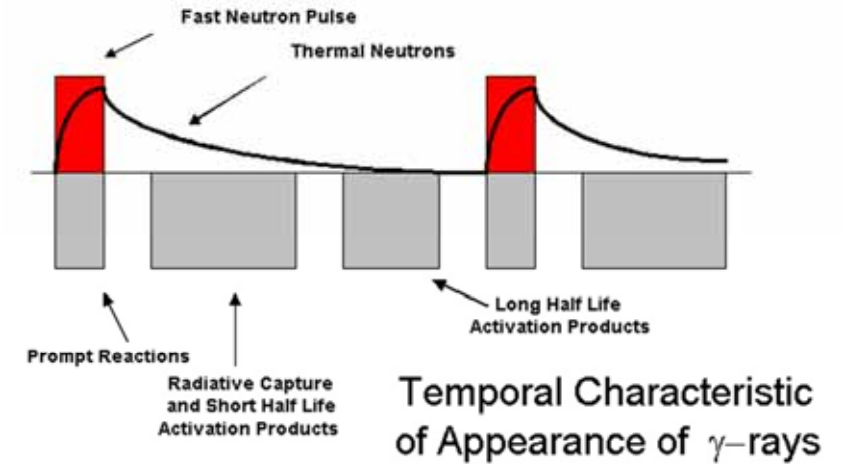

FIG. 15. Time domains of information available from a pulsed NG. A typical pulse has a width of 1–10 μs, which is represented in red. Repetition rates vary for each application. The most commonly found are in the range of 100 Hz to 100 kHz.

5.1.2. Potential overlap with test & research reactors

The traditional role for test and research reactors (TRTR) for teaching and material analyses relies on relatively high fluxes of thermal (less than 5×10^{-7} MeV) neutrons at levels of 10^{12} to 10^{14} neutrons $\cdot$ cm^{-2} $\cdot$ s^{-1}. NGs typically produce fluxes of fast (greater than 1 MeV) rather than thermal, and at flux levels ranging from 10^{5} to 10^{8} neutrons $\cdot$ cm^{-2} $\cdot$ s^{-1}. NGs output can be moderated to thermalize the flux, but this decreases flux and typically produces a high background of gamma radiation.

5.1.3. Industrial trends

In the area of homeland security, there is some activity to develop neutron based scanning systems for cargo and vehicles. High yield generators can be used for cargo inspection, but from a practical basis probably face obstacles from trade unions working in ports, because of radiation fears, and regulatory requirements that vary from country to country. Vehicle inspection applications would also require a high output neutron device, but this faces somewhat different obstacles. A vehicle inspection system would in theory need high output to cope with a quick analysis of a moving vehicle and a large standoff distance between the inspection system and the object under inspection. An isotropic device like a NG seems likely to be a non-starter because of the very radiation fields created everywhere in order to project enough flux out to a potentially moving vehicle. So while either of these applications could suggest the existence of market forces that would convince NG developers to invest in higher yield devices, current realities for either application temper the urge to invest.

Advances in sealed tube generators are focusing towards the development of modest output generators that are smaller, less expensive, low weight systems with longer lifetimes and higher outputs. Reduction in size and weight are particularly driven by the growing demand in the homeland security market for field portable applications while price, reliability and performance improvements are demanded by all markets. Also important are on-going advances in NG support systems such as the modernization of old analogue control systems to digital controls that incorporating advanced diagnostic routines and that can be remotely accessed for wireless operation and factory servicing and upgrading. Similarly, improvements in generator designs and power supplies have lowered the power consumption of these systems to allow longer operation while on battery.

5.2. Axial radio frequency induction plasma neutron generators

5.2.1. Generator structure and function

A new commercially available NG that also uses a simple diode to generate neutrons is the radio frequency induction (RFI) plasma NG. In this case, the deuterium ions are generated in a RFI plasma and accelerated across a DC potential towards a Ti target. The main components are located along a single axis, and tubes with this design are referred to as axial generators, as shown in FIG. 16.

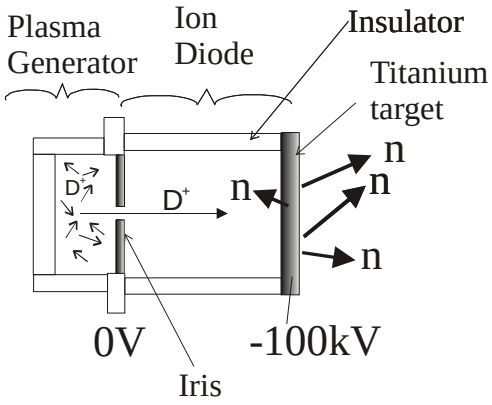

FIG. 16. Diagram of the principle components of the fast NG using the DD reaction.

Like the Penning diode, the RFI plasma NG is fundamentally a diode, but with a RFI plasma ion source instead of a Penning ion source. Also like the Penning diode, the RFI source uses a titanium target; however, the titanium is beam loaded in the initial few seconds of operation. Deuterium ions are generator in the RFI plasma and are accelerated across a voltage potential to the titanium target. The D^+ ions strike the titanium, and in the first few seconds of operation they form titanium hydride in the first few microns of the target surface. Subsequent deuterium ions fuse with D atoms of the hydride resulting in the DD reaction and emitting 2.5-MeV neutrons. Thus the generator's neutron emission is self-sustaining, the sealed penning diode which uses an impregnated target have the same properties. On the other hand, the RFI generator needs a compressed source of deuterium gas and an active vacuum system (e.g. turbo pump).

Previous generators of this type had various components exposed that were at high voltage potential, making the generator dangerous to operate. In the new design the high voltage is shielded by placing the entire accelerator structure and its components inside conflate

stainless steel piping (FIG. 17). The target and secondary electron shielding are inside and cooled through a unique insulator feed through structure.

FIG. 17. An axial RFI NG. The components at high voltage potential are shielded by placing the entire accelerator structure and its components inside modified conflate stainless steel vacuum pipe. Not shown are the generator's required subsystems (i.e. vacuum, cooling and power supplies).

These generators have been shown to be capable of yields of 10^8 n/s using an axial design and a DD reaction. Two new axial generators manufactured by Adelphi Technology Inc. are capable of yields of up to 10^{10} n/s. At the time of this writing, the DT reaction has not been attempted. A photo of a commercially available axial generator is shown in FIG. 17. A cross--sectional view of the 10^{10} n/s yield tube is shown in FIG. 18.

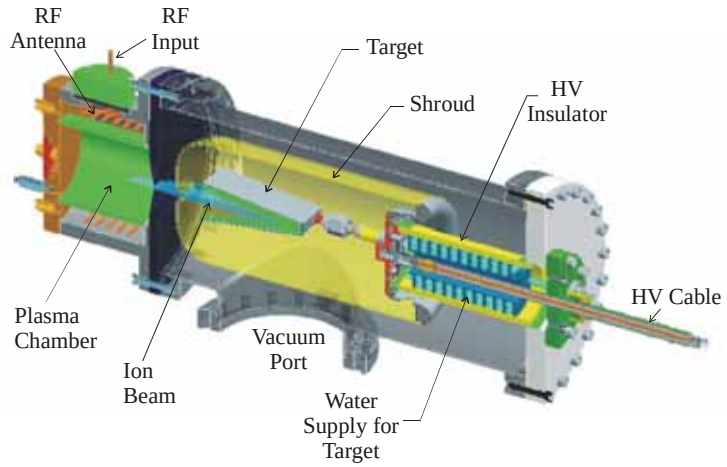

FIG. 18. The new 10^{10} n/s DD Fast NG.

5.2.2. Plasma ion source

The major innovation that makes these generators viable is the RFI plasma source [107, 112]. In the past, dielectric materials used in the NG with only moderate successful. The material of the discharge vessel was quartz, and, although quartz is an excellent dielectric material for

transmitting the radio frequency (RF) energy, its heat conductivity is poor. Thus, these ion sources were limited in operation power and were used only in a low duty cycle, or low power operation mode.

Incorrect coupling would also result in short lifetimes of these early ion sources for the NG. The capacitive coupling mode generates a high potential electric field between the anode (the metal front and back plates of the plasma generator) and the external antenna. This field accelerates ions towards the anode in the discharge chamber, resulting in sputtering of the metal from the back and the front plates of the source. The sputtered metal is then deposited on the inner surface of the dielectric plasma generator wall. When this sputtering continues for a while, it results in fully metalized inner surface of the plasma generator, shielding the RF fields from entering the source chamber from the external antenna coil, thus effectively stopping the source operation.

The correct RF coupling is done by using an impedance matching circuit to couple the RF power to the plasma. The purpose of the matching circuit is to match the 50-Ohm output impedance of the RF amplifier to the few Ohm impedance of the load, in this case the plasma. The basic design of the matching circuit is a tunable LC resonance circuit. Two distinctive features make this matching network design most suited to the external antenna driven plasma generator. First, the circuit is a balanced RF design. The antenna circuit is electrically isolated from the primary power feed. This minimizes the currents returning to the RF amplifier via the ground connection and the outer shield of the coaxial RF power cable, thus minimizing the radiative losses of the RF. The second distinctive feature is the use of a step down transformer in the matching circuit. This not only allows the balanced design of the antenna circuit, but also a fine tuning of the antenna circuit current and the resulting induced voltage in the antenna. Thus, the operator of the plasma generator is able to find perfect tuning parameters for the source without excessive antenna voltages, and without ion induced sputtering in the source.

Another innovation is that the RF antenna is outside the plasma. Two RFI D ion sources have been developed for the axial generators, one with (1) a solenoid antenna coupling and another with (2) spiral antenna coupling. In both cases, the RF power is coupled by an antenna that resides outside the plasma chamber. The RF is couple either through a ceramic cylinder or through a dielectric window in another. Having the antenna outside the plasma chamber prevents corrosion of the antenna, which occurred previously even when it was dielectrically coated. In previous internal antenna designs, water leakage could occur since water was being recirculated inside the antenna. Water contamination would be particularly dangerous if radioactive tritium gas were being used and, if a leak occurred, absorbed into the water.

5.2.3. Target

For neutron imaging, a bright neutron source is desirable. This means, that for a NG the beam spot size on the target has to be small and the beam power has to be high. In case of flat target, this leads to high surface temperatures and low neutron yield. Another improvement of previous designs is that of the conical target, which permit gives larger surface area for the D^+ ion beam to strike, while still giving an apparent small apparent source size along the generator axis. When viewed along the axis of the generator the fast neutrons appear to be coming from the small circular base of the cone. The shape of the cone increases the cooling surface area of the target, allowing a small beam spot size on the axis of the NG.

The brightness of the neutron source is primarily dependent upon the amount of deuterium beam power that can strike the Ti target. However, the maximum power density depends upon the maintaining the titanium hydride in the target and preventing the evaporation of the deuterium ions so that the DD reaction can continue with subsequent impinging D+ ions. Maximum beam power values of 500 W/cm^2 have been estimated.

The flat target can be altered to another geometry (e.g. tilting the target) so that the apparent source size when view from a particular direction is small. Conical and wedge shaped geometries can also be used to shrink the apparent source size. For example, if we wished a neutron yield of 10^9 n/s, a source size diameter of 3 mm would require a 10 mA of beam current and 120 kV of acceleration voltage. For flat target this would mean a beam power density of ~14 kW/cm^2. If a cone shape target is used the power density at the surface can be made to be less than 500 W/cm^2. Beam powers of up to 6 kW can be cooled with water using a high voltage feed through structure developed for the axial RFI NG (see FIG. 17).

The target cooling water hoses are coiled around the HV cable inside the insulator. The cooling water is of low conductance and, hence, there is a high resistance in the direction of water flow, and only a low leakage current can flow in that direction, minimizing possible HV breakdown.

5.2.4. Shroud

Secondary electrons are generated when the ion beam strikes the target. They are generated by ionizations at the target interface and in the beam column. Because of the potential difference between the target and the plasma source iris, these electrons attempt to stream back to the iris and around its aperture. They can be stopped or filtered out by surrounding the target with a metal shroud biased to be slightly more positive (e.g. 100 V) relative to the target potential. This biasing is done using a Zener diode embedded inside the insulator column. The shroud for the DD-110 generator is shown in FIG. 18.

5.2.5. Support systems

The systems required to drive the RFI plasma NG are shown in FIG. 19. These are a High Voltage Power Supply, an RF Power Supply, a RF matching Network, two Water Chillers, Gas Supply, and Turbo Pump.

- **High Voltage Power Supply**. A NG using the DD reaction makes up for its lower efficiency compared to the DT sealed sources by using a higher current HV supplies. For a yield of 10^8 n/s, a power supply of roughly 500 watt is required; for 10^{10} n/s, a 6 kW supply is required. Both these supplies would operate at 80–120 kV. Thus expensive and large supplies are needed as one increases the yield. Operating at higher voltage increases the yield, but not linearly with voltage as it is with current and voltage breakdown becomes more likely with increased voltage above 120 kV.
- **RF Power Supply and Matching Network**. An RF Power Supply of 13.5 MHz of approximately 2.5 kW is more than adequate for all three generators. As described above, the impedance of the RF supply is matched to the antenna's impedance via an RF Matching Network. Thus, when the source is first turned on, the impedance matching network must be tuned to maximize the forward, and minimize the reflected RF power. However, once this is achieved no further tuning is required.
- **Water Chillers**. Cooling for the target is obtained using a water supply that both cools and de-ionizes the water using a series of filters. Since the target is being cooled and is

at a high potential voltage (e.g. 120 kV) the cooling water must to de-ionized in order to have a high resistance. Cooling of the RF supply, matching box inductors and plasma chamber must also be done and is accomplished by using a single 2 kW chiller.

— **Turbo Pump and Gas Supply**. Since deuterium gas is constantly being fed into the RFI plasma ion source, the generator must be differently pumped to remove the gas. To prevent high voltage breakdown there has to be a vacuum level in the high voltage section. The gas pressure in the plasma chamber must be maintained at about 0.1 Pa (10^{-3} Torr). The plasma pressure is adjusted by a motor controlled precision valve on the deuterium gas source. The vacuum is maintained by a turbo and roughing pump, which are continuously operating. Since the operation of the DD NG does not require the use of any radioactive gases, it can be vacuum pumped by conventional pumping methods.

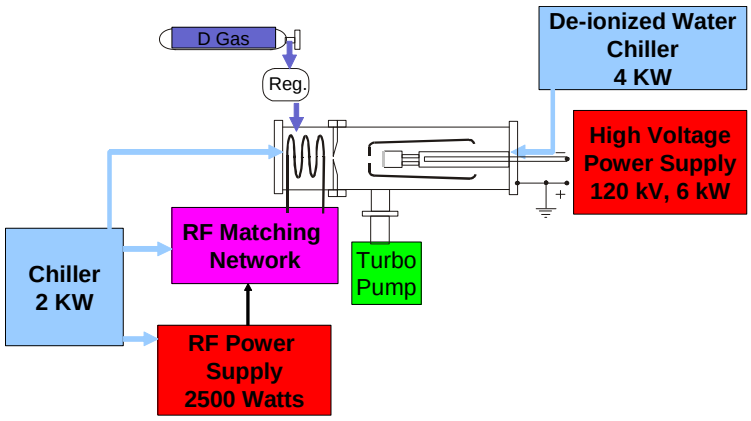

FIG. 19. The support systems for the NG. The power and voltage requirements are for the DD-110 generator.

5.3. Inertial electrostatic confinement sources

The inertial electrostatic confinement (IEC) concept also known as the Farnsworth-Hirsch Fusor, or Fusor, was originally conceived by Philo T. Farnsworth during his research on vacuum tube designs for television in the 1950s [113]. In the 1960s his associate, Robert Hirsch, improved the initial Farnsworth design by constructing a system with concentric inner and outer spherical electrodes, set in a large container filled with a dilute fuel gas of deuterium and/or tritium [114]. The corona discharge of the outer electrode provided the source of ions, which were drawn to and passed through the inner, negatively charged electrode to a central reaction region. The positive ion sheath at the inner negative electrode acted as an electrostatic barrier to contain positive ions in its interior. However, positive ions from the outer electrode however are accelerated from the outer electrode easily penetrated the inner electrode and its positive ion sheath. The collection of hot positive ions in the centre and cooler positive ions about the inner electrode created the necessary plasma temperature and pressure to allow fusion.

Generically, the IEC device confines plasma in a potential well, which is created by electrostatic fields or combination of electrostatic and magnetic fields. The fields are produced either by grids or by virtual cathodes, usually in a spherical or cylindrical geometry. The fields accelerate the ions toward the centre of the sphere or cylinder, where fusion occurs. Hirsch constructed an a 24 inch diameter IEC, which produced a steady state neutron yield of

2×10^{10} n/s since the late 1960s [115]. The University of Illinois IEC N-Device, which has a 55 cm diameter with an inner grid diameter of 10 cm, produces a steady state, DD neutron yield of 2×10^{7} n/s [116]. The IEC is useful for practical neutron sources. However, the existing IEC fusion devices have low fusion yields that are 0.01% of the input power, because the Coulomb collision cross-section is much greater than the fusion collision cross-section by several orders of magnitude. That is, the ion beams in the IEC devices rapidly lose energy by Coulomb collisions before producing fusion reactions, and this leads to a net loss of its energy [115]. The relative simplicity of design and construction, and low cost, as well as the allure of fusion have attracted and allowed many amateur individuals and groups to construct Fusors [117].

Presently, IEC research and development for fusion and neutron source applications is being pursued by the University of Wisconsin, Fusion Technology Institute [118], the Fusion Studies Laboratory at the University of Illinois at Urbana [119][120], the Los Alamos National Laboratory [121][123], and the NASA Marshall Space Flight Center for advanced space propulsion concepts [124]. Also, several Japanese University groups, coordinated by Yoshikawa of Kyoto University [125], directed IEC research toward the development of a NG for landmine detection, with participation by The University of Sydney in Australia led by Khachan [126]. There have been five US–Japan IEC workshops in the last 10 years, with the latest one at Argonne National Laboratory May 22–24, 2007.

The US IEC research is focused on the production of protons and neutrons for detection of clandestine materials, radioisotope production, and long range goals of electricity production and space propulsion, whereas the Japanese and Australians are focused on development of a neutron source for landmine detection. All the groups use DD fuels at voltages of up to 80 keV to produce neutrons. The University of Wisconsin uses voltages of up to 170 keV to produce D–^{3}He protons [118]. The Los Alamos National Laboratory explores the periodically oscillating plasma sphere mode of IEC operation [123]. In regard to DD neutron generation, which is produced by the typical IEC university laboratory devices, the neutron source diameter is approximately 10 cm, and the neutron yield is about 10^{8} n/s. However continued improvements of IEC based neutron sources may make them commercially viable in the future.

On November 9, 2006 Robert Bussard gave a Google Tech Talk on his fusion research experiments at Energy Matter Conversion Corporation (EMC2) in San Diego, CA which is a good overview of the history and principles of IEC [127]. Also, Brussard presented the Polywell IEC concept discussed in a paper by Krall in 1992 [128] and patented by Brussard in 1992 [129]. The Polywell IEC is an IEC with a polyhedral configuration, where magnetic coils are placed on the edges of the polyhedron so as to create a quasi-spherical magnetic field which can better contain the plasma at the device centre leading to a non-local thermal dynamic equilibrium. This better containment of the plasma causes an increase in ion density, velocity, temperature, and collisions, as well as an increased DD cross-section for fusion, and thereby increases the rate of fusion. The paper notes the Polywell IEC uses “low technology” engineering compared to a tokamak. The physics of the IEC is very complicated, however, the IEC is small, cheap, and quick to build compared to a tokamak [127]. The EMC2 company founded by Brussard received $10M from DARPA in the 1990s and an additional $20M support from the Navy from 1992–2005 to pursue research and development of the Polywell IEC. In 2005 the WB-6 IEC device (30 cm in diameter) built by EMC2 and funded by the US Navy, produced 2.5×10^{9} DD fusions per second [127]. Budget constraints forced the Navy to stop funding of the Wb-6 IEC project, and this project was shut down at the end of 2005.

CHAPTER 6
INSTRUMENTS AND SYSTEMS

6.1. Overview

6.1.1. Isotope based systems

Isotope based systems have the potential to be used for activation analysis applications located outside scientific laboratories, such as field logging and on-line measurement in industrial plants. Consequently, these sources generate a relatively low neutron flux compared to that available from reactors.

The principal isotopic sources used are ^{252}Cf and ^{241}Am–Be (or occasionally other α-Be sources). Neutrons generated by ^{241}Am–Be sources produce prompt γ rays by both, neutron inelastic scattering and thermal capture reactions. In contrast, the substantially lower energy distribution of ^{252}Cf neutrons tends to create activities generated only by thermal capture. Detection of delayed activation analysis reactions is difficult in most cases because of the substantial irradiation times required.

The advantages of a radioisotope source are its predictable behaviour and relatively low capital and operating costs. Disadvantages are primarily occupational, health, safety & environment (OHSE) related issues, such as disposal costs and the potential for radiation exposure. Isotopes have been used in activation analysis for many years and extensive literature on the subject is available. Details of the relevant physics and some examples of industrial applications can be found in Refs. [130, 135].

6.1.2. Reactor based systems

In this limited space it is impossible to give an adequate account of the great variety of reactor based systems for neutron activation analysis, already differentiated by applications, half-lives of the activation products and available neutron fluxes. An excellent overview of the present state of the technique is given, e.g. Ref. [136] while basic information on NAA may be found in Ref. [9].

Instead, a rather specific system for NAA of short lived isomeric transitions at a small research reactor is described briefly as it shares some peculiarities with accelerator based systems, namely low fluxes and mainly short lived activation products, for which it offers viable solutions.

Low neutron flux is compensated to a certain extent by an above average sample size of 5 ml as well as by the possibility to use the rabbit system in the cyclic mode of operation. Short half-lives are taken into account by a transport time of the rabbit system of 250 ms, for a distance of 15 m, and a high counting rate gamma spectroscopy system with real time correction of counting losses.

Fully automatic operation at a high sample throughput is made possible by a sample changer, and a software system calculating elemental concentrations immediately after the measurement by means of a list of specific saturation activities of all activation products under consideration. This list may be determined experimentally, by means of standard reference materials, or calculated from system parameters, by means of the IAEA_k_0 program. References of two recent papers [137, 138] describing the system in more detail are given below.

Further, a paper of 1984 is cited [139], already describing a high rate gamma spectroscopy system with real time correction of counting losses, and a fast rabbit system, for neutron activation analysis of short lived isomeric transitions. The system is based on a 14 MeV NG.

6.1.3. Accelerator based systems

Accelerator based NGs are also powerful tools fast, easy and accurate analysis of important element and hence, complementing reactor NAA. Four types of accelerators can be used for generating neutrons, such as sealed tube, electrostatic accelerators, cyclotrons, and linear accelerators [140].

Radiofrequency quadrupoles (RFQ) linear accelerators or drift-tube Linacs or a combination of the two are potentially a very good solution to the delivery of large beam currents at energies of a few MeV. NGs based on the compact linear accelerator can produce from 10^8 to more than 10^{13} n/s using either proton or deuteron beams to bombard beryllium targets [141].

These generators can replace conventional sources in non-destructive testing applications such as thermal or fast neutron radiography, and can also be used for cancer therapy. They exhibit long lifetimes at full output, as there is little target or beam degradation. Since they do not use radioactive materials, licensing requirements are less stringent than for isotopic sources or tritium sealed tube generators. These pulsed systems based on the RFQ accelerator are well suited for applications requiring a high peak neutron flux, including activation analysis of very short lived reaction products. Problems related to the optimal use of accelerator based NGs were reported and one of important problems is a human factor; the skills and the experiences of the technical staff in laboratories [142].

The choice of NAA technique as a very effective method of training scientists in basic and applied nuclear research led to the purchase of two KAMAN A-711 NGs for two research centres in Nigeria, namely, the Centre for Energy Research and Training, (CERT) in Zaria, and the Centre for Energy Research and Development (CERD) in Nsukka [143].

6.1.4. Neutron generator based systems

Various types of NG based systems for activation analysis as a replacement and/or alternative to reactor and isotope based systems are developed to compensate the disadvantages of isotope and reactor based systems.

Proven analytical techniques such as NAA and PGNAA could be possible in a non-reactor based activation facility. High enough neutron fluxes for analytical purposes are now achievable with an incoming new generation of DD NGs. For this system several factors such as generator supplies, radiation shielding, sample preparations and gamma spectrometer should be considered carefully. In view of all of these considerations, a large generator based activation facility can be compared with a small research reactor, without the requirement of complicated nuclear regulation restrictions of it. For most of universities and non-reactor trained research institutions those kinds of systems could be an option for beginning on nuclear analytical techniques. Some aspects regarding technical progress and various fields of application are still under development.

6.2. Technical considerations for neutron generator based systems

6.2.1. Technical considerations – the move to neutron generators

There is a need for the development of a NG based system for activation analysis as a replacement and/or alternative to reactor and isotope based systems. Isotope based systems suffer from both technical and commercial limitations:

- The source cannot be pulsed.
- The maximum available flux is low compared to reactors and generators.
- Purchase prices and disposal costs are escalating and it is becoming harder to buy new sources.
- "It is essential that activities involving radiation exposure, such as the production and use of radiation sources and radioactive materials, and the operation of nuclear installations, including the management of radioactive waste, be subject to certain standards of safety in order to protect those individuals exposed to radiation" [144]. These safety standards increase the complexity and cost of both reactor and radioisotope based systems.

Reactor based systems also have their own disadvantages:

- Purchasing and operating costs of reactors are very high. In addition, the construction cost of associated infrastructure is also very high.
- There are limited legitimate disposal routes for nuclear waste
- Social concern over the potential for nuclear accidents is growing.

By contrast, NGs are relatively inexpensive compared with reactors, offer the option of pulsed beams, cease emitting radiation when power is switched off and produce very little radioactive waste for disposal.

6.2.2. An accelerator based compact neutron generator compared to radioisotopes

The most common radioisotope neutron sources used recently are ^{226}Ra/Be, ^{241}Am/Be, and ^{252}Cf. In the first two sources alpha particles emitted by radium or americium are absorbed by the nucleus of ^{9}B with the subsequent emission of neutron. The last neutron source produces neutrons by spontaneous fission. The neutron flux of these radioisotopes is in the range of 10^4–10^9 n/s dependants upon their amounts. An accelerator based compact NG can be replaced with these radioisotopes with similar or higher neutron flux. In addition to that, a compact NG has an advantage that it can be turned off while not being used.

6.3. Large generator based systems

Proven analytical techniques such as NAA and PGNAA could be possible in a non-reactor based activation facility. High enough neutron fluxes for analytical purposes are now achievable with an incoming new generation of DD NG. For this kind of systems, it has to be considered:

(1) **The generator supplies**: A large NG (>10^{11} n/s) needs high voltage and RF power supplies, cooling and vacuum systems. Those equipments require special electrical power and mechanical installation, for preventing electrical noise and microphoning on

detectors. A computer based control system could be recommendable for assisting the scientific staff in the operation of the generator. (see Section 6.1.4 for details).

(2) **Neutron and gamma shielding surrounding the generator**. The NG does not only produce neutrons, also X rays from stopping radiation of ions onto the target, and capture radiation of neutrons. Those radiations need shieldings for protecting the personnel and the equipments against neutron damage. For thermal neutron activation techniques a moderator is also needed. In this work is presented a study on the optimization of a thermal PGNAA and NAA facility based on a DD NG. (see Section 6.4.8 for details).

(3) **Sample preparation and handling**. The intensity of the achievable neutron fluxes enables the possibility of large sample instrumental activation analysis, for example between 10 g to 1 kg. A dedicated laboratory space and equipment are needed for preparing, homogenizating and manipulating those large samples before and after the irradiation. Automatic fast large sample transfer systems are needed for studying short life radionuclides. (see Section 6.4.7 for details)

(4) **Gamma spectroscopy systems**. High efficiency HPGe detectors can be used for partially compensating the low fluxes (compared with a reactor) and for reaching a comparable sensitivity. The use of Compton suppression systems could be used as active shielding for reducing the background. Also coincidence techniques with a couple of detectors are a possibility for the same purpose. (see Section 6.4.4 for details)

Large generator based activation facilities can be compared with a small research reactor, without facing the complicated nuclear regulation restrictions. For most of universities and non-reactor trained research institutions those kinds of systems could be an option for beginning on nuclear analytical techniques.

6.4. Instrumentation issues

6.4.1. Choice of detector for neutron generator based systems

The choice of detector for NG based systems depends on the exact requirements of the application. Such requirements include sample geometry, range of energies, and range of count rates, spectrum complexity, and harshness of the measurement environment.

Explanations of the various types of γ ray detectors can be found in many references (e.g. Gilmore & Hemingway [145]). The three most common γ ray detector types are high purity germanium (HPGe), sodium iodide (NaI(Tl)) and bismuth germanate (BGO). Selection of detector type is dependent on the degree of resolution required and the environment in which they are to be used.

HPGe is distinguished by the excellent resolution achievable, typically a few keV FWHM. However, HPGe detectors have to be cooled, either using liquid nitrogen or electromechanical cooling mechanisms. The cost to counting efficiency ratio is significantly lower compared with NaI and BGO. Those HPGe detectors designed only for laboratory use are also relatively fragile. New, more robust HPGe detectors are becoming available.

In PNGAA systems scintillation detectors are most often used. NaI and BGO are available in large dimensions. In NAA systems, where lower energy gamma lines are to be detected, and where spectra may be relatively complex both HPGe detectors and scintillation detectors are conventionally employed.

At higher energies (several MeVs), the higher *Z* value of scintillators provides more NET counts in the photopeak than in HPGe detectors although the energy resolution of HPGe detectors are by far superior (typically 2 keV). For scintillation detectors typical values are 4% at 2.6 MeV for NaI(Tl) and 6% at 2.6 MeV for BGO. The disadvantage of BGO is its rather large temperature coefficient (approx. –1% per degree C) which implies that the detectors should be temperature stabilized. New scintillation materials are becoming available (see Section 6.4.2)

Since in PNGAA systems the count rates can be rather high, HPGe detectors may have more problems coping with these. This is due in part to the fact that the charge collection time in a semiconductor detector is long compared with the time required to collect a light flash in a scintillation detector. NaI(Tl) or BGO scintillation detectors can be used up to approx 500 kHz in spectroscopic mode.

Scintillation crystals such as NaI and BGO have significantly poorer resolution than HPGe. The resolution for NaI is better than that for BGO, although the latter can be slightly improved by cooling. NaI is also cheaper than BGO. However, NaI suffers from mechanical and thermal shock, and activation of iodine in the crystal can cause substantial contribution to gamma background. The photopeak efficiency of BGO is higher at high energies and the crystal is more robust than NaI. NaI(Tl) detectors offer the advantage of a better energy resolution compared to BGO detectors but BGO detectors have more NET photopeak counts due to the higher *Z* value. Typical sizes are 152 mm diameter, 152 mm high or 102 × 102 × 102 mm in NaI(Tl) and 76 × 76 mm or 127 × 76 mm in BGO. Details can be found in Refs. [146–149].

6.4.2. Detector development trends

It is a remarkable fact that the high resolution Germanium semiconductor detector (in “GeLi” form) has been with us for almost 50 years, and that the first sodium iodide scintillation detector was reported in 1948. During this period development has been “steady”. In recent times the heightened need for large numbers of improved spectroscopic detectors for applications associated with “homeland security” is adding impetus to development. It is these “external forces” which provide the funding to develop instrumentation for the otherwise “niche market” of neutron activation analysis.

6.4.2.1. Scintillation detectors

NaI (Tl) detectors can now be manufactured in almost arbitrarily large sizes. Unlike HPGe detectors where a single crystal must be grown, large NaI detectors can be manufactured by gluing together smaller crystals.

New Scintillation materials such as $LaCl_3$(Ce) and $LaBr_3$(Ce) offer improved energy resolution, better linearity and higher light outputs. While currently only available in modest sizes, and at relatively high cost, it would be reasonable to expect over time that these issues would be resolved. Therefore the expectation of “typical” energy resolution for a scintillation detector, which is currently in the region of 6–7% for NaI at 662 keV, might in the not too distant future be around 3% as these new materials become more common.

Scintillation detectors have classically suffered from temperature instability. This occurs because of temperature variation of light output, especially in NaI, and instabilities in the photomultipliers themselves. Developments in stabilization methods are taking place and

solid state devices are appearing which promise to supplant photomultipliers for read out purposes.

6.4.2.2. HPGe detectors

While HPGe detectors have always offered vastly superior energy resolution to Scintillators (20 to 40 times better), their drawbacks have been restricted size, complexity in use (cooling) and lastly, cost. Practically speaking, the size restriction is basically a cost restriction. HPGe detectors approaching 200% relative efficiency have been made and larger would be possible if required.

The fact that HPGe requires cooling to cryogenic temperatures has historically been achieved through the use of liquid nitrogen. This has represented a major limitation in the deployment of these detector systems, especially in industrial environments. A new generation of miniature high reliability cryocoolers based upon the Stirling Cycle is now available. The much larger external commercial need, this time in the Cell telephone market, is driving these developments, from which γ ray detection instrumentation benefits. The availability of these coolers is leading to the development of much more rugged and easier to deploy HPGe detectors. The fragility of HPGe detectors, mentioned earlier is now on the decline.

6.4.3. Neutron damage in scintillators

All materials suffer to some extent from radiation damage from γ rays and neutrons. In scintillators radiation damage manifests itself by the formation of absorption bands in the material (coloration) which negatively affects the energy resolution and the light output of the scintillator. The onset of radiation damage in NaI(Tl) or BGO starts at doses of approx. 500-1000 Gray. Part of the damage is self-annealing.

The effect of fast neutrons on the performance of germanium detectors is described in detail in the literature [150]. A summary of the results of greatest practical interest follows; HPGe coaxial and planar detectors show energy resolution degradation when bombarded with fast neutrons. The approximate threshold fluences are:

- 2×10^8 cm^{-2} for P-Type detectors up to 20% in efficiency
- 1×10^7 cm^{-2} for P-Type detectors up to 70% in efficiency
- 4×10^9 cm^{-2} for N-Type detectors up to 30% in efficiency
- 1×10^9 cm^{-2} for N-Type detectors up to 70% in efficiency
- 1×10^9 cm^{-2} for planar detectors

Evidence suggests that in order to achieve the highest possible resistance to neutron damage, the detector should operate at a temperature as close to 77K as possible. Streamline HPGe detector cryostats may be equipped with an internal heater and companion hardware to allow in cryostat neutron damage repair at the place of detector use. Typical annealing temperatures and duration of the annealing cycle for 30% relative efficiency detectors with severe damage are given in TABLE 5 Larger volume HPGe detectors start showing energy resolution degradation at lower fluences than smaller detectors.

TABLE 5. TYPICAL ANNEALING TEMPERATURES AND DURATION FOR 30% RELATIVE EFFICIENCY DETECTORS WITH SEVERE DAMAGE

Detector	Temperature (°C)	Time (h)
P-Type	120	168
N-Type	100	24

The increase in resistance to neutron damage of N-Type detectors versus P-Type can be as high as a factor of 20. However, this increase depends on a variety of factors including detector size, configuration of electric field internal to the detector, energy spectrum of the neutrons, and probably other variables.

When P-Type detectors are annealed, there is a significant loss in relative efficiency because of inward diffusion from the lithium outer contact. Such loss is negligible for N-Type detectors because the lithium diffusion is at the inner contact where an increase of the lithium diffusion depth has little effect on the detector's active volume.

There is no known limit to the number of times that a neutron damaged detector can be annealed if proper precautions are taken. There is no evidence of a radiation hardening effect. Slightly neutron damaged N-Type detectors show some improvement in energy resolution when cycled to room temperature. However, severely neutron damaged N-Type detectors show a catastrophic deterioration of energy resolution when cycled to room temperature. As a general rule, it is best to maintain neutron damaged detectors at LN_2 temperature until they are annealed.

6.4.4. Spectroscopy electronics

The wide range of electronic instruments and modules commercially available for implementation of spectroscopy systems for NAA is best reviewed at manufacturers Web sites, for example [146, 148, 151, 152]. New developments in instrumentation are often described in journals such as Nuclear Instruments and Methods [153], at conferences such as the IEEE Nuclear Science Symposium, or the Modern Trends in Activation Analysis meetings (MTAA). Increasingly, the analogue spectrometers of previous times are being superseded by digital implementations. A good overview of the basic issues involved is given in Ref. [145].

6.4.5. Electronics development trends

The advent of the first commercial digital γ ray spectrometer occurred in the early 1990's. While analogue systems are still in manufacture, new development is on the decline. The developments of digital technologies for consumer markets are enabling adaption into the needs of spectroscopy instrumentation. The direction of the technology is "faster", "smaller", "lighter", and "cheaper". This will mean improved performance in spectroscopy instrumentation, especially in portable configurations and allow more and more sophisticated algorithms to be implemented which can process signals pulse by pulse. These techniques will lead to increased system resolution and throughput, improved stability, background reduction, and the ability to perform spectral imaging. Some of these techniques are already being applied to these problems.

The upward trend in the computing power of the PC will offer the opportunity for further advancement of analysis algorithms as more sophisticated approaches fall within the scope of practical implementation

6.4.6. Count rate issues

The filtering of pulses from a radiation detector, whether scintillation or HPGe is always a trade-off between energy resolution and count rate (or range of count rates). The event rate at which data is stored into data memory is referred to as the system throughput. Throughput defines that number of events stored per unit time, which in turn defines detection limit in an NAA system. By reducing pulse processing time, the system throughput may be increased. This, however, generally results in a loss of energy resolution, so once the system hardware is chosen, the analyst must make the best choice between resolution and throughput, consistent with his needs. Loss of events from the spectrum due to system dead time generally requires the use of an accurate "live time clock" which compensates for the dead time losses. The more advanced implementations of dead time correction operate in "real" time, which is, they correct the spectrum "pulse by pulse" for dead time losses.

Short half-lives often predominate in accelerator based neutron activation analysis. Consequently, spectroscopy electronics should be able to cope with both elevated and variable counting rates. Necessary prerequisites are, therefore; a) a transistor reset preamplifier for virtually unlimited maximum energy rate and b) a pulse processing system with best possible resolution at minimum pulse processing time [154]. "Energy rate" is measured in units of energy per second, being the product of the γ ray count rate and the γ ray energy. It is a measure of the rate at which charge is deposited in the detector itself. For quantitative analyses under conditions of rapidly varying counting rates and spectral shapes, an ideal spectroscopy system should be equipped with real time correction of counting losses.

Discussion of what constitutes the ideal shaped filter with which to optimize the signal to noise ration in a spectroscopy system is beyond the scope of this document. Suffice it to say that this is a mathematical concept which was initially implemented in close approximation in an analogue electrical circuit fabricated from discrete components. The advent of very high speed sampling ADC's from the consumer electronics industry has made it possible to cost effectively produce instruments in which detector output waveforms are sampled at high speed and the resulting stream of digital numbers are then processed by high speed digital techniques.

Digital systems are intrinsically much more stable than their analogue predecessors and moreover it is possible to implement in the analogue domain digital filtering schemes which allow pulse by pulse corrections to be applied which will remove or at least reduce effects which result in undesirable spectral artefacts [155, 156]. Examples include loss free counting correction, charge trapping correction, elimination of period noise effects, ballistic deficit correction.

The Preloaded Digital Filter (PLDF) combines low to medium rate resolutions comparable to those of high quality Gaussian amplifiers with input rates of up to 1000 kcounts/s and throughput rates of up to 100 kc/s, by automatically adapting the noise filtering time to individual pulse intervals. High rate resolutions superior to those of state-of-the-art gated integrator systems are possible. In contrast to commercially available digital filters, the PLDF in its new implementation performs pulse shortening as well as pole zero cancellation in the analogue domain [157]. This not only results in a simpler digital core but also, for the first

time, makes possible the use of a low cost ADC in a spectrometric application. Combined with real time correction of counting losses according to the Loss Free Counting method [158, 159], the PLDF is the core of a novel multichannel analyzer system for NAA of short lived isomeric transitions [137, 138].

6.4.7. Sample handling and data analysis

To be able to cope with short half-lives a fast rabbit system is the preferred medium of sample handling in accelerator based NAA [139]. Above average sample volumes of several ml may compensate lower fluxes to a certain extent [138]. A transport rabbit with automatic sample separation makes possible a low cost aluminium construction of the irradiation position [138]. Suitably designed, an automatic sample changer makes possible unattended system operation in the normal as well as in the cyclic mode, to further increase sensitivity under low flux conditions [137, 138].

As reported, automatic activation analysis is rendered possible at a small reactor by a unique neutron activation analysis facility for short lived isomeric transitions, based on a fast rabbit system with sample changer and sample separation, and an adaptive digital gamma spectrometer for very high counting rates of up to 10^6 c/s. The system is governed by a computer program performing irradiation control, neutron flux monitoring, and gamma spectrometry with real time correction of counting losses, spectra evaluation, nuclide identification and calculation of concentrations in a fully automatic flow of operations. As spectrometry is done by means of hundreds of sequentially measured pairs of concurrently recorded loss corrected and non-corrected spectra, concentrations are derived from an optimally weighted average of all individual occurrences in this sequence of spectra which also enables the separation of isomeric transitions with coinciding energies but different half-lives such as ^{116m2}In (162.4 keV, $t_{1/2}$ = 2.2 s) and ^{77m}Se (162.2 keV, $t_{1/2}$ = 17.4 s).

6.4.8. Data analysis

A detailed discussion of the issues involved in data analysis software is beyond the scope of this document. Excellent overviews of the analysis of γ ray spectra are available [145, 160]. Numerous intercomparisons of commercial γ ray analysis packages are to be found in the literature, e.g. [161, 162].

Analysis software for any γ ray spectrum has a set of basic functional requirements: Extraction of net peak areas, energies and associated uncertainties, including the unfolding of multiplet peaks, calibration for efficiency, interpretation of the net peak areas in terms of neutron flux, source activity or elemental concentrations, as well as correction for spectral distortions due to count rate, sample geometry, and source effects.

NAA spectra can be particularly complex with many overlapping peaks requiring deconvolution techniques. The presence of short half-life components[2] can require correction for decay of activity during irradiation, between irradiation and measurement in a spectrometer, and during the actual measurement itself. The short half-life aspects can result in the requirement for automatic rapid sample handling systems of “rabbit systems”. In PGNAA, short lived radionuclides will exhibit increasing count rates, perhaps reaching saturation levels, as irradiation and spectrum acquisition continues.

[2] “Short” in this context generally means short compared to the acquisition time of the data.

PGNAA spectra are not essentially different from other NAA spectra. However, the energy range is much larger, up to 10 MeV rather than up to 4 MeV. The spectra are riddled with escape peaks, where the single escape peaks are Doppler broadened and easily mistaken for doublets by conventional data analysis methods. Anti-Compton shields are being used to reduce the continuum in the spectra, at the cost of rendering efficiency curve usage virtually impossible. Excellent references on the topic are available [84].

Short half-life components in the spectra will mean that "real time" dead time correction needs to be applied during acquisition of the data. In general this correction is carried out in specially developed hardware (see Section 6.4.6).

NAA samples vary from bulk samples such as samples on a conveyor belt within an industrial process, to very small samples such as are encountered in forensic analysis. Small samples may require counting very close to the detector or even within it in the case of so called "well" detectors. The reason is to maximize geometric efficiency and thereby optimize sensitivity. This "close geometry" counting brings with it another potential problem of "true coincidence" summing of multiple γ rays from a single decay being recorded by the electronics subsystem as a single spectral event.

Efficiency calibration in NAA is a topic all in itself. In the "traditional" approach of comparative NAA, standards which are physically identical to the sample and which contain known amounts of the element of interest are sequentially irradiated with the batch of samples. The analysis then is reduced to determining the elemental ratio of sample and standard directly from the peak area ratios. Ideally, the spectral artefacts mentioned above affect sample and standard equally and cancel out in the concentration calculation. These methods are generally referred to as "comparative".

It is often the case, however that "identical" standards are not available. In this case, an absolute method is required, in which, knowing the flux from the reactor or generator and the cross-sections for activation, it is possible to calculate elemental concentrations from the spectrum and these absolute quantities. A well-established method of this type is the single comparator k_0 method developed at In Gent and Budapest [163, 164]. This method is also applicable to PGNAA. Most often, however, internal standardization is used in PGNAA, where one elemental concentration in the sample is considered to be known, and others are determined relative to the known one.

6.4.9. Special considerations for industrial systems

There are substantial differences between industrial environments and those in which most scientific laboratories exist. These differences need to be considered during selection and implementation of instrumentation for industrial applications. Most industrial environments include one or more of the following characteristics:

- Personnel will consist almost entirely of occupationally exposed workers.
- There are very few or no staff with specialised skills relevant to operation / maintenance / calibration of sophisticated nuclear equipment.
- Continuous well controlled production and safety are top priorities.
- Infrastructure and site access may be extremely limited.
- There is a wide ambient temperature and/or pressure range.

— The environment is extremely dusty with potential for mechanical impact from particulate material.
— High levels of vibration and noise are present either intermittently or continuously.

Thus, any industrial activation analysis system needs to have ‘turnkey’ operation, and it should run reliably without maintenance or recalibration for months at a time. Usage and maintenance must fit with the production schedule without compromising safety. The individual components must be mechanically robust and/or well protected against any adverse environmental conditions. The overall system needs to be designed to comply with radiation protection standards that are appropriate for the general public.

6.5. Compton suppression

By surrounding an HPGe detector by a layer of scintillation material and detecting γ rays Compton scattered out of the primary detector, the peak to total ratio can be improved by generating a “veto” pulse to reject these events from the spectrum. In practice, this is applicable only for HPGe or NaI(Tl) detectors. This technique is employed in both, in PGNAA systems and in NAA systems. The Anti-Compton shield is usually an annulus of scintillator around the primary detector. The thickness of the scintillation material depends on the maximum energy of the scattered γ rays. A typical Compton Suppression Annulus is shown in FIG. 20.

An excellent review of Compton suppression counting in NAA has been given by Landsberger and Peshev [165] concluding that reductions of detection limits are possible together with an increase of accuracy due to a substantial reduction of the background of gamma spectroscopy. It was also concluded, however, that the method does not provide accurate quantification of isotopes when the overall dead time exceeds ~10%. Not substantiated in this review, it may be attributed to the fact that random coincidence losses have not been properly taken into account.

Generally, Compton suppression adds to system complexity. As well as removal of Compton scattered events from the spectrum, the Compton Suppression system will remove events from spectrum peaks associated with cascade γ rays. This effect is undesirable: “full energy events” which because of the specific nuclide decay scheme are in time coincidence with other full energy γ rays may be captured in both primary and Compton suppression detector. This effect requires “true coincidence” correction techniques to be applied. This effect is quite common: Co-60 is an example of a coincidence emitter. The 1332 keV and 1173 keV γ rays are emitted simultaneously, without angular correlation.

Recently [166], random coincidence losses in a Compton suppression spectrometer have been corrected instrumentally by comparing the random coincidence rate to the counting rate of the Germanium detector in a pulse counting busy circuit [167] which is combined with the spectrometer's “loss free” counting (LFC) loss correction system. The normally unobservable random coincidence rate is reconstructed from the rates of Germanium detector and scintillation detector in an auxiliary coincidence unit, after the destruction of true coincidence by delaying one of the coincidence partners. Test measurements have been performed comparing the ratios of peak areas of ^{137}Cs with and without coincidence loss correction (CCLC) versus counting rate of the Germanium detector. While losses of ~25% are observed at 200 kc/s for a mere correction of dead time and pileup losses without CLCC, true loss free counting was possible with CLCC.

FIG. 20. Typical Compton Suppression Annulus (courtesy Scionix).

Quantitative system response has been tested also in two source measurements with a fixed reference source of ^{60}Co of 14 kc/s, and various samples of ^{137}Cs, up to aggregate counting rates of 180 kc/s for a HPGe well type detector, and more than 1400 kc/s for its BGO shield [168]. In these measurements, the net peak areas of the 1173.3 keV line of ^{60}Co remained constant at typical values of 37000 with and 95000 without Compton suppression, with maximum deviations from the average of less than 1.5%.

When a system is being designed to a limited budget, it may be practically more effective to use a larger HPGe detector (with higher peak to total ratio) than smaller, lower efficiency, HPGe detector with the added complexity of the Compton Suppression Electronics.

6.6. Coincidences techniques

This section is adapted from Ref. [169]. Coincidence detection of γ rays (γ–γ coincidence) is a well-established technique in nuclear structure studies [170]. It is well known that coincidence methods can substantially reduce interference, and hence also the complexity of spectra. The usefulness of the γ–γ coincidence technique in elemental analysis [9] has already been demonstrated in the case of the INAA by several authors [171, 174]. Their main goal was to

improve the sensitivity of the method by suppressing the continuous background and reducing spectral interference.

The conventional method for doing γ–γ coincidence is to require a coincidence relation with a selected full energy peak. This constraint reduces the spectrum to the signals of those gamma photons which are in a cascade relation with that peak. It lowers the background substantially, increasing the peak to background ratio. The peak count rate is also reduced, since it is proportional to the product of two full energy peak efficiencies. A significant disadvantage is that this method is extremely time consuming due to the low coincidence count rate. Instead of using the peak coincidence method, Ember et al. propose to define a coincidence relation not with a single peak, but with a selected region of the spectrum containing several peaks and a part of their Compton continuum to increase the coincidence efficiency.

CHAPTER 7
COMPACT NEUTRON GENERATORS

7.1. Introduction

Compact NGs are becoming an attractive alternative to nuclear reactors and radioactive neutron sources in variety of fields of neutron science [108], medical research [175] and various material analysis applications, ranging from coal and cement analysis [176] to various explosive detection schemes, from homeland security applications [108, 56, 177] to other explosive detection applications, like land mine detection [39]. Traditionally compact NGs have been used in oil well logging industry, using DT fusion reaction for high energy 14 MeV neutron production. Currently the main commercial manufacturers of compact NGs are Thermo Electron [178], Sodern EADS [179] and Schlumberger [180]. These NGs generate DT neutron yield in the range of 10^8 to 10^{11} n/s. There are yet others, which are made by universities or national laboratories, like VNIIA [181] made generators (sold in US by Del Mar Ventures [182]) and Lawrence Berkeley National Laboratory's Plasma and Ion Source Technology Group (generators commercialized by Adelphi Technology Inc. [183]). The NGs designed and made by the LBNL group are highlighted in this section.

The Plasma and Ion Source Technology Group (P&IST) at the E.O. Lawrence Berkeley National Laboratory has been developing high power DD NGs for various applications. These NGs are differentiated from the commercial manufacturers mainly by the method the plasma is generated and by the use of DD, instead of DT, fusion reaction. The P&IST group has been pioneering in RF induction discharge for different applications for more than twenty years [184]. This RF technology with unique impedance matching circuitry and source designs capable of high power operation is being used in various NGs, developed by the group. RF induction discharge ion source has unique features that make it an excellent source type for high power, high yield NGs. These features include the high plasma density generation for high beam current extraction, extremely high atomic ion generation from molecular gases like hydrogen, and reliable, long life operation. These ion sources are currently used in three different types of NGs; axial, single ion beam NG; coaxial, multibeamlet, high current NG; and point NG with high instantaneous neutron yields. The most suitable NGs for PGNAA and for NAA are the single beam axial NG and the high yield co axial NG.

7.2. Axial neutron generators

The axial, single beam NG is a development from the sectioned insulator, single beam neutron source, which was developed mainly for pulsed beam applications. The sectioned accelerator axial NG was developed to demonstrate the extremely long lifetime operation of a DD NG, driven by RF induction ion source. The NG has a unique sectioned accelerator design, where the accelerator voltage is split into three segments evenly. These segments have two purposes, first, they shield the high voltage insulator from charging, due to the travelling ion beam, and second, by splitting the high potential into multiple segments, the electrostatic field stresses are minimized. See FIG. 21 for a picture of the NG.

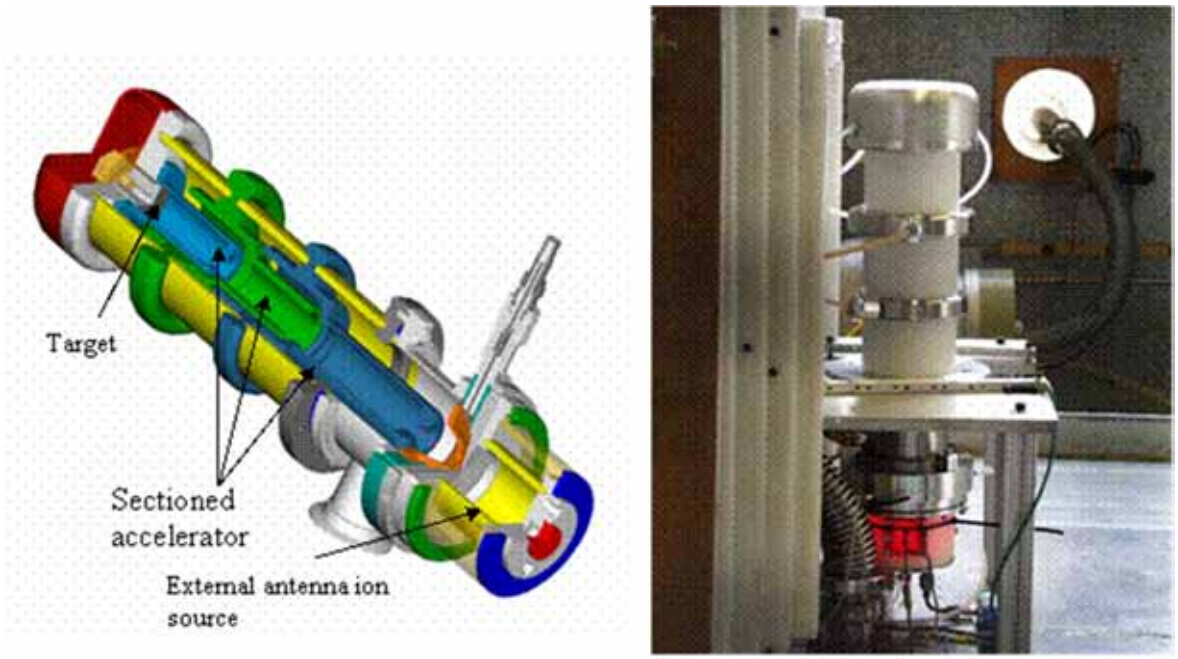

FIG. 21. Sectioned accelerator axial DD NG, with three stage accelerator section, puller electrode for the initial beam extraction and acceleration and the RF induction ion source with an external.

The sectioned accelerator NG was operated during the first prototype neutron imaging system tests during November and December 2004 at the Lawrence Berkeley National Laboratory. During the runs the NG was run continuously up to 10 hours in a day for 6 weeks. The generator proofed extremely reliable during these tests, neutron flux only to be limited by the dose considerations in the test stand. The external RF antenna ion source has thus proofed the ability to provide long life time operation with extremely stable operation characteristics. In the following discussion, three main axial NG components are highlighted.

7.3. Ion source

The external antenna, water cooled ion source design is used in all of the axial NG developed at the LBNL. The most important operation characteristics of an ion source in conjunction with NG operation is the extractable ion current, ion mass distribution in the ion beam and the operation gas pressure.

The neutron yield produced by the NG is directly depending on the intensity of the ion beam, the ion beam current. RF plasma generators are known to be able to produce extremely high current densities for various applications. The P&IST Group has been developing RF based plasma generators for these applications. These applications include H^- injectors for large accelerator systems [185] and for tokamak fusion applications [186], positive ion sources for advanced focused ion beam systems [187] and for semiconductor applications [112]. The externally driven RF induction ion source is shown in FIG. 22.

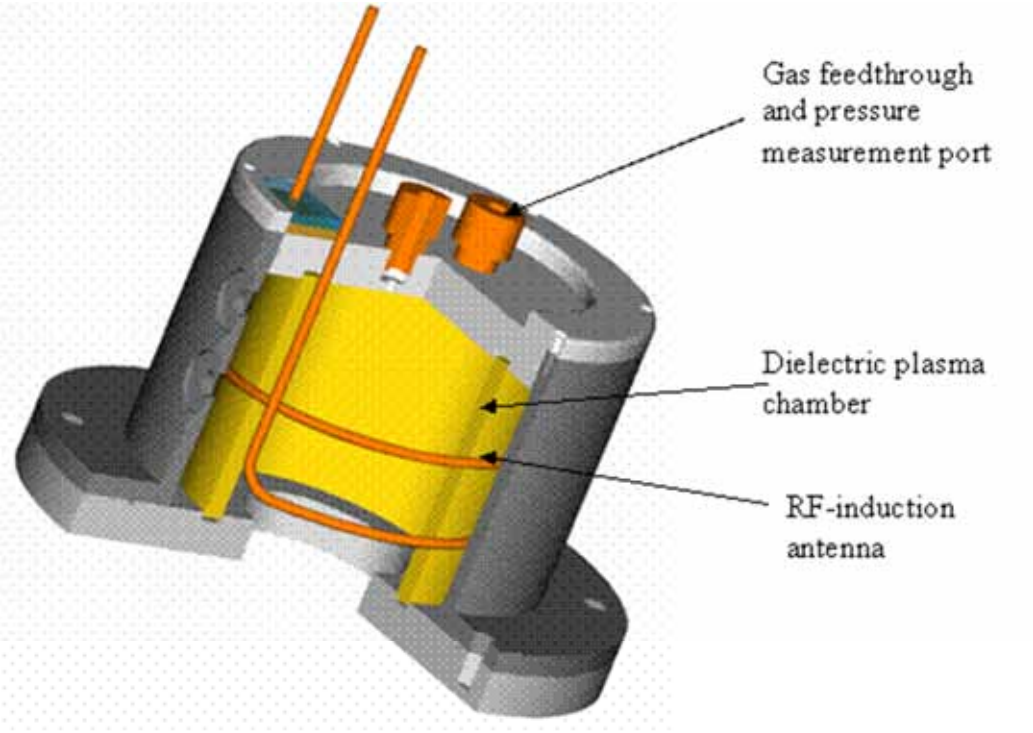

FIG. 22. External antenna driven ion source for high power DD or DT NG applications.

The extractable ion beam current is a function of various parameters, like the RF power and the source pressure. The external antenna ion source can be operated at a wide range of operating parameters, depending on the needs of the application. During the testing of these ion sources, the operation gas is hydrogen, instead of deuterium, due to the radiation safety issues. Hydrogen operation gives a good estimation of the source behaviour, when operated with deuterium. The hydrogen current as a function of pressure and RF power is shown in FIG. 23. Typically the output ion current is proportional to the discharge power.

Hydrogen gas forms three ion species in plasma: proton (H^+), molecular ion (H_2^+) and H_3^+. The same applies for deuterium and tritium gases. The ion species distribution is an important parameter in determining the overall efficiency of the NG. Some of the widely used NG ion sources produce significant fraction of molecular ion species, thus reducing the energy per deuterium or tritium nuclei. The RF discharge has demonstrated nearly monatomic ion species with a wide range of operating parameters. This can be seen in FIG. 24, where the hydrogen species are measured as a function of the discharge power.

For sealed tube operation one of the most important parameter in the ion source operation is the efficiency of the operation at low operating gas pressure. In the sealed tube, the ion source pressure determines the operating pressure also in the target chamber of the generator. Reliable high voltage operation cannot be achieved, if the gas pressure is too high in the sealed tube. Typically these sealed NG require gas pressure of <0.7 Pa (5×10^{-3} Torr). With penning discharge this is easily achievable, with RF induction discharge, on the other hand this requirement is more difficult to achieve. The RF induction sources can be configured to operate at low pressure regime by using higher RF frequency, internal, electron confining magnetic fields or by utilizing an additional electron source for low pressure plasma ignition. For DD NG, the operation gas pressure is not as critical because the NG is constantly being

vacuum pumped. Thus, pressure gradient is formed across the extraction aperture allowing higher pressure in the ion source chamber than in the target chamber. The RF induction sources are typically operated at ~1 Pa (10^{-2} Torr) range. The pressure dependence of the extracted ion current is shown in FIG. 25.

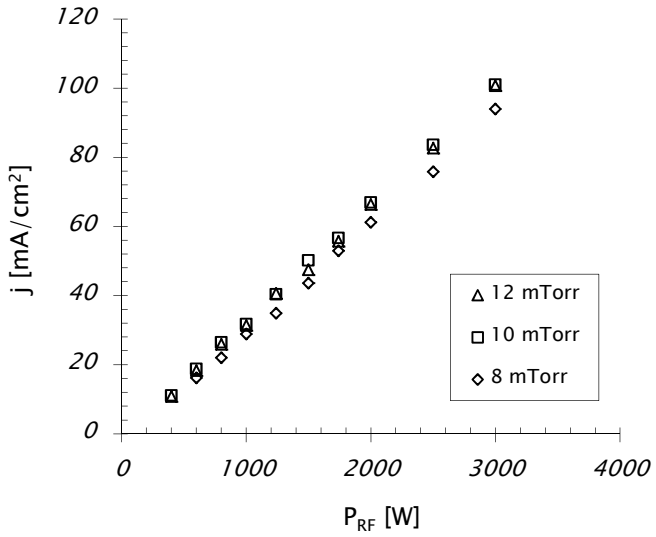

FIG. 23. Extracted hydrogen ion current density as a function of the operation gas pressure from externally driven RF induction ion source, used in the axial NG.

In some applications there is a need for a NG not having any exposed high voltage elements included. Thus the NG can be placed close to various moderator materials or experimental devices. Also various samples for neutron activation can be placed next to the target, outside the vacuum vessel. In the latest axial NG development, a grounded vacuum/target chamber shields the high voltage element. FIG. 26 shows a drawing of the fully high voltage shielded NG. The RF induction ion source is similar to the section insulator NG. The accelerator structure is a single gap design with biased target shroud for secondary electron filtering. The high voltage feed through integrates the HV cable and the water feeds for the target. The fully high voltage shielded NG is designed for up to 10^9 n/s DD operation.

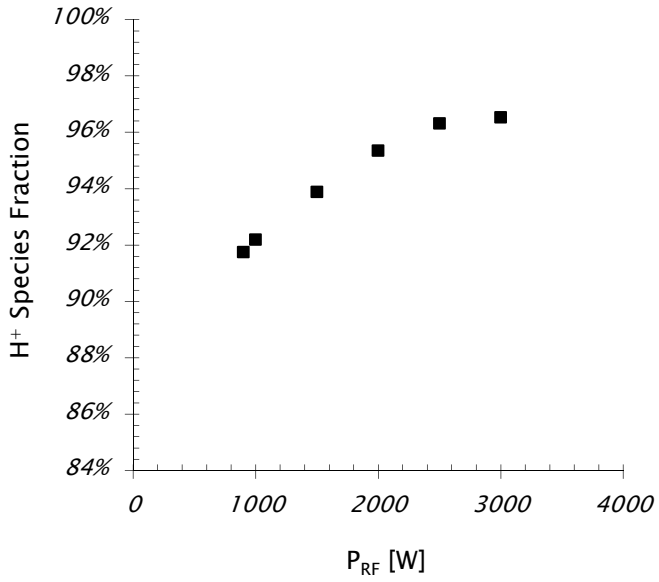

FIG. 24. Atomic hydrogen (proton) species fraction of the total extracted ion beam. Ion source operated at 8 mTorr of hydrogen gas pressure.

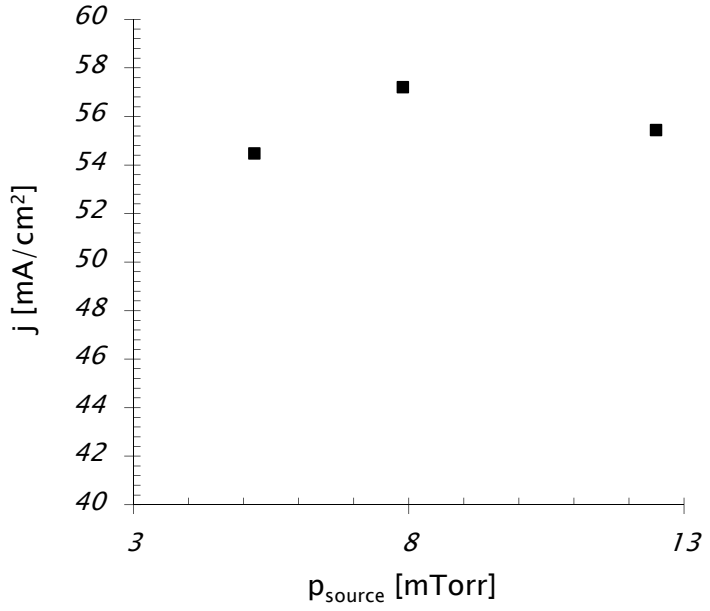

FIG. 25. Extracted ion current density as a function of the source pressure for hydrogen with 2 kW of discharge power.

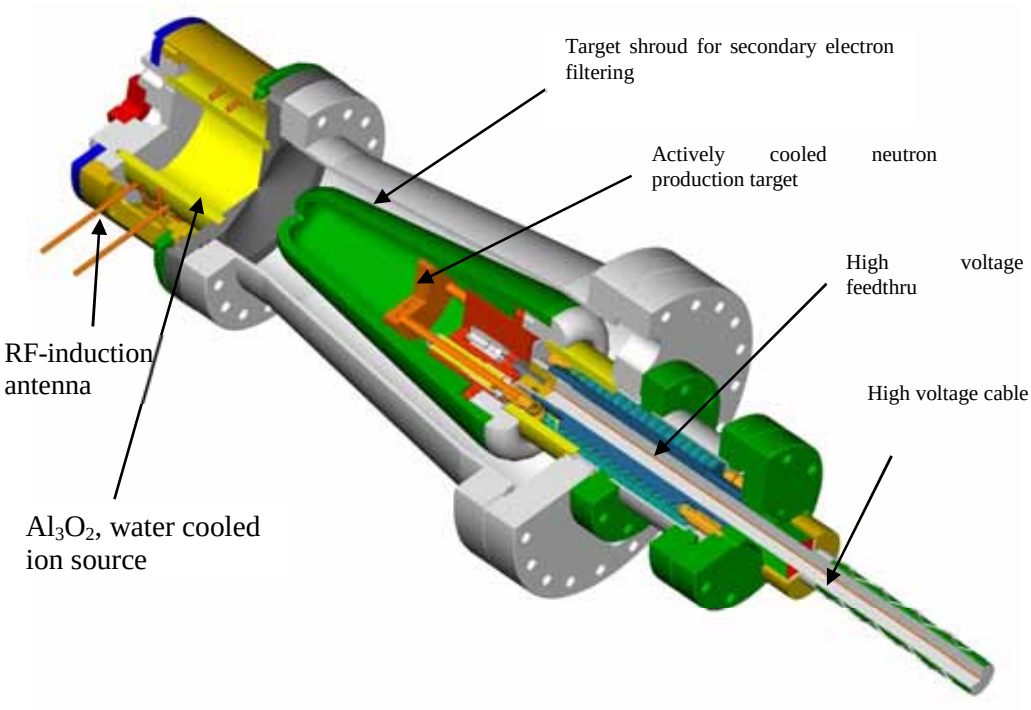

FIG. 26. Fully high voltage shielded axial NG. The length of the generator is ~50 cm.

7.4. Accelerator

The extraction and the accelerator system of a NG are modelled using dedicated computer codes. The codes used in the P&IST Group are: IGUN [188], PBGUNS [189], SIMION 3D [190] and KOBRA 3D [191]. For single cylindrically symmetric beam simulations, 2D codes are used, and for slit beam extraction systems, 3D simulation codes are necessary.

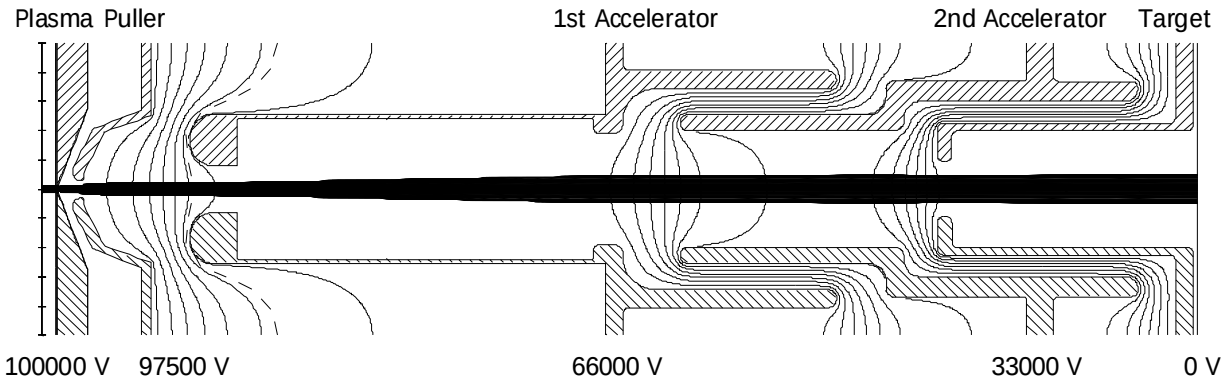

FIG. 27. Ion beam extraction simulation using IGUN code. The multistage accelerator structure of the sectioned insulator NG is shown in this simulation.

The purpose of the extraction design is to match the plasma density for the extraction field in order to produce lossless beam transport to the target. In case of single gap extraction design, the plasma meniscus (boundary layer between the plasma and the extraction field) determines the initial ion beam optics characteristics. This will lead to a situation, where the ion beam and the beam spot size vary depending on the discharge power (plasma density) and the acceleration voltage (extraction electric field). A single gap accelerator NG operation is thus limited to a certain range of these parameters for optimum operation. IGUN simulation of the beam behaviour in the case of sectioned insulator NG is shown in FIG. 27.

7.5. Target

Titanium is widely used as a neutron production target material. When the deuterium (or tritium) ions are implanted in to the target, they form titanium hydrates, effectively 'trapping' the ions into the titanium matrix. When the generator is operated, the surface temperature will increase, causing temperature induced diffusion of these atoms toward the surface (and toward the bulk) of the titanium. After the NG has been turned on there is a 45–60 min loading period where the neutron yield increases ~20% from the initial yield. See FIG. 28 for a typical 'fresh target' yield as a function of time.

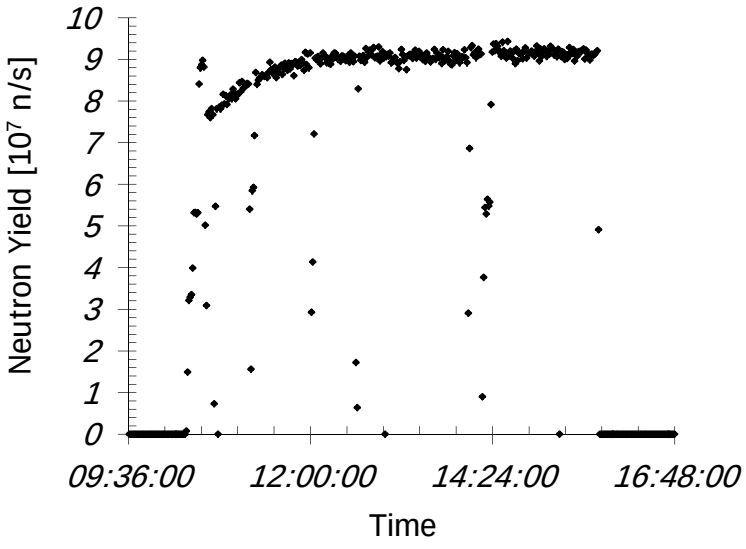

FIG. 28. Neutron yield as a function of time in a sectioned insulator, axial NG.

The LBNL NGs are using explosive bonded titanium on copper or aluminium bimetal targets, made by Atlas Inc. Some of these targets have been operated ~1000 hours without failures. In some cases the target surface is overheated by the beam. See FIG. 29, of a coaxial NG run, where the target surface was over heated. In case of preloaded target this would result in target failure and loss of neutron yield. In the case of beam loaded target, the neutron yield can be recovered by operating the NG at lower power level. This can be seen on FIG. 29, when the extracted beam current is dropped back to 20 mA from 24 mA, the yield increases back to original value, before the overheating.

There are secondary electrons generated when the ion beam strikes the target. These secondary electrons may cause catastrophic failure of the NG, if not properly filtered out. The secondary electron filtering is done using electrostatic field next to the target surface. This field is formed by biasing the target to more positive potential than the surrounding shroud. This biasing is done using a Zener diode, high voltage divider stack or with multiple high voltage power supply.

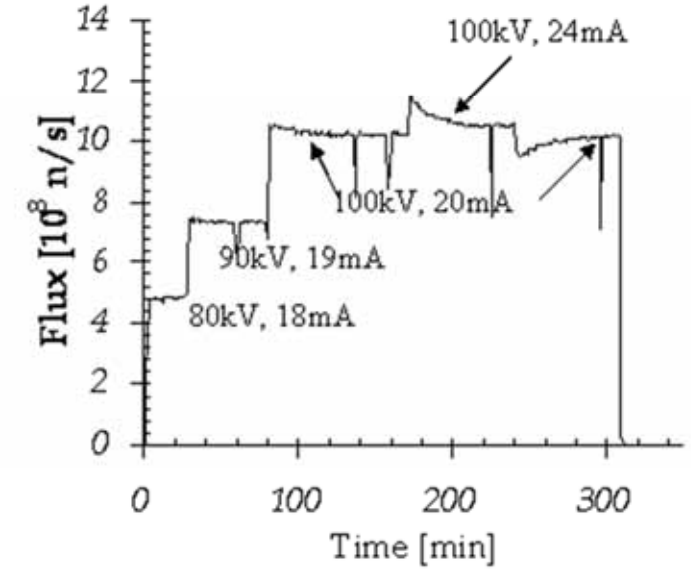

FIG. 29. Neutron yield as a function of time in a case of overheating the target surface. The overheating starts at the 90 kV/18 mA level, continues to 100 kV/24 mA level, resulting in greatly reduced neutron yield. When the beam power is dialled down back to 100 kV/20 mA level, the yield recovers.

The beam power at a neutron yield level of 10^8 n/s DD is ~100 W. This heat needs to be water cooled from the target. The target cooling water is feed from the ground potential to the target potential via non-conducting water hoses and preferable Low Conductance Water for low leakage current.

Target assembly and the vacuum vessel with the RF induction ion source of an axial, high voltage shielded NG are shown in FIG. 30. The secondary electron shroud and the high voltage insulator are clearly visible.

FIG. 30. The axial NG shown with target assembly separated (in the lower half of the picture) from the vacuum vessel and the ion source. The generator is 50 cm in length.

7.6. Coaxial neutron generator

The coaxial NG has the capability of operating at high beam current regime and thus producing high neutron yields. This is possible, because of the unique target arrangement of the coaxial NG. The basic structure of the generator consists of an ion source with an internal antenna, a target cylinder surrounding the ion source, and an insulator cylinder surrounding the target as shown in FIG. 31. The advantage of this coaxial design is that the target area can be maximized in a given volume and the HV insulator is protected from the sputtered target particles. The outer dimensions of the coaxial NG, operating in the neutron facility at the LBNL, are: 30 cm in diameter, 40 cm in height. The neutron output of this source is 5×10^9 n/s.

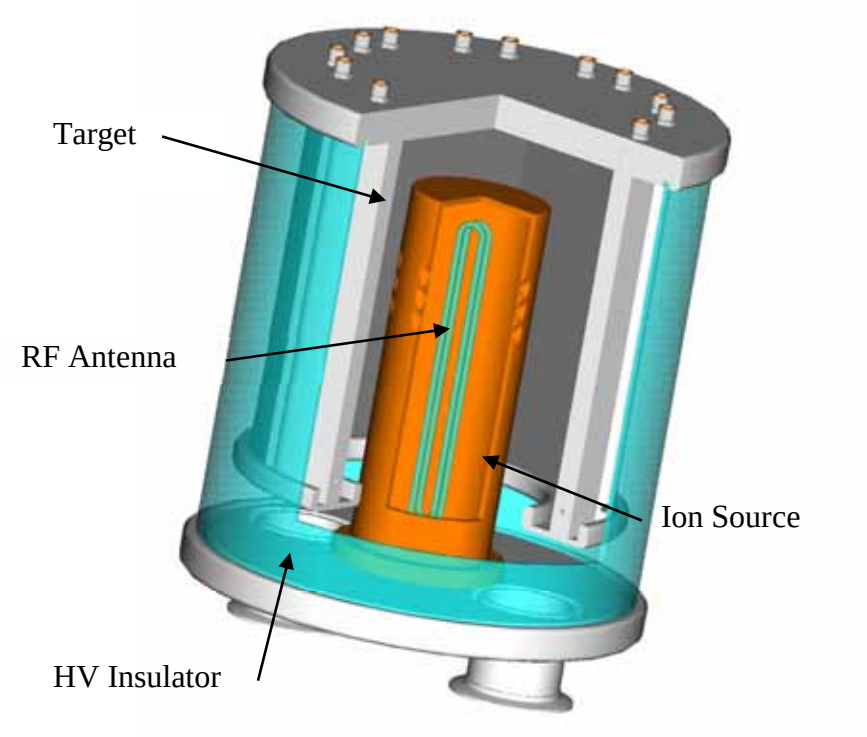

FIG. 31. The main components of the coaxial NG.

The P&IST Group has developed a 10^{11} n/s NG, based on the coaxial NG concept, for an Italian hospital/university consortium (EUROSIA) in Turin, Italy for Neutron Capture Therapy (NCT) applications.

7.7. Ion source

The coaxial NG has a fairly large discharge chamber. The plasma density and other operation characteristics are thus different. The current density as the function of the RF discharge power and the source pressure are shown in FIG. 32 and FIG. 33, respectively. The ion source uses internal, water cooled, quartz RF antenna. This antenna type has been tested extensively with various sources and it has proven reliable for more than 1000 hours.

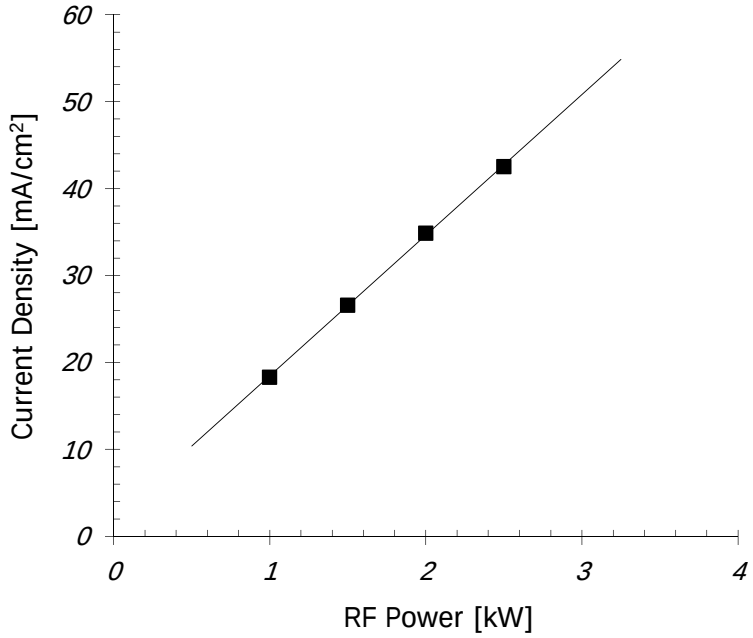

FIG. 32. The extracted current density of a coaxial NG plasma generator. The ion source chamber is 30 cm in height and 10 cm in diameter.

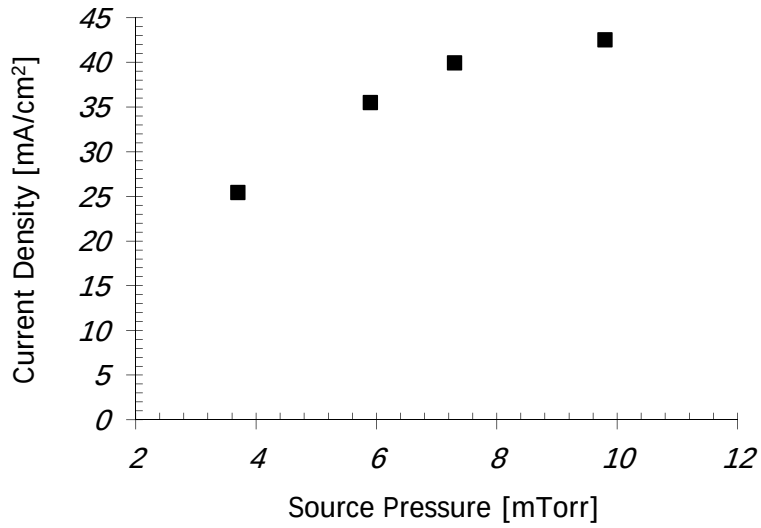

FIG. 33. The extracted current density of a coaxial NG plasma generator as a function of the operation gas pressure. The minimum operation pressure is less than in the case of axial NG ion source due to the larger size of the RF antenna used.

7.8. Extraction and acceleration system

The coaxial NG uses single gap extraction/acceleration system. The NG used in the neutron facility at the LBNL, the generator has a 24, 2.5 mm in diameter extraction apertures, capable of producing in excess of 50 mA of beam current at 90 kV of acceleration voltage. The EUROSIA NG has seven 1.5 mm wide slit apertures of 75 mm in height. The total extraction area is ~8 cm^2. When the ion source is operated at 2.5 kW, more than 330 mA of ion beam is being extracted. There is also an electrostatic secondary electron shield structure to protect the ion source. See FIG. 34 for a drawing of the EUROSIA NG.

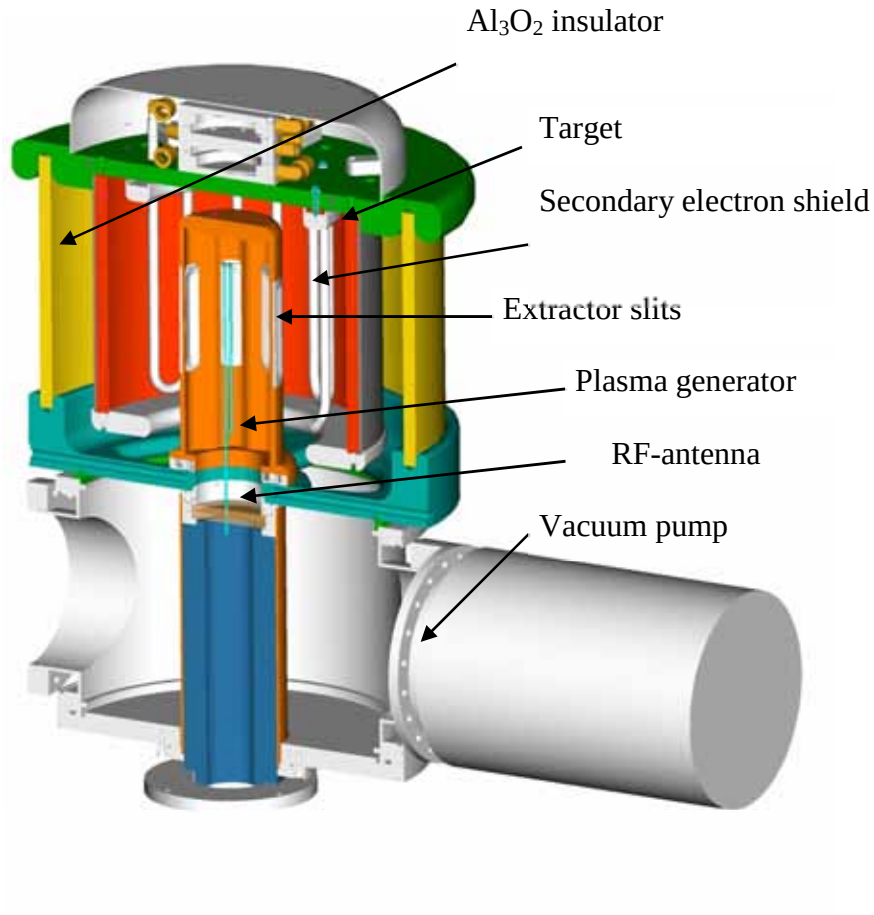

FIG. 34. The main components of the EUROSIA coaxial NG.

7.9. Target and high voltage insulation

The target cylinder is insulated from the ground potential ion source by a dielectric cylinder, in the case of the LBNL coaxial NG by Pyrex glass, and in the case of the EUROSIA coaxial NG be Al_2O_3 cylinder. The high voltage insulator is protected from the sputtered metal by the target cylinder. In the EUROSIA NG, the vacuum pumping is integrated to the base support structure of the generator. See FIG. 35, for the fabricated EUROSIA NG at one of the two NG test stands at LBNL. The generator is 80 cm in height and 40 cm in diameter.

FIG. 35. Fabricated EUROSIA coaxial NG at the NG test stand at LBNL.

7.10. Experiments with the LBNL deuterium–deuterium neutron generator

The LBNL high intensity DD NG has been described elsewhere in this report. It is surrounded by 30 cm of polyethylene that acts as both a moderator and neutron shield. The generator is coaxial, with multiple deuteron beams striking a cylindrical titanium target with a radius of 15 cm. The thermal and fact neutron flux, were determined by ^{115}In(n,γ)^{116m}In and ^{115}In(n,n′)^{115m}In reactions respectively. These results are summarized in TABLE 6.

TABLE 6. NEUTRON FLUX AT DIFFERENT LOCATIONS AROUND THE NG
(The uncertainty is ≥20%)

Sample location	Distance from the centre of the NG cylinder	Thermal neutron flux ($n \cdot cm^{-2} \cdot s^{-1}$)	Fast (≥0.5 MeV) neutron flux
Pneumatic terminal	~28.2 cm	1.1×10^4	1.4×10^5
Inner shielding	~26.2 cm	1.3×10^4	1.0×10^5
Top of NG		1.1×10^4	1.5×10^5

The NG was operated at 80 mV and 40 mA for this calibration test and the total neutron yield into 4π was measured as 10^9 n/s. At full power this NG would by 10^{10} n/s. The thermal

neutron flux in the LBNL NG can exceed 10^5 n · cm $^{-2}$ · s $^{-1}$. FIG. 36 shows that the flux through the moderator, measured at various depths next to a removable plug, compares well to MCNP calculations.

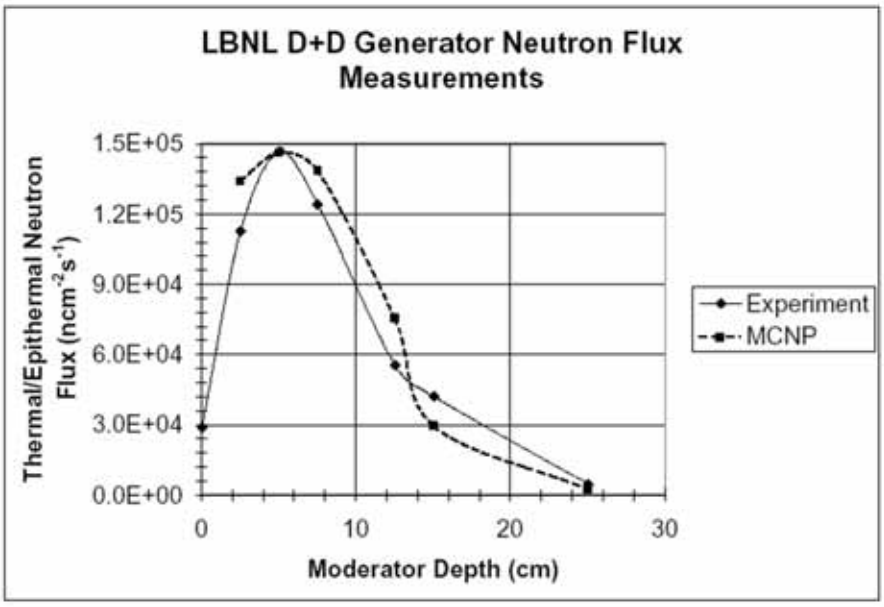

FIG. 36. Thermal flux in the LBNL NG (solid line) compared to MCNP calculations (dashed line).

Sample thermal neutron capture spectra are shown for aluminium (FIG. 37), bromine (FIG. 38), copper (FIG. 39), cobalt (FIG. 40), hafnium (FIG. 41), NaCl (FIG. 42), iodine (FIG. 43), and antimony (FIG. 44).

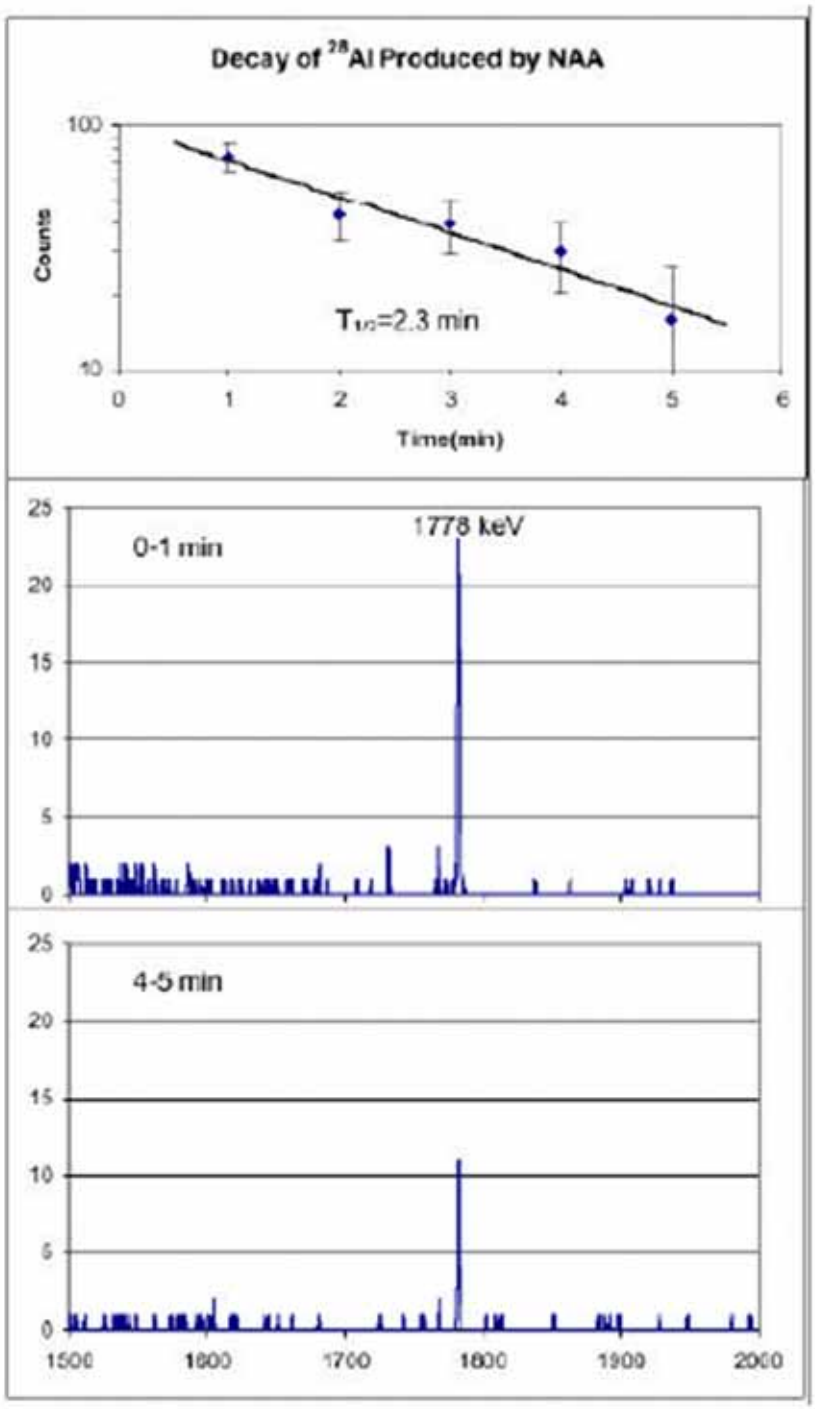

FIG. 37. Analysis of aluminium by $^{27}Al(n,\gamma)^{28}Al(2.24\ m)$.

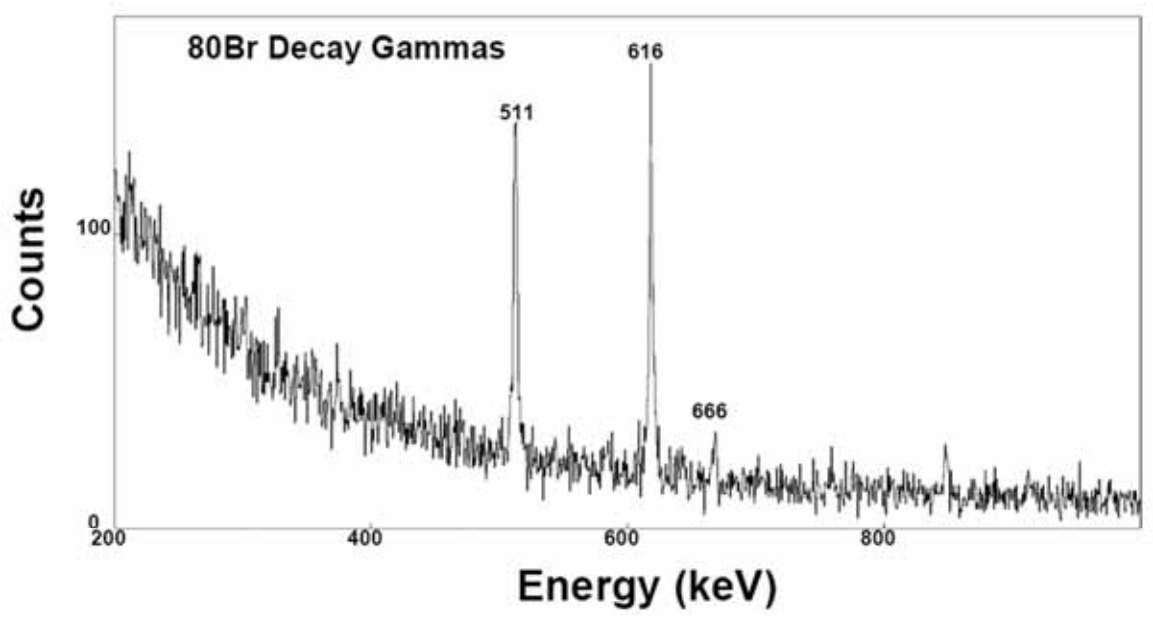

FIG. 38. Analysis of bromine by $^{79}Br(n,\gamma)^{80}Br(17.68\ m)$.

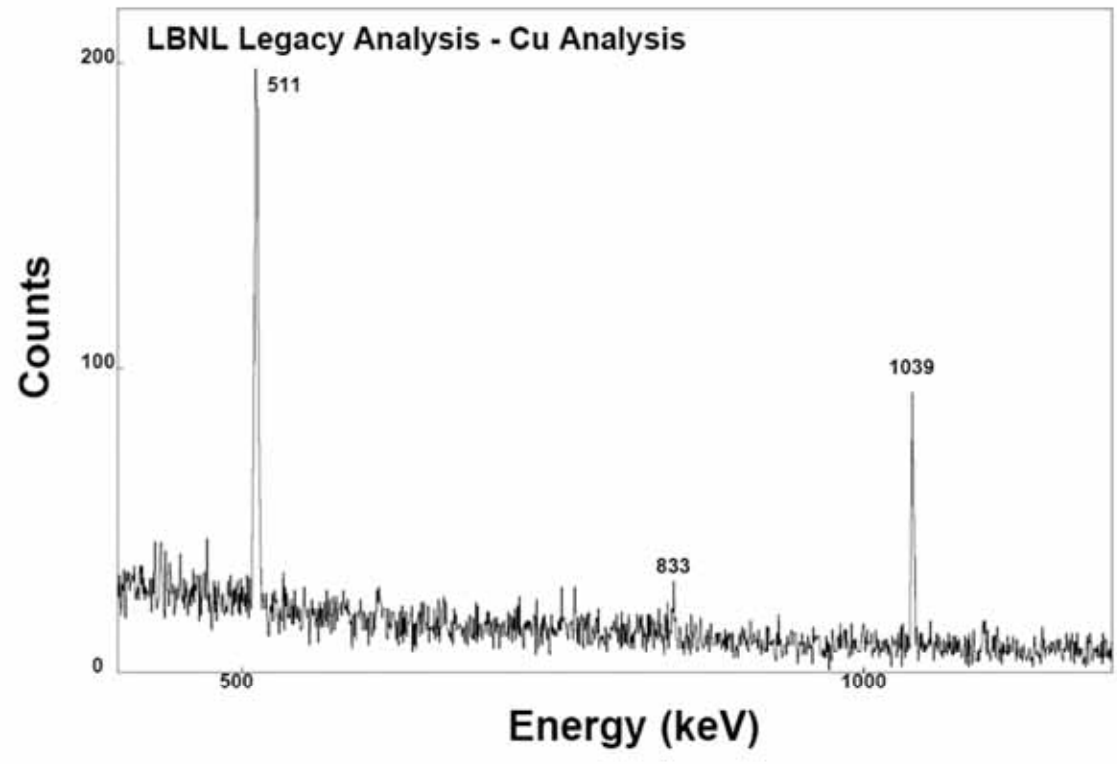

FIG. 39. Analysis of copper by $^{65}Cu(n,\gamma)^{66}Cu(5.12\ m)$

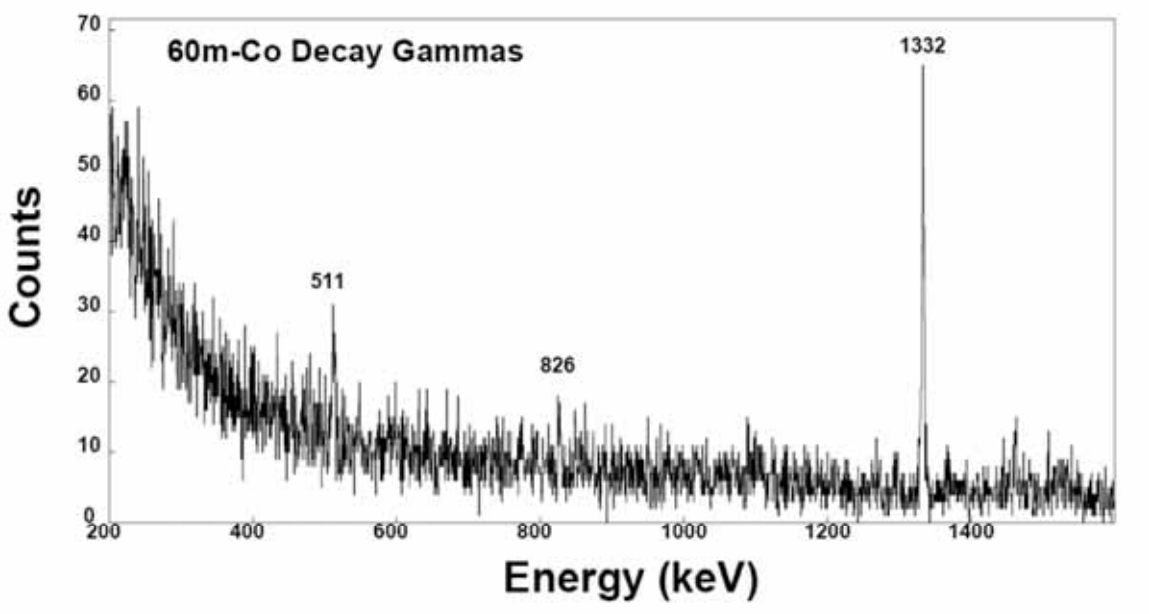

FIG. 40. Analysis of cobalt by $^{59}Co(n,\gamma)^{60m}Co(10.47\ m)$

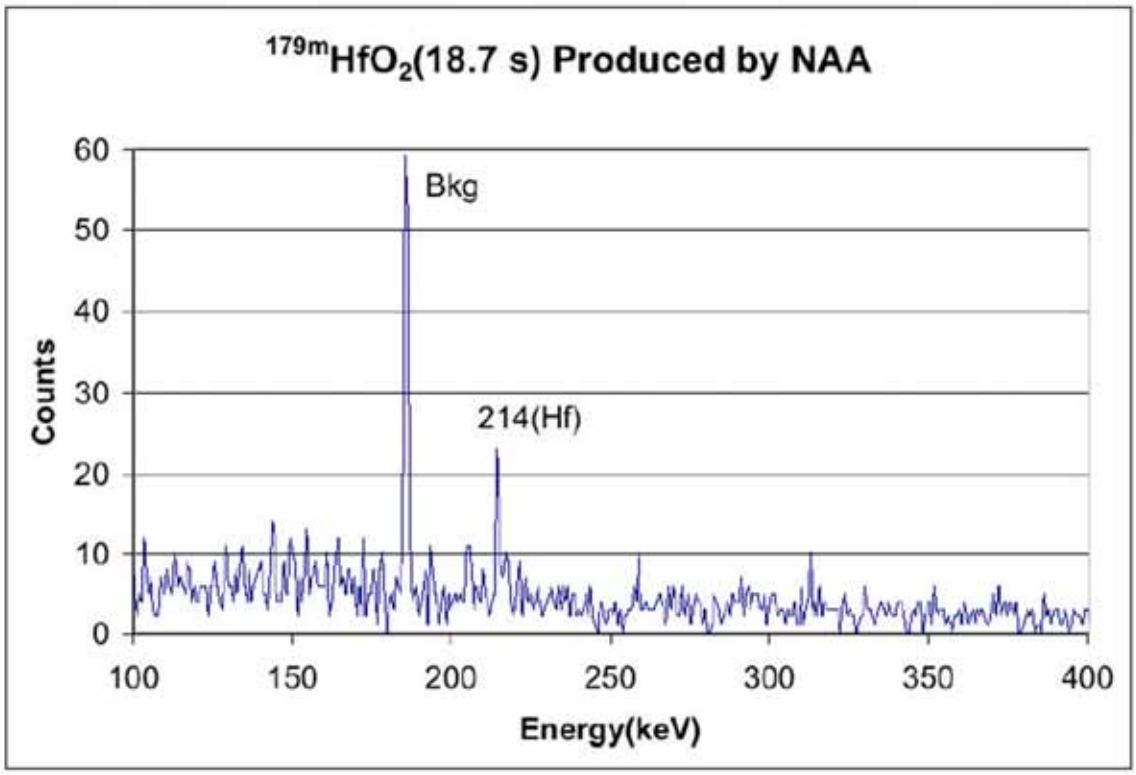

FIG. 41. Analysis of hafnium by $^{178}Hf(n,\gamma)^{179m}Hf(18.67\ s)$.

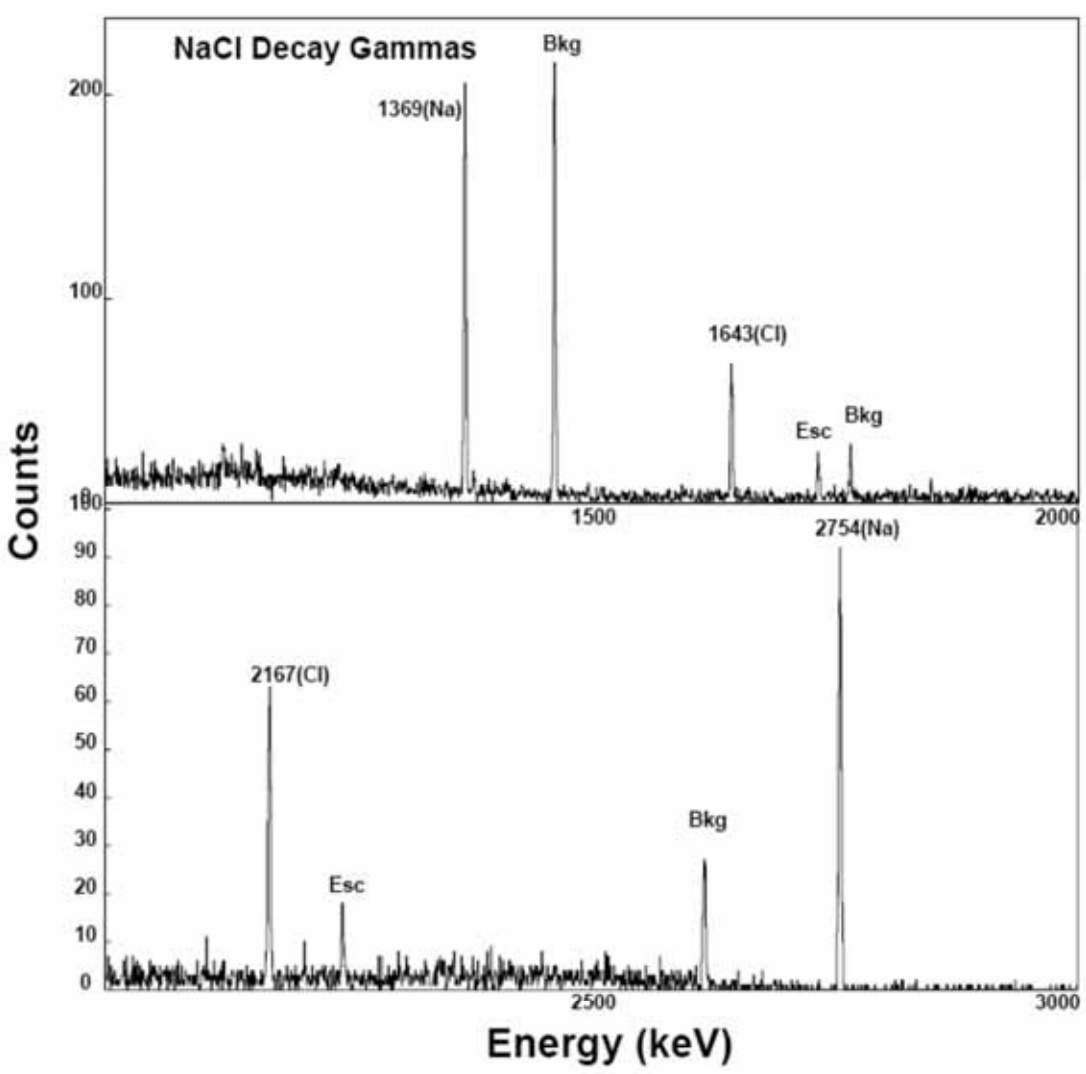

FIG. 42. Analysis of NaCl by $^{23}Na(n,\gamma)^{24}Na(14.95\ h)$ and $^{37}Cl(n,\gamma)^{38}Cl(37.24\ m)$.

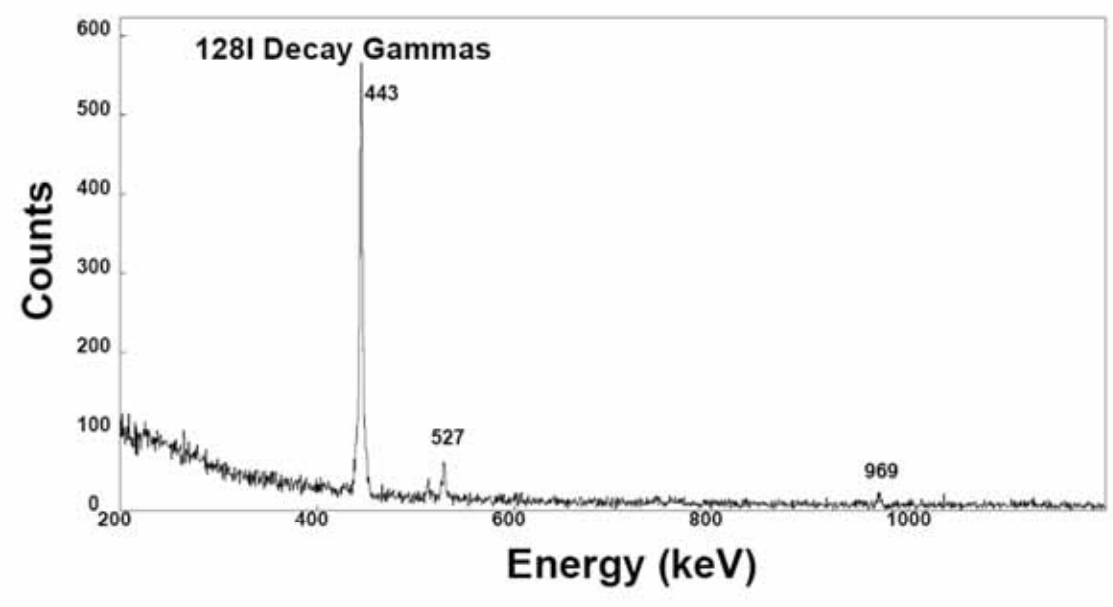

FIG. 43. Analysis of iodine by $^{127}I(n,\gamma)^{128}I(24.99\ m)$.

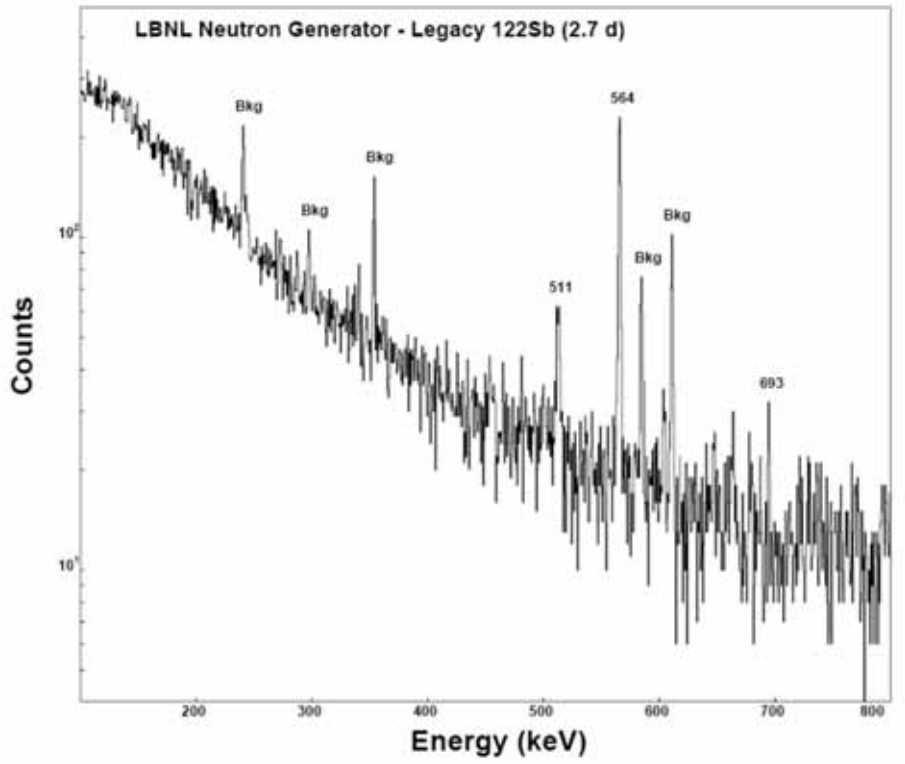

FIG. 44. Analysis of antimony by $^{121}Sb(n,\gamma)^{122}Sb(2.72\ d)$ in LBNL legacy waste.

The fast (>0.5 MeV) neutron flux at the LBNL NG exceeds 10^5 n/s which is suitable for analysis with (n,γ) (n,n'γ) and other fast neutron reactions. FIG. 45 shows a typical spectrum for ^{199}Hg(n,n'γ) from the LBNL NG.

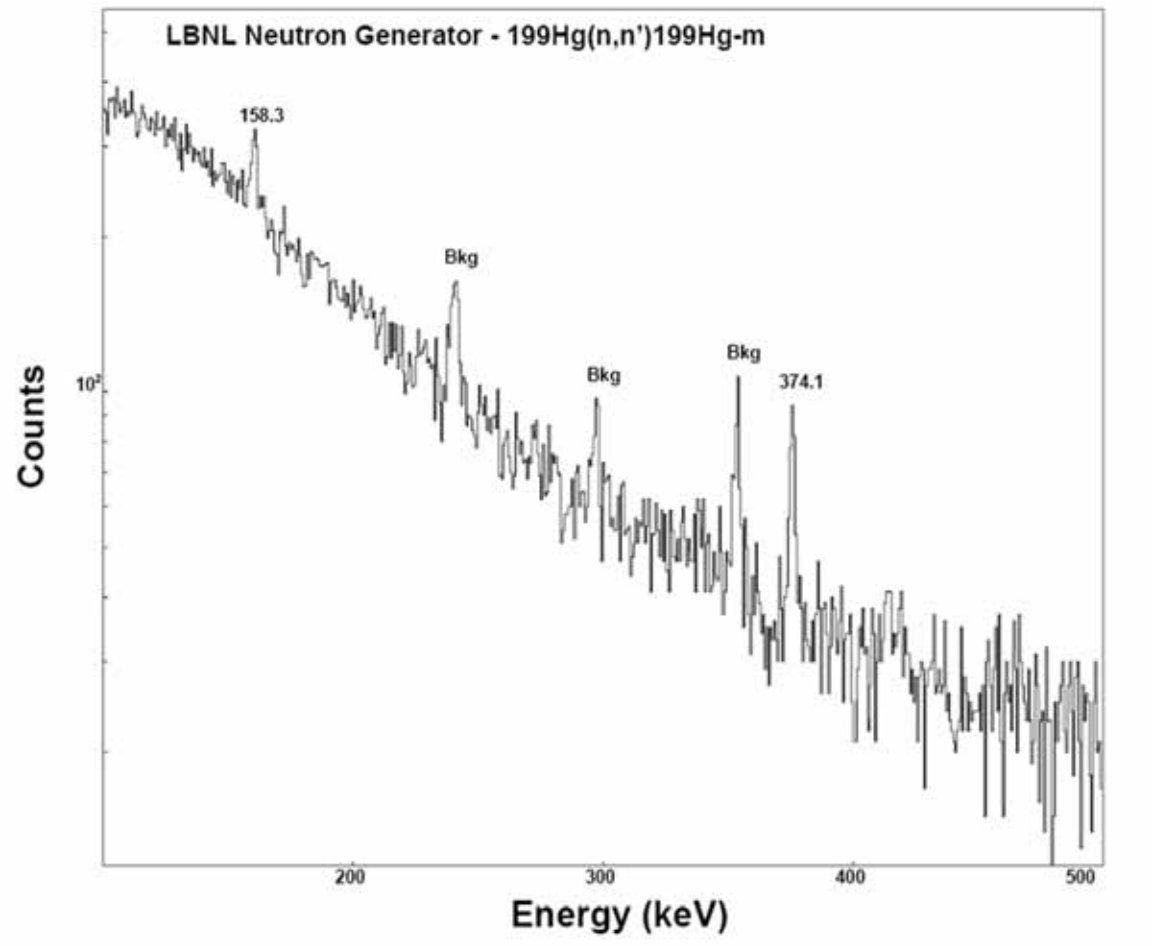

FIG. 45. Analysis of mercury by ^{199}Hg(n,n'γ)^{199m}Hg(42.67 m).

Fast neutrons can also be used for the analysis of uranium by the ^{238}U(n, fission) reaction as shown in FIG. 46. Although uranium can be detected by its natural radiations, the high energy γ rays produced in fission can be used to analyze concealed uranium or determine the uranium enrichment.

A prompt γ ray spectrum recorded at the LBNL NG is shown in FIG. 47. All of the elements contained in the NG and the surrounding shielding are clearly seen. The analyzed C/H ratio from this spectrum is 0.5 consistent with polyethylene.

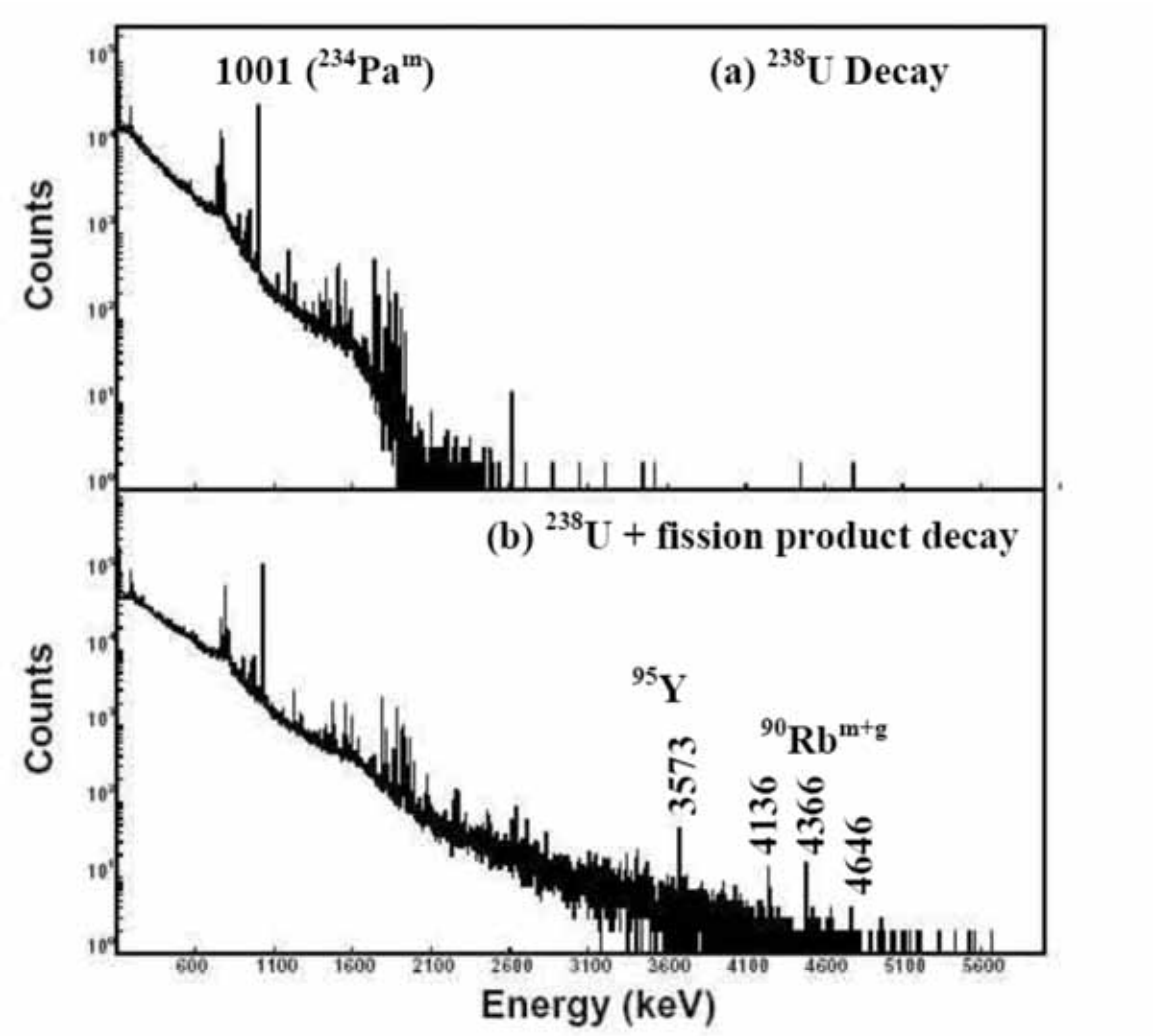

FIG. 46. Analysis of depleted ^{238}U by ^{234m}Pa daughter decay and by ^{238}U(n,fission). Thermal neutrons from DD NG can also be used for PGNAA that is sensitive to all elements from hydrogen to the actinides.

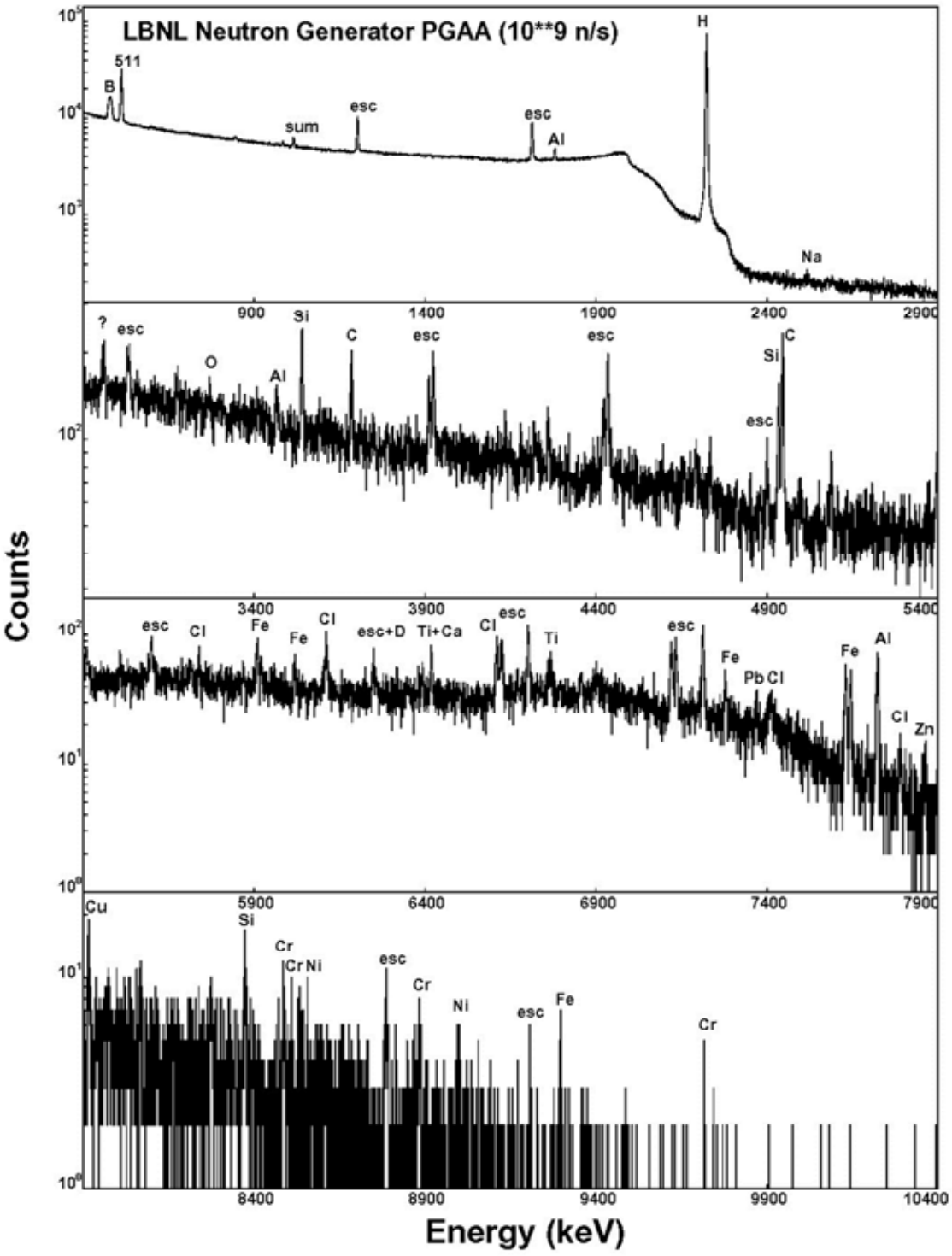

FIG. 47. PGNAA spectrum of the LBNL NG and shielding. 15 observed elements include H, C (polyethylene), Ti (generator target), Fe, Al (support structures), Si, O (concrete floor), Cu, Zn (cooling lines), B (neutron shielding), Pb (gamma shielding), Cl (PVC) and Na, Ni, Cr (miscellaneous).

7.11. Pneumatic transport system

A simple pneumatic transport system for transferring samples from the LBNL NG to a low background counting area is shown in FIG. 48. Samples can be transported for counting in less than one second allowing the analysis of short lived activities.

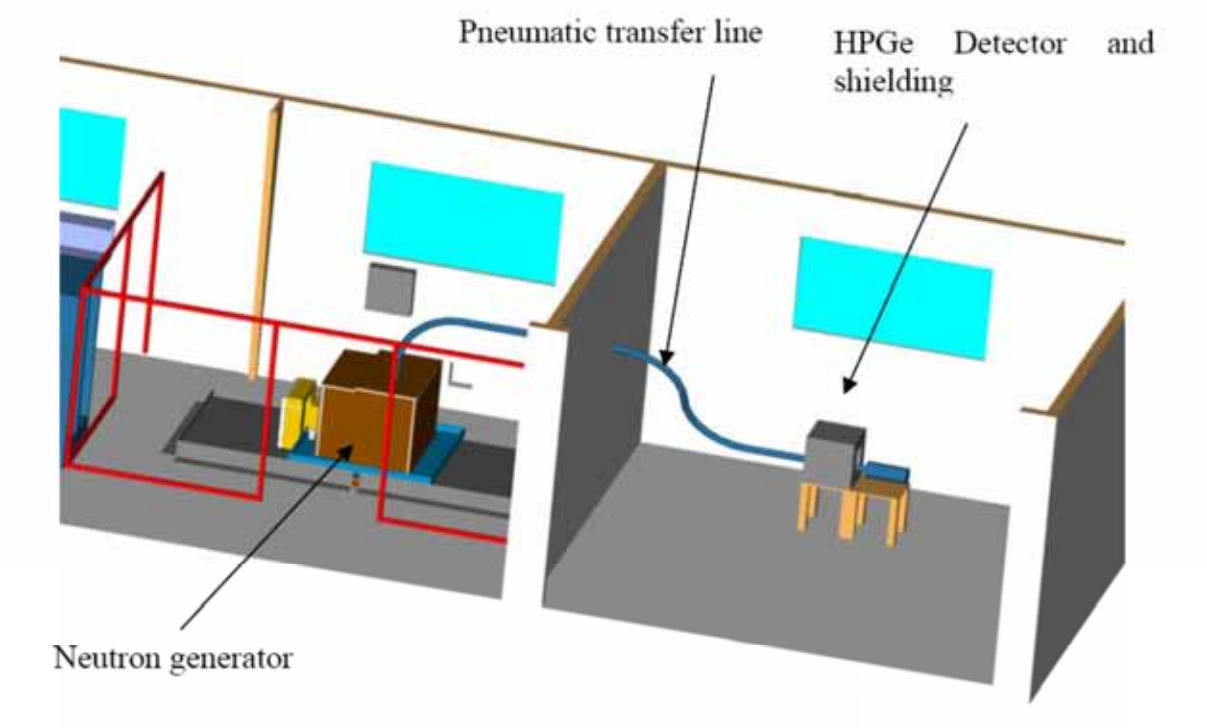

FIG. 48. LBNL pneumatic transport system.

CHAPTER 8
SAFETY AND REGULATIONS

8.1. Introduction

Neutron generators have in the general public a reputation of hazardous material that they do not deserve. They are seen as far more dangerous than familiar X ray instruments of which everybody has received radiation at his dentist or at the hospital. In reality NGs are not so dangerous however they are radiation sources and must be operated in ad hoc installations by specifically skilled people.

The use of NGs with the knowledge of and in compliance with the safety rules and regulations is extremely important. It will allow correcting the wrong image of NGs, and help to develop the use of neutron technology in all industrial applications where it can be beneficial due to its great analytical or imaging capabilities. The willingness of making NG users be aware of safety aspects in order to develop the neutron technology justifies the presence of this chapter, which is not so obvious.

The goal of Chapter 8 is not to be a reference or applicable document. Users are strongly encouraged to refer to official documents provided by the Nuclear Safety Agency of their country. This chapter will not be completely exhaustive and moreover not "official" on this safety subject. The goal is to give a safety overview through the topics 'technical aspects', 'general rules to follow' and 'regulation aspects' in such a way that allows one not to be completely lost in complicated official documents.

8.2. Technical aspects of the neutron generator safety

There are two main hazards with NGs: the electrical hazard and the radiation hazard.

8.2.1. Electrical hazard

As seen in previous chapters, NGs generate neutrons thanks to a nuclear reaction obtained in a target on which ions have been accelerated by an electrical field. To obtain a high level electrical field (typically 100 kV/cm) a high voltage power supply (typically 100 kV) is needed.

However, if the generator is designed according to the norms of the manufacturer, there are no naked pieces under voltage that are accessible. If the connections (mains, ground) are done as indicated in the user manual, and if the generator elements are not modified or opened, there is no electrical hazard. However, in compliance with the legislation (depending on the country), the user will discover legal labels on some parts of its generator warning him against Very High Voltage (VHV) hazards.

8.2.2. Radiation hazards

Neutron generator radiation hazards can be divided into three different categories:

(1) Radiation hazard due to the fact that 14 MeV neutron tubes[3] contain tritium, a radioactive gas.

[3] On the contrary, 2.5 MeV neutron tubes only contain deuterium, which is not radioactive.

(2) Radiation hazard due to neutron and γ emission of a NG during normal operation.
(3) Radiation hazard due to the neutron activation phenomena that makes objects and materials radioactive, including the NG itself.

8.2.2.1. Radiation hazard due to the fact that 14 MeV neutron tubes contain tritium, a radioactive gas

Tritium is a hydrogen isotope that consists of one proton and two neutrons. It is a β emitter (emission of a β particle from one of the neutrons, which becomes a proton) with a half-life of 12.33 years, the maximum energy of the β particle is 18 keV and the average energy is 5 keV. No radiation is measurable outside the tube, because the electrons do not have enough energy to penetrate the wall of the tube.

Tritium is known for the manufacturing of objects that are self-luminous in the dark, for example: exit signs for hotels or airplanes [192], and watches. Tritium is present with Deuterium in 14 MeV neutron tubes. The order of magnitude of the quantity is between 10 and 1000 GBq for specific and high flux NGs.

Generally 3 barriers are present to prevent the tritium from escaping the tube (see FIG. 49):

(1) The barrier of the emission module housing. This housing contains the tube, the VHV connection and also the VHV insulator between the tube's VHV metallic parts and the metallic grounded housing.
(2) The tube barrier itself.
(3) The getter barrier (zirconium, titanium, vanadium, erbium, etc.) that stores the gas inside the tube as metallic hydride.

The escape of tritium is very rare. Moreover, if a leak occurs because of a mechanical problem, air immediately starts to flow inwards, because the pressure inside the tube is generally very low (~0.1 Pa (10^{-3} Torr)). If a leak occurs, the right course of action is to put the tube in a plastic bag and close it. No radiation will come out then.

The toxicity of tritium is very low [193], but it has to be considered. The transient time in the human body is just 10 days [194].

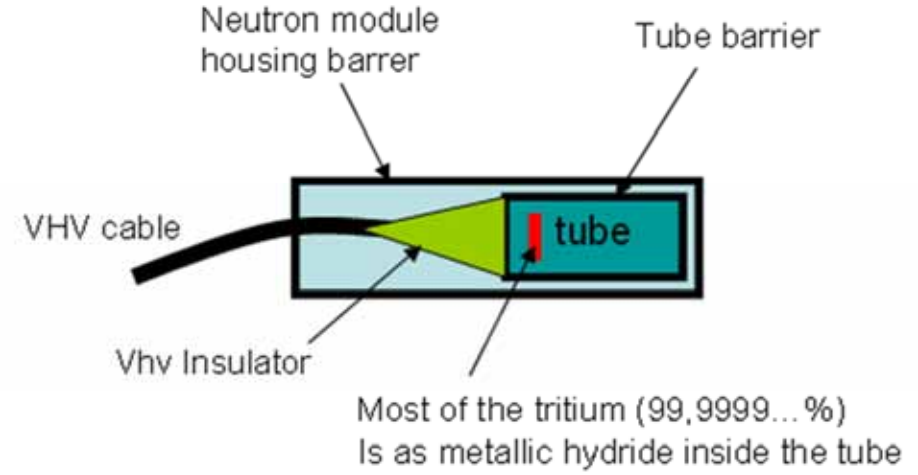

FIG. 49. Scheme of the tritium containment of a 14 MeV NG. The containment consists of three barriers: housing barrier, tube barrier and getter barrier.

8.2.2.2. Radiation hazard due to neutron and γ emission of a NG during normal operation

The main hazard of NGs is obviously the fact that they are radiation emitters, which is what they are built for. The user must take that into consideration before operating them, and he has to know how to protect himself and others from their radiation.

Neutrons are to be considered, and also gammas that are a consequence of the neutron interactions with the materials around the neutron tube target, where the neutrons are created. The neutrons and gammas are produced in 4π sr. Biological consequences of the NG operations must be evaluated before any use. This must be done by calculating the biological dose rate due to neutrons and gammas. To calculate the neutron flux at a given distance from the neutron tube, the following formula can be used:

$$\phi = \frac{S}{4\pi r^2}\ [\mathrm{n \cdot cm^{-2} \cdot s^{-1}}] \qquad (8.1)$$

Where ϕ is the neutron flux at a given distance r from the source, and S is the neutron emission per second. The formula is valid only if there are no obstacles between the source and the location at distance r. Taking into account the energy of the neutrons of 14 MeV, the biological dose rate can be calculated thanks to a conversion factor like those given in TABLE 7 [195]. For instance a flux of 17×10^8 n · cm $^{-2}$ · h $^{-1}$ gives 1 Sv/h, which is 10^6 µSv/h. So 1 µSv/h corresponds to $17 \times 10^8 / (10^6 \times 3600) = 0.47$ n · cm $^{-2}$ · s $^{-1}$

TABLE 7. MEAN QUALITY FACTORS (Q) AND FLUENCE PER UNIT DOSE, EQUIVALENT FOR MONOENERGETIC NEUTRONS

Neutron energy (MeV)	Quality factor[4] (Q)	Fluence per unit dose equivalent[5] (10^8 neutrons · cm^{-2} · Sv^{-1})
2.5×10^{-8}	2	980
1×10^{-7}	2	980
1×10^{-6}	2	810
1×10^{-5}	2	810
1×10^{-4}	2	840
1×10^{-3}	2	980
1×10^{-2}	2.5	1010
1×10^{-1}	7.5	170
5×10^{-1}	11	39
1	11	27
2.5	9	29
5	8	23
7	7	24
10	6.5	24
14	7.5	17
20	8	16
40	7	14
60	5.5	16
1×10^2	4	20
2×10^2	3.5	19
3×10^2	3.5	16
4×10^2	3.5	14

[4] Value of quality factor (Q) at the point of the maximum dose equivalent in a 30 cm diameter cylinder tissue equivalent phantom.

[5] Monoenergetic neutrons incident normally on a 30 cm diameter cylinder tissue-equivalent phantom.

In most cases distance alone is not sufficient to lower the dose rate to an acceptable level and the NG must be operated with shieldings to reduce the dose rate to operators. These shieldings could be the walls of a lab room or shielding put directly around the neutron source. Typical thickness of shielding to reduce the neutron flux and dose rate by a factor of ten is about 38 cm of water or concrete. Highly sophisticated materials are developed to optimize the shielding, namely for fusion reactor research purpose (see FIG. 50).

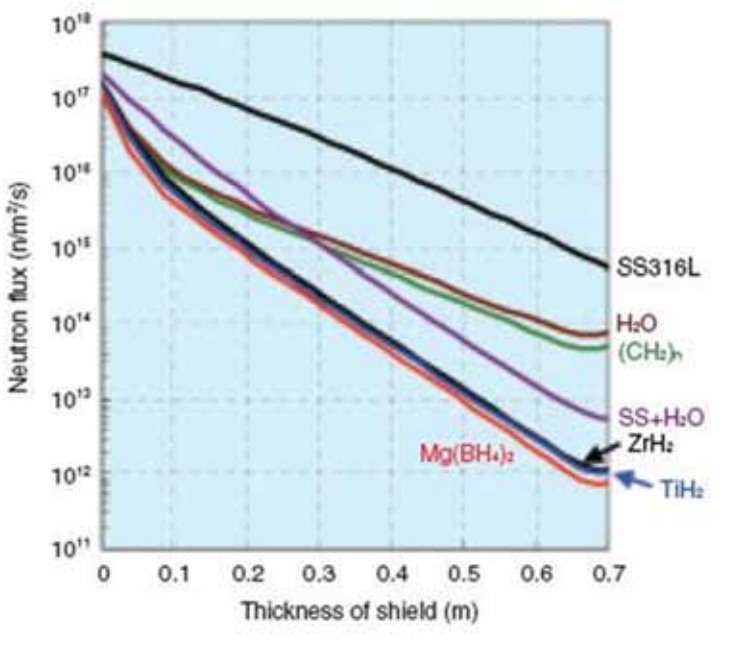

FIG. 50. Attenuations of fast neutron fluxes in 0.7 m thick shields made from various materials. The hydrogen rich hydrides show superior neutron shielding capability compared to the conventional materials. Neutron transport calculations of the 0.7 m thick outboard shields indicated that $Mg(BH_4)_2$, TIH_2 and ZrH_2 can reduce the thickness of the shield by 23%, 20% and 19%, respectively, compared to the combination of steel and water.

NGs generally must not be directly accessible while operational. If accessibility is possible by opening a door or moving a mobile shielding, the NG must be switched off. NGs are usually provided with a safety loop that can be connected to the safety circuit of the lab.

8.2.2.3. Radiation hazard due the neutron activation phenomena

Neutron activation is usually the required physical effect of neutron irradiation, as it allows performing measurements on the sample being irradiated. It is also a drawback as the sample becomes immediately active. Consequently ad hoc operations have to be considered for the management of the activated samples. The activation hazard risk is low with standard NGs, and most importantly one has to deal with the regulations aspects (see Section 8.4).

Levels of activation can be very different depending on the considered object. The final level of activation depends on the mass of the object, the flux it receives and the duration of irradiation. Ranking the activated objects regarding their radioactivity from most activated to least activated generally gives the following list:

(1) NG emission module
(2) Lab structures supporting the NG emission module
(3) Fixed samples exposed to flux
(4) Mobile samples

FIG. 51 shows the approximate dose rate at 4 different distances from a NG emission module, a few minutes after shut down following a continuous emission period varying from a few minutes to 1000 hours at an emission level of 2×10^9 n/s. The dose rate varies from 1 µSv/h to a few mSv/h. For mobile samples the residual artificial radioactivity created in one kilo of cement ore at the output of an industrial analyzer is less than its natural radioactivity (i.e. 450 Bq).

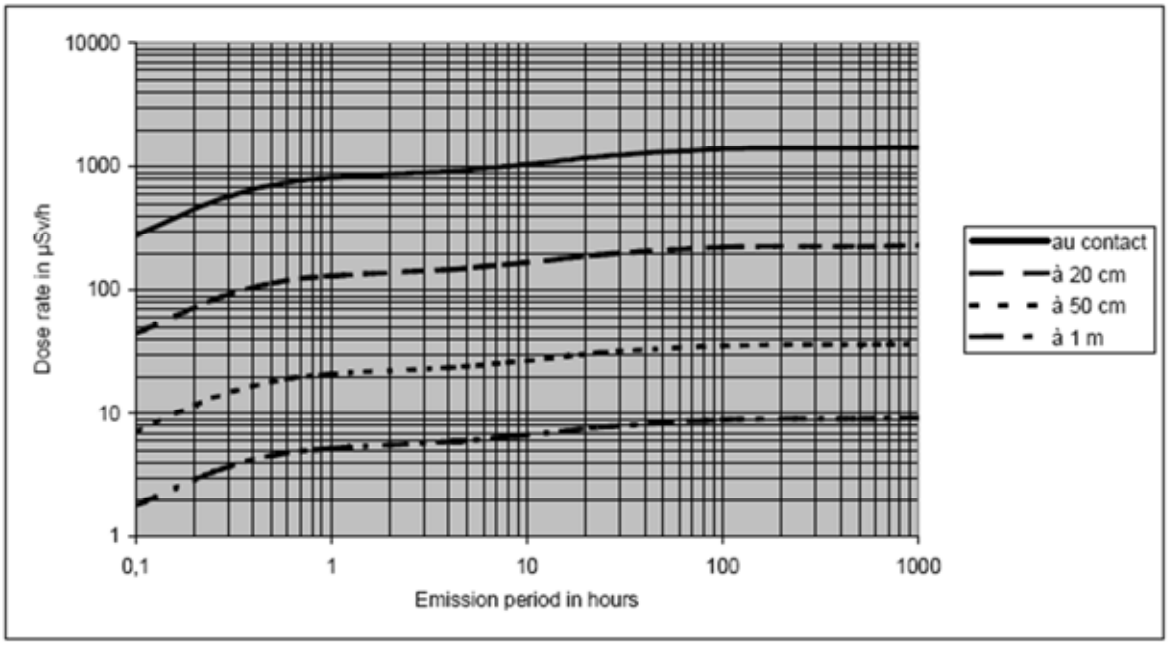

FIG. 51. Dose rates at 0, 20, 50 and 100 cm from a NG emission module after a continuous emission period.

8.3. General rules

The rules mentioned in this section are just common sense rules. They are not part of a safety procedure. Check local and official rules for safety procedures.

8.3.1. Dealing with electrical hazards

— Read and follow all notices from the user's manual.
— Insure that equipment is properly grounded.
— Do not open sub assemblies.

8.3.2. Dealing with radiation hazards

8.3.2.1. Tritium hazards

Tritium can be inhaled, ingested, or absorbed through skin. There is no major leakage of tritium when working with a properly functioning NG (if there is a tritium leakage, some major defect is happening to the sealed tube and the NG can no longer sustain a VHV, thus does not work). A potential problem could arise due to permeation. Few tritium atoms could permeate the walls of the sealed tube, the neutron module housing and other barriers. The final amount of released tritium atoms would be very low, but not null. Permeation can be checked with smear sample measurements.

Some rules to minimize the risks of tritium are:

- Do not open neutron modules.
- Install air extraction in the laboratory (mandatory in some countries).
- Emergency protocol exits. In case of hazards enclose NG in plastic bags.

8.3.2.2. Radiation hazards due to neutron and gamma emission of the NG during normal operation

Some rules to minimize the risks due to radiation emission during normal operation are:

- Design shielding and walls according to the expected maximal flux (or limit the flux according to the existing facility).
- Map the expected dose rate through calculations and compare it with measurements.
- Close the active area access with a safety loop. If safety loop is broken, NG will automatically be stopped.
- Follow local rules to train people and insure utilization of individual dosimeters.

8.3.2.3. Radiation hazards due to activation phenomena

Some rules to minimize the risks of activation radiation are:

- Keep in mind the order of magnitude of level of activation for activated objects (see Section 8.2.2.3).
- Measure the activated objects when samples have to be moved.
- Use labels to store activated objects.
- Follow local rules.

8.4. Regulations

Regulations strongly depend on national rules and policies. Moreover, it depends on national regulations of the NG supplier, and on the national regulations of the NG customer, buyer and user.

8.4.1. Administrative work before buying a NG

Two important topics:

(1) Obtaining authorization according to radiological safety.
(2) Obtaining authorization according to antiproliferation rules.

8.4.1.1. Radiological aspects

The philosophy is: according to national safety organization rules, NG suppliers can only send NGs to proven authorized.

The usual procedure is:

(1) Customers must ask their local authorities for the right to detain and use NGs (NG suppliers are asked to supply a NG brochure for local authority information purposes).
(2) Customers must send their certificate to NG suppliers.
(3) Based on the customer's certificate NG suppliers ask their local authorities for the right to sell and supply customers with the requested NGs.

8.4.1.2. Anti-proliferation rules which apply for any NG

The philosophy is: the NG supplier national administration has (likely) committed to the United Nations about controlling the export of 'dual use' products (civilian and military). Based on a filed form by the customer, NG suppliers must get a license from its administration before delivering the NG to a customer.

(1) Customers must provide information for the NG provider. This information could be defined by specific forms that the NG provider can send to his prospect. Typically the minimum information required to fill in these forms is the identification of end-users, typical use of NG and place where the NG will be used and stored. Information about final use should also be a commitment to use it as described.
(2) NG suppliers provide information and commitment to their national authorities to get the license.

When the NG supplier has all authorizations, NG can be shipped. The administrative procedure typically takes several weeks to months.

8.4.2. Regulations for operation

Only national regulations apply. Users must receive authorization from their administration to operate NG. This process could be simple or complicated, be short or long time consuming, depending on the level of details that has to be provided, which depends highly on the neutron flux that has to be considered.

8.4.3. Regulations about NGs end of life

Regulations about NGs end of life depend also only on the supplier's and customer's national regulations. Some countries require the neutron tube to be sent back to NG suppliers after ten years. NG suppliers usually have the necessary equipment to recycle NGs at their end of life.

It must be noticed that sending back NGs at their end of life (or at any time) must be done according to the process described in Section 8.4.1.1 where customer and NG provider switch roles.

CHAPTER 9
STUDY OF THE OPTIMAL PERFORMANCE OF A NEUTRON ACTIVATION ANALYSIS FACILITY BASED ON A DD NEUTRON GENERATOR

9.1. Introduction

In FIG. 52 a basic neutron activation facility is represented. The sample can be placed for PGNAA in two positions, inside the moderator in an internal configuration or in a neutron beam in an external configuration. For NAA, the sample is irradiated using “rabbit tubes” enabling fast transfer to a counting facility. The variables of design of this system are many, but the most important are:

(1) The intensity, energy and geometry of the deuteron beam of the NG.
(2) The material, geometry and size of the moderator.
(3) The material and thickness of neutron shielding.
(4) The material and thickness of gamma shielding.
(5) The sample’s place, in an external or internal configuration.
(6) The material and size of the gamma detector.
(7) The electronics’ settings, one or two detectors can be used by either coincidences or summing modes.

Other variables are:

(1) Construction materials and size of the NG.
(2) Temperature of the moderator.
(3) Impurities of the moderator.
(4) Sample container materials.
(5) Structural materials of the system.

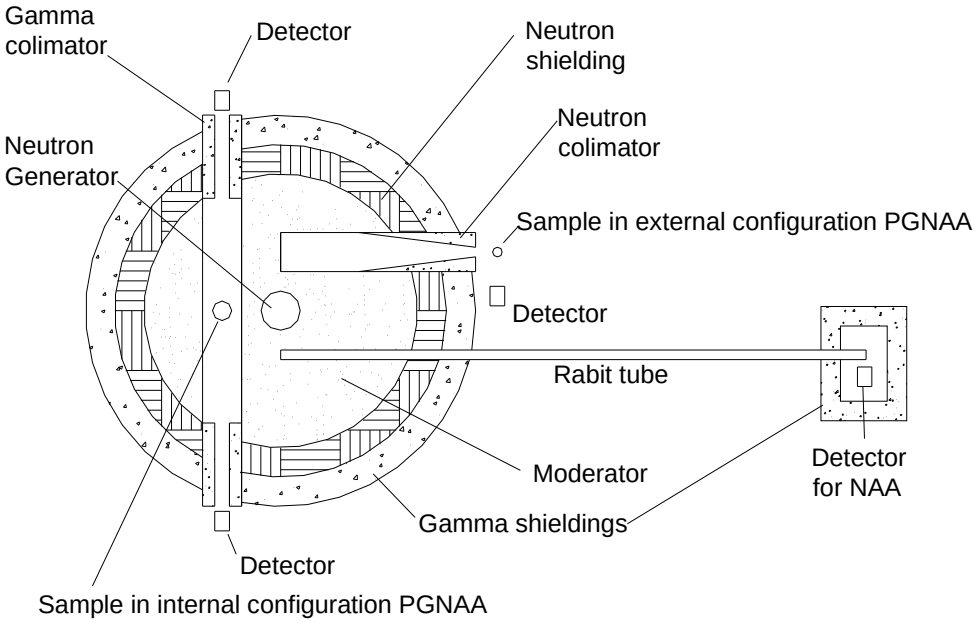

FIG. 52. Basic schema of a NAA and PGNAA facility.

The performance of the facility depends on the selection of all those variables. Some of them can be studied using simplified models, but others need more complex calculations such as Monte Carlo simulations. The purpose of this chapter is to explain and justify the design criteria for optimizing a neutron activation facility based on a DD NG.

9.1.1. The optimal design concept

For PGNAA the number of gammas of energy E_{ijk} due to the presence of the element *i* is:

$$C(E_{ijk}) = \frac{m_i\, I_{ij}\, N_A}{M_i}\, \sigma_{ij}\, G\, \phi\, \Gamma_{ij}(E_{ijk})\, S(E_k)\, \varepsilon(E_k)\, Tc \tag{9.2}$$

where:

- m_i is the mass of the element *i* in the sample
- I_{ij} , the isotopic abundance of the emitting isotope
- N_A , the Avogadro number
- M_i , the molar mass of the element.
- σ_{ij} , the mean activation cross-section of the isotope.
- G , the neutron self-shielding factor.
- ϕ, the total neutron flux.
- Γ_{ij} , the prompt gamma yield per capture.
- $S(E_k)$, the gamma self-shielding in the sample
- $\varepsilon(E_k)$, the total efficiency of counting
- Tc , the counting time.

The subscripts *i*, *j*, *k* indicates the element, the isotope and the gamma energy respectively. For NAA the number of gammas is

$$C(E_{ijk}) = \frac{m_i\, I_{ij}\, N_A}{M_i}\, \sigma_{ij}\, G\, \phi\, \Gamma^*_{ij}(E_{ijk})\, S(E_k)\, \varepsilon(E_k)\, F_T \tag{9.3}$$

where:

- $F_T = \frac{\left(1 - e^{-\lambda Ti}\right) e^{-\lambda Tw} \left(1 - e^{-\lambda Tm}\right)}{\lambda}$, is the time factor.
- λ, the decay constant.
- Ti, the irradiation time.
- Tw, the time between the end of irradiation and the beginning of counting, and.
- $\Gamma_{ij}^*(E_k)$, the gamma emission yield per decay

The mean cross-section σ_{ij} depends on the neutron flux energy spectrum $\phi(E)$ and it is given by:

$$\sigma_{ij} = \frac{\int_0^\infty \sigma_{ij}(E)\,\phi_0(E)\,dE}{\int_0^\infty \phi_0(E)\,dE} = \frac{\int_0^\infty \sigma_{ij}(E)\,\phi_0(E)\,dE}{\phi_0} \tag{9.4}$$

And the *G* factor, by:

$$G_{ij} = \frac{\int_{SampleVolume} \int_0^\infty \sigma_{ij}(E)\ \phi(r,E)\,dE\,dV}{V\int_0^\infty \sigma_{ij}(E)\,\phi_0(E)\,dE} = \frac{\int_{SampleVolume} \int_0^\infty \sigma_{ij}(E)\ \phi(r,E)\,dE\,dV}{V\sigma_{ij}\,\phi_0} \tag{9.5}$$

where the sub index "0" indicates the flux at the surface of the sample. In most of cases the neutron flux can be described approximately as the sum of three components: a maxwellian thermal flux, an epithermal moderation spectrum and the fast neutron source's spectrum:

$$\phi(E) \approx \phi_T \frac{E}{E_T} e^{-\frac{E}{E_T}} + \phi_E \frac{\Delta(E)}{E^{1+\alpha}} + \phi_F(E) \tag{9.6}$$

ϕ_T is the integrated thermal neutron flux, E_T is the most probable energy of the maxwellian distribution, ϕ_E the epithermal constant, $\Delta(E)$ the "joint function" and $\phi_F(E)$ is the fast neutron source spectrum. If the number of thermal reactions is much bigger than the others, the mean cross-section can be easily calculated:

$$\sigma_{ij} = \sqrt{\frac{\pi}{4}}\sqrt{\frac{T_0}{T}}\sigma_0^{ij}\ g(T) \tag{9.7}$$

where *g(T)* is the Wescott factor, *T* the temperature of the maxwellian distribution,(E_T=k_B *T*) and the sub index "0" here indicates the reference energy, 0.0253 eV.

Also, the G_{ij} factor can be more easily calculated with thermal neutrons because the cross-sections are almost *1/√E*, and it becomes independent of the element and the isotope. This is very useful in relative determinations in PGNAA where this factor could be cancelled. In NAA small samples (~milligrams) are used in order to make it as close to 1 as possible and minimizing the relative uncertainty in its calculation. For this reason a high flux ($>10^{10}$ n · cm^{-2} · s^{-1}) is needed for analyzing ppm or ppb concentrations.

The analysis of the sample is first performed identifying the lines of the gamma spectra produced by each component. The net number of counts $C(E_{ijk})$ is determined subtracting the background area, $B(E_k)$, from the gross area, ($C(E_k)$ + $B(E_k)$), around the energy E_k in the gamma spectra:

$$C(E_{ijk}) = \big(C(E_k) + B\big) - B \tag{9.8}$$

The minimum number of counts above the background to reach a required uncertainty in $C(E_{ijk})$ is known as the "determination limit" L_Q and it is expressed as [145]:

$$L_Q(i) = \frac{1}{2} k_Q^2 \left(1 + \sqrt{1 + \frac{4\sigma_B^2}{k_Q^2}} \right) \tag{9.9}$$

where k_Q is the inverse of the required relative standard deviation and σ_B is the standard deviation of the background. So, for PGNAA (thermal reactions), the minimum mass of the element *i* that can be measured with a relative uncertainty k_Q in the counts is:

$$m_i = \frac{M_i}{0.886\, I_{ij}\, N_A\, \sigma_0^{ij}\, \Gamma_{ij}(E_{ijk})\, g(T)\, G\, S(E_k)} \frac{L_Q(i)}{\sqrt{T_0 / T}\, \phi\, \varepsilon(E_k)} \frac{1}{Tc} \tag{9.10}$$

And for NAA is:

$$m_i = \frac{M_i}{0.886\, I_{ij}\, N_A\, \sigma_0^{ij}\, \Gamma_{ij}^{*}(E_{ijk})\, g(T)\, G\, S(E_k)} \frac{L_Q(i)}{\sqrt{T_0 / T}\, \phi\, \varepsilon(E_k)} \frac{1}{F_T(Ti, Tw, Tc)} \tag{9.11}$$

The first factor of Eqs (8.9) and (8.10) are constants; the second one depends of the facility performance and the last one on the experimenter considering the needed uncertainty, the cost of the analysis and his/her patience. When the background count rate is higher than count rate of the sample, $L_Q \approx k_Q\, \sigma_B$. So, it can be concluded to obtain the optimal design for measuring the minimum mass of every elements in the worst counting conditions, the following condition must be met:

$$\textbf{The maximum } \frac{\sqrt{T_0 / T}\, \phi\, \varepsilon}{\sigma_B}$$

Two other parameters must also be considered in the optimization:

(1) The (thermal + epithermal) to fast fluxes ratio, $(\phi_T + \phi_E) / \phi_F$.
(2) The thermal flux to epithermal constant ratio, ϕ_T / ϕ_E.

The first one determines the relation between the absorption to fast reactions rates, and it is related with probability of the production of the same isotope by different components of the sample. This possible interference could complicate the analysis. The second parameter must be considered in the calculation of the total reactions. The epithermal absorptions are difficult to quantify because of the neutron self-shielding in the cross-section resonances. Furthermore, the prompt gamma yields of the epithermal absorptions are not measured yet. So, a second criterion of optimization can be established[6]

The more thermal the flux, the easier is the analysis.

A thermal to epithermal ratio (*T/E*) and a thermal to fast ratio (*T/F*) of about 1000 is enough to depreciate other reactions.

[6] also exists NAA with fast neutrons, but they aren't considered here.

9.1.2. Radiological safety and practical limits

The highest recommended radiation dose for workers is 20 mSv per year in the USA. This limit establishes a reference dose rate of 10 μSv/h for a 2000 hours working year. In the surroundings of a NAA facility this rate is enough because the sample can be measured far away from it. But in PGNAA, where the detector must be close to the wall of the facility, this dose rate can saturate the spectrometer or destroy the detector. It is reported that 3 fast neutrons per square centimetre can severely damage one HPGe in 10 years [84]. A common gamma spectrometer can process approximately count rates of the order of 10^4 cps without an important dead time. If it is considered that the tenth part of it could be background, for a 3-inch detector, this means approximately 20 photons $\cdot$ cm $^{-2} \cdot$ s $^{-1}$. On the other side, a reasonable and practical lower limit could be the same count rate produced by the environment through a 10 cm thick lead shield: ~0.1 ph $\cdot$ cm $^{-2} \cdot$ s $^{-1}$.

9.1.3. Design requirements

As a conclusion of this chapter it can be summarized and established the following optimal requirements:

- 3 $n_F \cdot$ cm $^{-2} \cdot$ s $^{-1}$ (~5 μSv/h for neutrons) and 1 ph $\cdot$ cm $^{-2} \cdot$ s $^{-1}$ (~0.01 μSv/h for gamma) at the detector position.
- 3 $n_F \cdot$ cm $^{-2} \cdot$ s $^{-1}$ (~5 μSv/h for neutrons) and 100 ph $\cdot$ cm $^{-2} \cdot$ s $^{-1}$ (~1 μSv/h for gamma) at facility wall.
- The maximum $\sqrt{T_0 / T}\ \phi \varepsilon / \sigma_B$.
- A thermal to fast neutron flux ratio $(\phi_T + \phi_E) / \phi_F$ of ≥1000.
- A thermal to epithermal neutron flux ratio ϕ_T / ϕ_E ≥1000.

9.2. Optimization description

A NAA facility is performing better when the neutron flux is high and most thermalized as possible; no other parameters have to be considered in the design. The sample is placed inside the facility and the activity of the sample is subsequently measured in a counting room. But a PGNAA facility is more complicated because the measurement and the irradiation are simultaneous. A minimum shield's thickness is needed for protecting the detector against the fast neutrons. The sample can be placed either near the neutron source where the flux is high but counting has low efficiency, or close to the detector in the opposite situation. The design is optimized in increasing order of complexity. The applied steps are:

(1) Selection of the best moderator.
(2) Determination of the minimum size of moderator and shielding.
(3) Determination of the best configuration and sample placing.
(4) Test of the best design.

By testing a very simple facility model with MCNP the best moderator is selected. This calculation tool represents as accurately as possible, the neutron and γ rays transport with the minimum number of assumptions. The model consists of a point isotropic neutron source of 2.5 MeV surrounded by a moderator. The tested moderators are:

(1) Light water (LW) (100% Pure)
(2) Polyethylene (Poly) (100 % Pure)
(3) Heavy water (HW) (reactor grade 99.8% molar).
(4) Heavy water (HW) (99.99% molar).
(5) Graphite (G) (100% pure)
(6) Beryllium (Be) (100 %Pure)
(7) Beryllium Oxide (BeO) (100% Pure)

The test consists in the calculation of the maximum thermal flux, the minimum moderator's and gamma shelving's thickness in order to fulfil the proposed requirements. The selected shielding materials are:

(1) Boron Carbide. (CB_4): Boron has a very high cross-section and its γ rays have low energy. It is not toxic in the manipulation, it doesn't produce any radioactive isotope and it is chemically inert. In addition to that, it has very low fast neutron yield by the bombarding of the produced alphas.
(2) Lead. (Pb): It is one of the highest *Z* materials, it has low neutron absorption cross-section and it is cheap. Some care has to be taken in the manipulation and melting because it is toxic if it is ingested or inhaled.
(3) Enriched Lithium Fluoride. (^{6}LiF): This material does not produce any gamma in the absorption reaction, but it is very expensive, it produces tritium and it has a high fast neutron yield per triton (~10^{-4}). It is needed only in the neutron irradiated surfaces viewed by the gamma detector.

To study the variations on the geometry and the configuration: internal versus external (with the selected materials) a very simply mode is used. The thermal neutron flux is calculated with the theory of age and the gamma detection efficiency is simply the geometric efficiency. Here the MCNP is not applied because a continuous variation on the geometry is needed, and the number of possible configurations is almost infinite. A more versatile and faster tool is needed to guess if some configuration is better than another, and then the best of them are tested with MCNP.

9.2.1. The simplified model

The optimal configuration is deduced by modelling the geometric dependence of the flux and the efficiency with the following equations: For the internal configuration the thermal neutron flux inside a spherical non-hydrogenous heavy moderator, can be calculated as follows [196]:

$$\phi_{th}(r) = \frac{Q}{2\Sigma_a R^2 r} \sum_{l=1}^{\infty} \frac{l}{1+\left(\frac{l\pi L}{R}\right)^2} e^{-\frac{l^2\pi^2}{R^2}\tau} \sin\left(\frac{l\pi r}{R}\right) \tag{9.12}$$

where

— *Q*, is the intensity of the NG,
— Σ_a, the macroscopic cross-section of the moderator,
— *R*, its radius,
— *L*, its diffusion length,
— τ, the age of neutrons,

— *r*, is the position, for example where can be placed the sample.

For an external configuration, the flux outside the system could be approximated roughly as:

$$\phi_{beam}(r,R,re,rs) \approx \frac{\phi_{th}(re,R)}{2}\left(1-\frac{1}{\sqrt{1+\left(\frac{rs}{r}\right)^2}}\right) \tag{9.13}$$

where

— *r* is the position of the sample measured from the inner end of the extraction tube,
— *R* is the radius of the moderator,
— *re* is the position of the inner end of the tube relative to the NG,
— *rs* is the radius of the inner end of the tube.

This equation considers that the inner end of the tube emits the neutrons isotropicaly with an intensity equal to the half of the flux without the tube perturbation. The geometric efficiency in both configurations is calculated as:

$$\varepsilon(rd,D) = 1-\frac{1}{\sqrt{1+\left(\frac{rd}{D}\right)^2}} \tag{9.14}$$

where *rd* is the detector diameter and *D* the distance to the sample. The intrinsic efficiency of detector is not considered in this work and a typical 3-inch wide detector is assumed for all the calculations. For PGNAA it could be recommended a minimum *D* ~20 cm in order to avoid “true coincidences” in the compound nucleus cascade de-excitation.

As it has been explained in the introduction, the system has to have a minimum size for reducing the dose at its surface up to maximum required levels. This minimum size due to the attenuation of fast neutrons can be calculated from the equation:

$$\phi_{fast}(R+X_{NS}) = \frac{Q}{4\pi\left(R+X_{NS}+X_{GS}\right)^2} e^{-\left(\Sigma_M R+\Sigma_{NS}X_{NS}\right)} \tag{9.15}$$

where X_{NS} is the thickness neutron shielding, X_{GS} is the thickness gamma shielding, and Σ are the macroscopic removal cross-section for fast neutrons (E>1 MeV) for each material. The minimum thickness of the gamma shielding with an attenuation constant of μ is given approximately by:

$$\phi_{\gamma}(R+X_{NS}+X_{GS}) \approx \phi_{\gamma}(R+X_{NS})\, e^{-\mu X_S} \tag{9.16}$$

Eqs. (8.11) to (8.15) are modelling the geometric dependence of the flux, the efficiency and the fluxes outside the facility in order to find the optimal configuration with the selected materials.

9.2.2. Monte Carlo N-particle transport code modelling

The MCNP is a useful and accurate tool for studying this type of systems where neutrons produce γ rays in complex geometries. The MCNP5 running in a PC [197] is used for this work. The MCNP input includes the following definitions:

(1) The source geometry, energy and angular distribution of generated particles.
(2) The geometry and materials of moderators and shielding.
(3) And the "tallies", the places where is calculated the flux.

The neutron source is modelled as a simply point emitting neutrons of 2.5 MeV. An intensity of 10^{11} n/s (of the most powerful DD NG found at the moment [198] is assumed to dimension the system. By using tallies type 4 the neutron flux at the sample positions is calculated, by using type 5 at the detector position and by type 2 at the surface of the facility. The following definitions of neutron energy ranges are considered: fast (E>1 MeV), epithermal (0.5 eV< E <1 MeV) and thermal (E<0.5 eV) neutrons.

The applied factors to convert photon and gamma fluxes to dose are taken from the ICRP criteria extracted from the MCNP manual. A maximum uncertainty of 20% for this estimation is assumed. An interpolation curves from these factors are shown in FIG. 53 and FIG. 54.

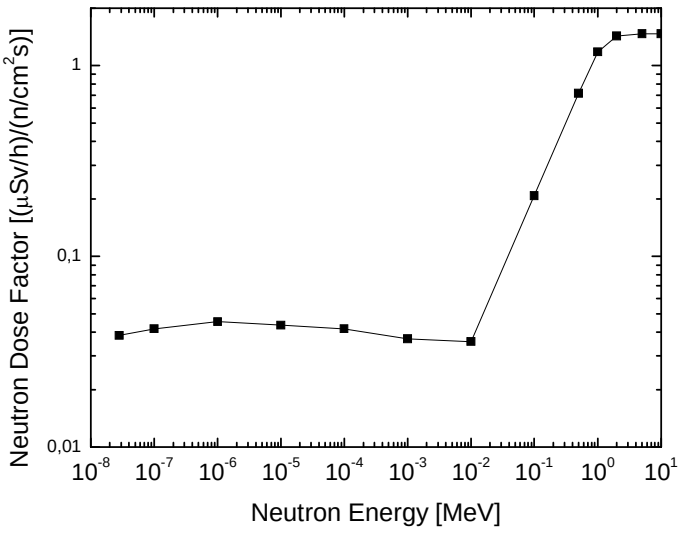

FIG. 53. Neutron Flux to dose conversion factor.

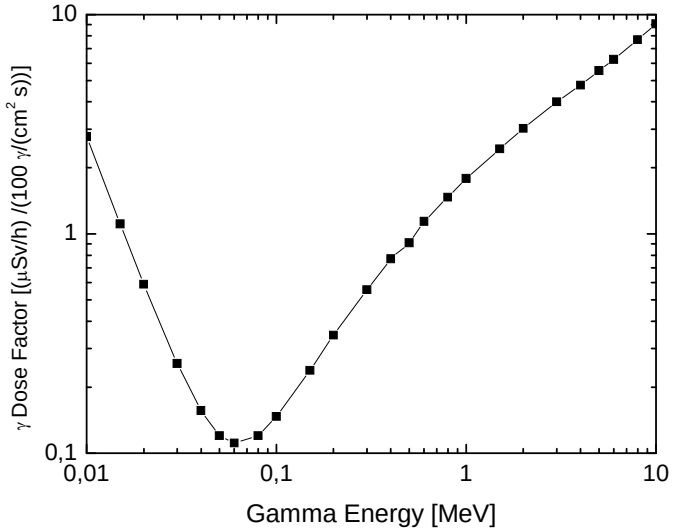

FIG. 54. Photon flux to dose conversion factor.

9.3. Results

9.3.1. Selection of the best moderator with MCNP

The attenuation of the neutron group from 1 to 2.5 MeV is shown in FIG. 55. This case corresponds to an isotropic source of 2.5 MeV inside a spherical moderator of 100 cm of radius. It can be seen that the best fast neutron shielding is polyethylene, and the worst is graphite. Heavy water, Beryllium and Beryllium Oxide have almost the same behaviour, and light water is a little better than these, but not as good as the polyethylene. The minimum radius needed to accomplish the proposed maximum fast flux at the detector is shown in TABLE 8.

The thermal flux produced by those moderators is shown in FIG. 56. The polyethylene and the water have the highest ones, but they decrease very fast. On the other hand, the other moderators have lower values, but they have almost a constant spatial distribution. The maximum values are summarized also in TABLE 8.

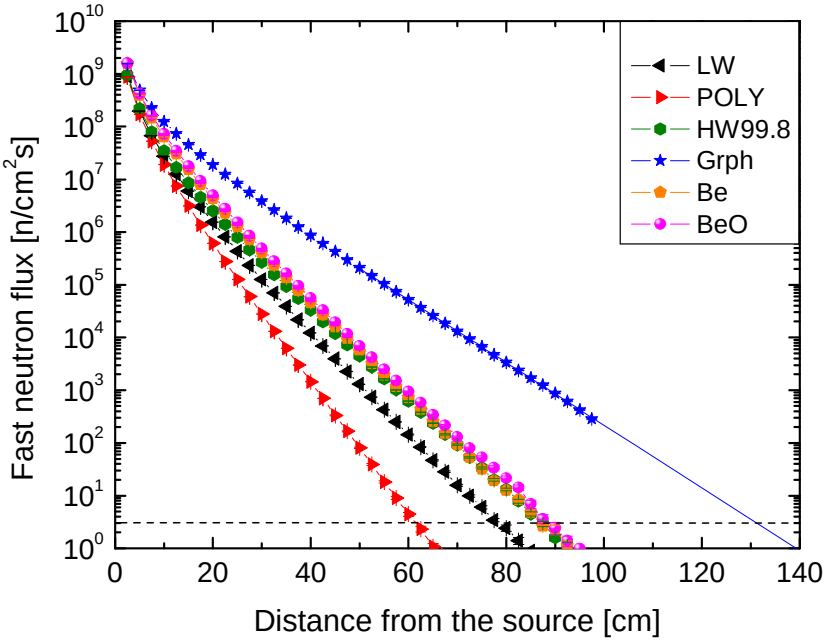

FIG. 55. Distribution of fast neutron flux over different moderators: light water (LW), polyethylene (POLY), heavy water 99.8% molar (HW99.8), Graphite (Grph), Beryllium (Be) and Beryllium Oxide (BeO).

The gamma photon distributions can be seen in FIG. 57 and the integral of those distributions are shown in TABLE 8. In spite of the very low absorption of Be, BeO, Graphite and the D_2O, they produce a very large number of photons of high energy. The needed thickness of lead for shield this radiation is also shown in TABLE 8.

TABLE 8. TESTED MODERATOR'S PERFORMANCE

Material	Min. R (cm)	Max. ϕ_{TH} (10^8 n · cm^{-2} · s^{-1})	ϕ_γ at surface (ph · cm^{-2} · s^{-1})	Min. X_{Pb} (cm)	Max. $\phi_{TH}\,\varepsilon$ (n · cm^{-2} · s^{-1})
LW	78	8.3	4.1×10^5	28	5.6×10^5
POLY	63	12	1.2×10^6	30	1.0×10^6
HW99.8	85	4.05	7.3×10^4	25	2.6×10^5
HW99.99	85	4.08	4.7×10^4	24	3.1×10^5
GRPH	130	1.8	4.3×10^5	30	5.8×10^4
Be	85	5.1	4.9×10^5	30	3.0×10^5
BeO	85	5.5	1.2×10^6	32	3.1×10^5

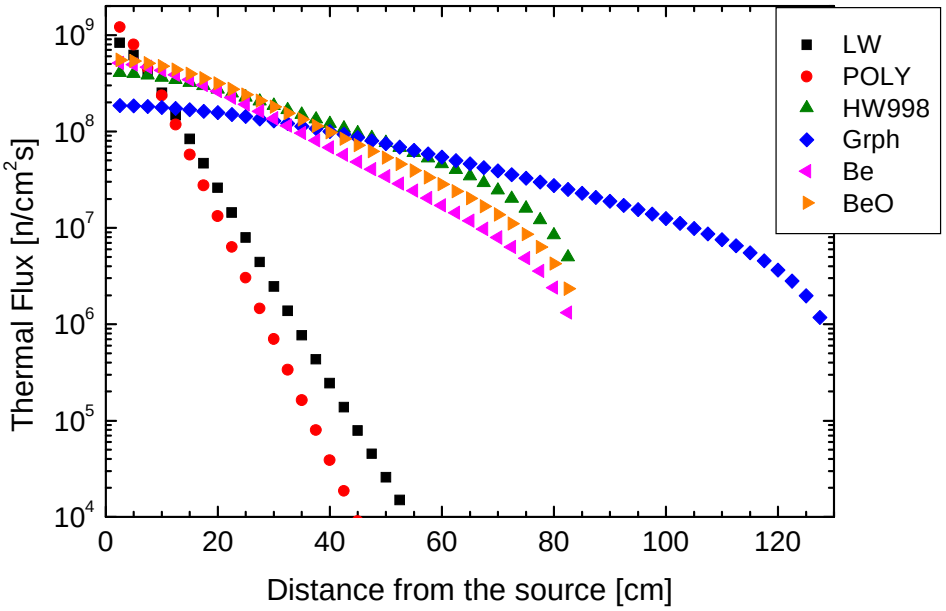

FIG. 56. Thermal neutron flux over different moderators.

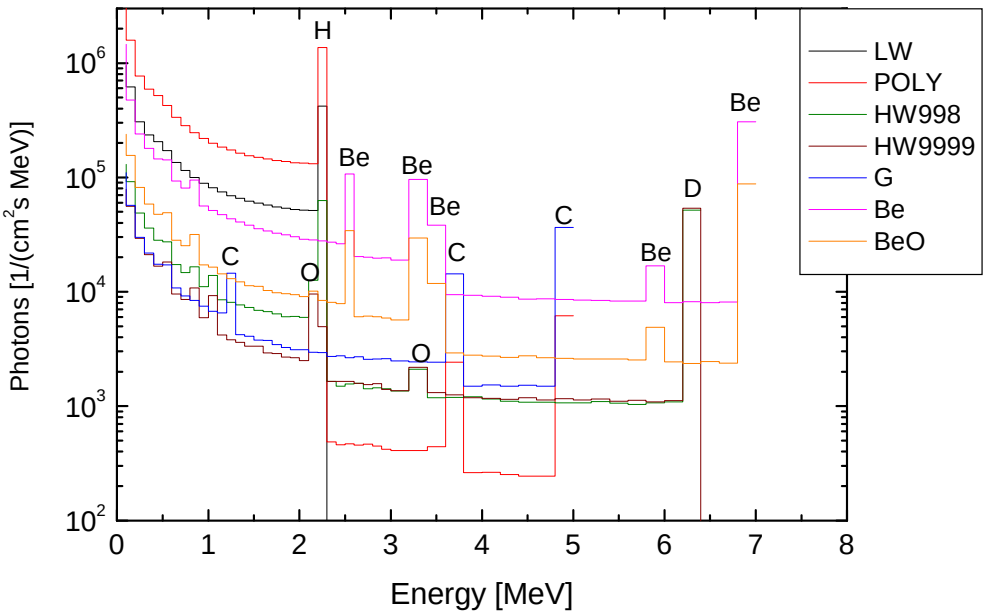

FIG. 57. Gamma spectra at the surface of the moderator.

By applying the simplified model the performance of the internal configuration facility can be calculated. This model does not consider the perturbation of inserted voids on the flux. In TABLE 8 and FIG. 58 the results are shown. The highest flux and compactness of the polyethylene produce the best performance, 3 times better than the non-hydrogenous moderators.

The other quality parameters $(\phi_T + \phi_E) / \phi_F$ and ϕ_T / ϕ_E are shown in FIG. 59 and FIG. 60 respectively. Here, the best moderators are the Be, BeO, Graphite and the D_2O, and the worst are the hydrogenated ones that reach a maximum of about $(\phi_T + \phi_E) / \phi_F$ ~20 and ϕ_T / ϕ_E ~100. The maximum values for the non-hydrogenous moderators depend on their sizes. For example, the D_2O has $(\phi_T + \phi_E) / \phi_F$ (r=80) ~10^6 and ϕ_T / ϕ_E (r=80) ~10^5, becoming a real thermal column.

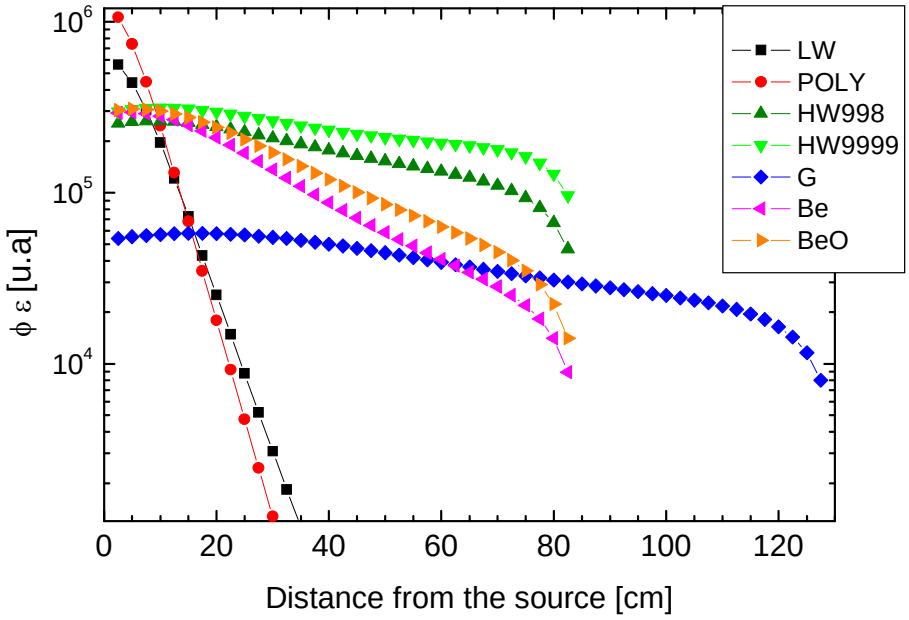

FIG. 58. Imaginary performance $\phi\varepsilon$ for the selected moderators.

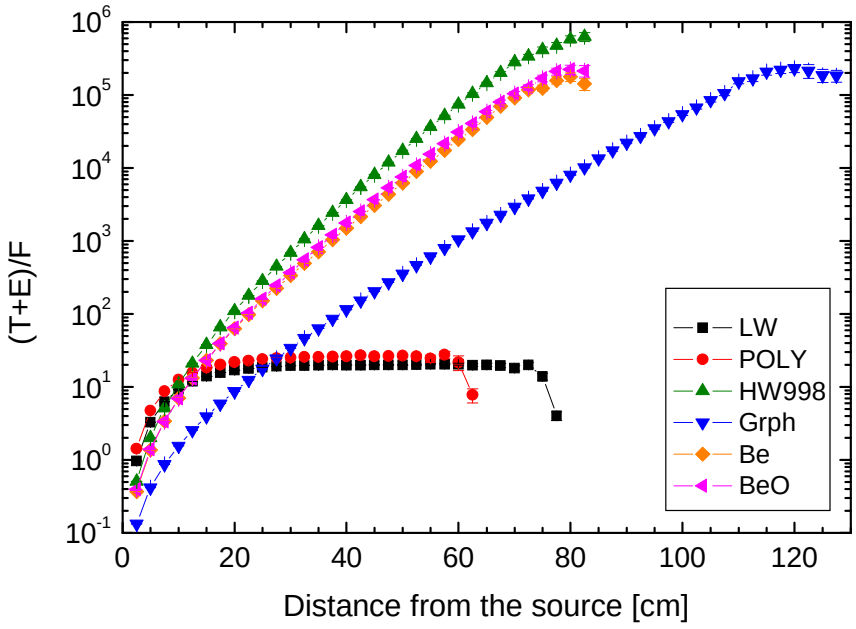

FIG. 59. Thermal plus epithermal to fast neutron fluxes ratio.

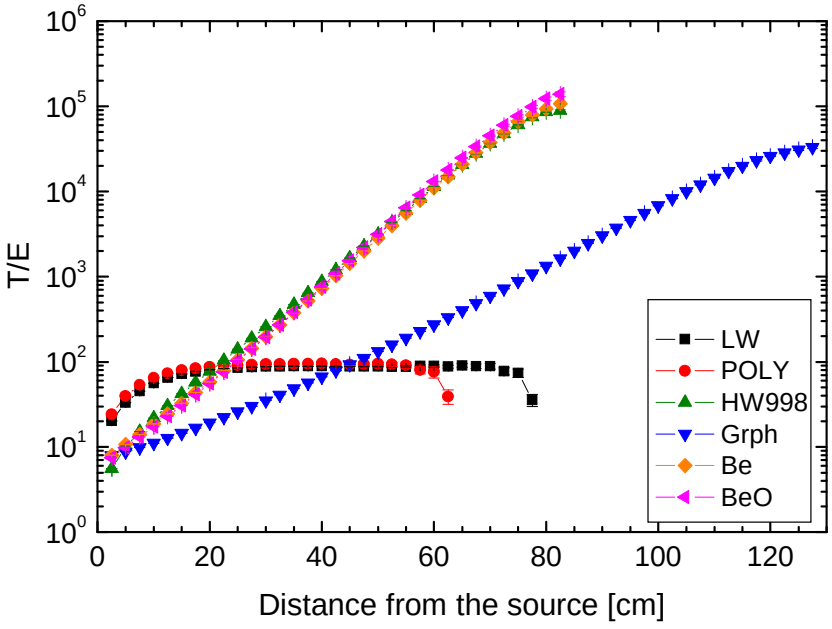

FIG. 60. Thermal to Epithermal neutron fluxes ratio.

Up to this stage of calculation, two moderators can be selected: Polyethylene because it has the best $\phi\varepsilon$ and heavy water because it has a high $\phi\varepsilon$ and the highest ϕ_T / ϕ_E. But close to the neutron source, where the polyethylene is the best, ϕ_T / ϕ_E is low for analytical purposes and the NG fills this place. For example, a comparison between thermal flux distributions produced by an empty space of 5 cm and 10 cm of radius are shown in FIG. 61. The space produces a flat distribution inside with a lower flux in both materials. The product $\phi\varepsilon$ is greater in heavy water for radius greater than 5 cm as FIG. 62 shows. Therefore heavy water has the best performance if the space for the NG is considered.

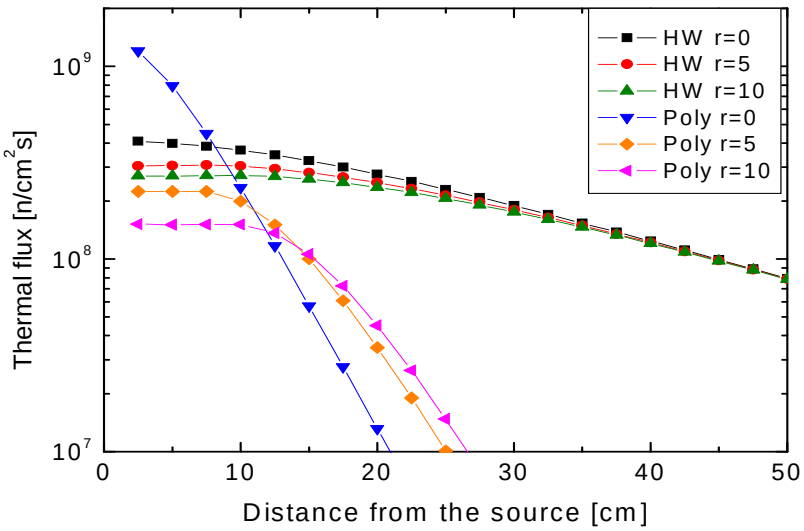

FIG. 61. Thermal flux in heavy water and polyethylene leaving a space of 5 and 10 cm, and without considering it.

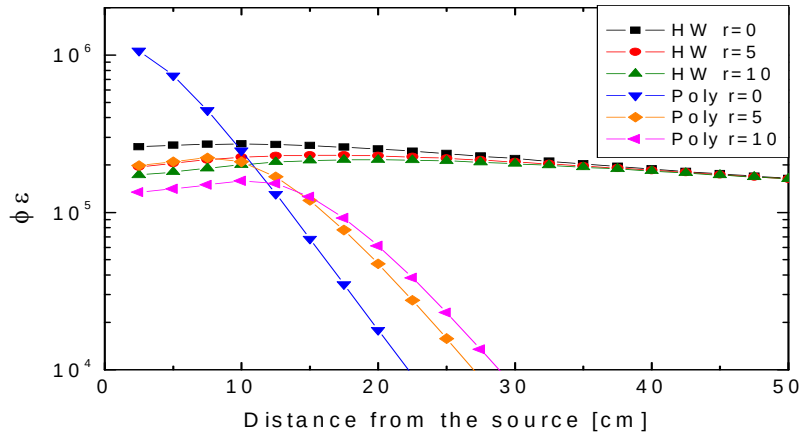

FIG. 62. Flux multiplied by efficiency in heavy water and polyethylene leaving a space of 5 cm and 10 cm, and without considering it.

Heavy water has also the following properties:

- It is available in large quantities because it is produced for natural uranium reactors. A higher purity than the “reactor grade” is recommended for reducing the Hydrogen lines. This element is a very interesting material in many applications, and it can be characterized very well with PGNAA.
- It is not toxic if not ingested. Beryllium and its compounds are extremely toxic if they are inhaled or touched.
- It can be purified from ions impurities by exchanging resins or activated carbon.
- It is not explosive. Beryllium decomposes the moisture of the air, eliminating Hydrogen, which is very flammable.
- It is easier to modify the geometry changing its container
- It is cheaper than high purity beryllium.

9.3.2. Optimization of the shielding and geometry with the simplified model

Two questions can be asked: Is the minimum size of a moderator the optimal choice? What happens if some thickness of heavy water is replaced by a hydrogenated fast neutron shielding?

To answer those questions the simplified model is applied. The internal and the external configuration are compared using heavy water as a moderator. Although heavy water is not considered a heavy moderator such as beryllium or graphite, the differences with an MCNP calculation are small (see FIG. 63). The parameters of Eq. (8.11) are obtained from Ref. [196]. The selected fast neutron shielding is borated polyethylene with a composition of 30%wt of boron carbide. This mixture has the slowing down properties of Hydrogen and the absorption of Boron; hence, it is one of the best shielding material for fast neutrons. This material has a fast neutron attenuation coefficient of 0.22 cm^{-1}. In order to avoid any H photons, the surface of the moderator should be lined with 1 cm of pure Boron Carbide.

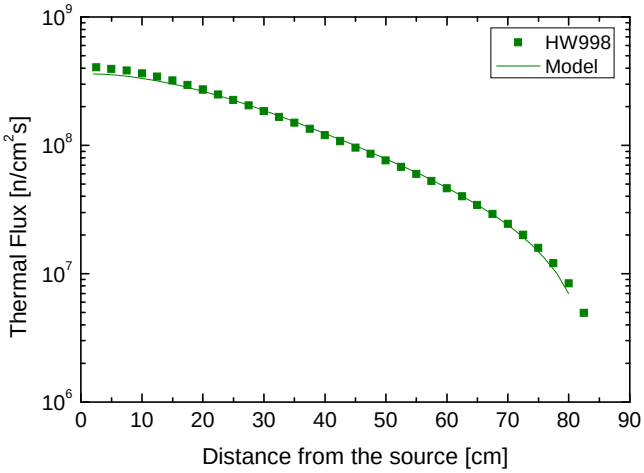

FIG. 63. Thermal neutron flux inside a spherical moderator calculated with Equation (8.11) and with MCNP.

9.3.2.1. Internal configuration

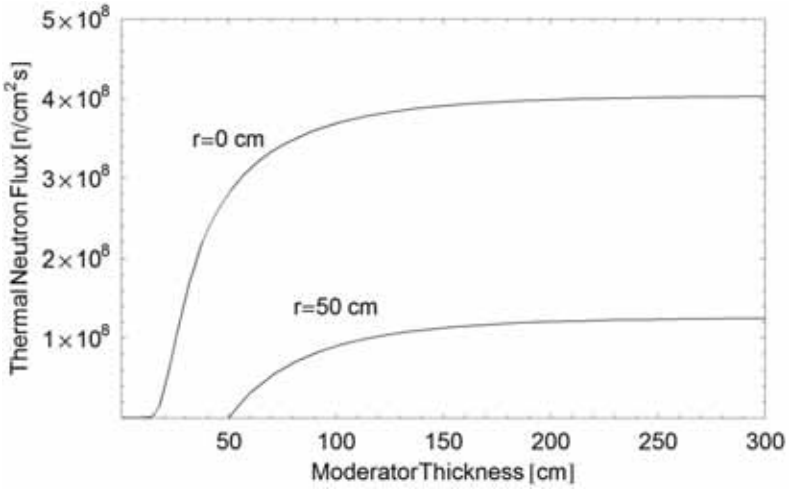

FIG. 64. Thermal neutron flux at r=0 and r=50 depending of the radius of the moderator.

The thermal neutron flux at the centre of a heavy water moderator (r=0 cm) reach a maximum value of approximately 4×10^{-3} Q, (see FIG. 64). So, by increasing the moderator radius, the flux is not higher and the detection efficiency outside the facility is worse. The same happens with other sample positions, for example r=50 cm:

To study this competition between the flux and the efficiency, all possible configurations of moderator and shielding thickness are analyzed by calculating the product $\phi\varepsilon(X_M,X_{NS})$. The sample is placed at a distance H=50 from the NG in order to have a ratio ϕ_T / ϕ_E ~1000. The situation is explained in FIG. 65 (left) On the bottom the contour plot of $\phi_{TH}(10cm+X_M)\ \varepsilon(D)$, where $D(R,X_{NS})= ((10cm + X_M + X_{NS} + 25\ cm)^2 - 50^2)^{1/2}$, is shown. Each change to a clearer gray means an increment of 5×10^3 from 2×10^4 to 6×10^4. The line that crosses FIG. 65 represents the limit of the allowed configurations that produce less than 3 $n_F \cdot cm^{-2} \cdot s^{-1}$at the surface of the facility. So, the best configuration is R= 10 cm+ 76 cm =86 cm, without any hydrogenated neutron shielding. The performance estimated with this model is about $\phi\varepsilon \approx 5.7 \times 10^4$ $n \cdot cm^{-2} \cdot s^{-1}$.

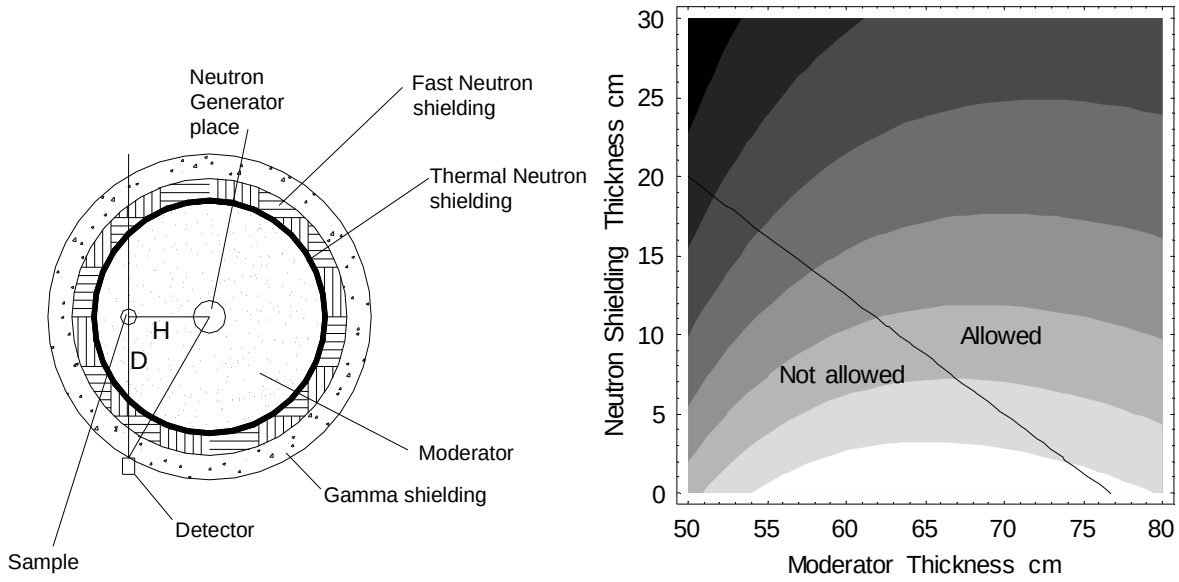

FIG. 65. Contour plot of the product $\phi\varepsilon$ for an internal configuration. Each colour level raises a value of 5×10^3, from 2×10^4 to 6×10^4.

9.3.2.2. External configuration

The number of variables to optimize the external configuration is more than the internal one and the optimization is more difficult. The flux through the length of the tube described by Eq. (8.12) is shown in FIG. 66. The radius of the tube and the radius of the heavy water moderator are fixed at r_d= 20 cm and R= 86 cm respectively. It can be seen that the extraction of the beam from the high flux region is better than the extraction from the external positions. The only one limitation for placing the tube close to source is the ϕ_T / ϕ_E ratio. Approximately at r=50 cm a ratio of 1000 could be obtained as FIG. 60 shows.

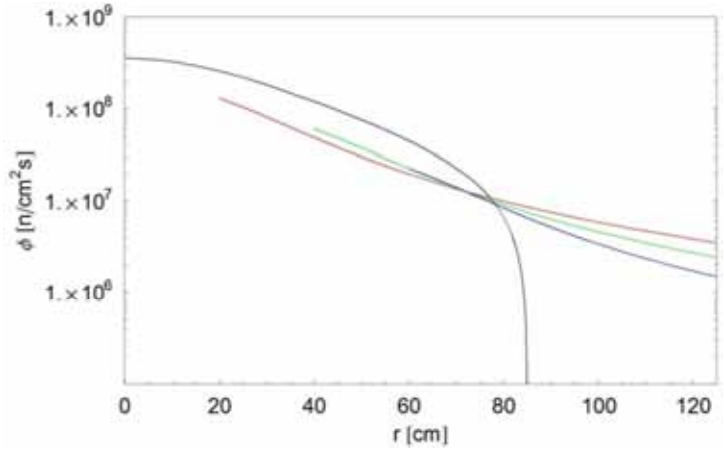

FIG. 66. Thermal flux calculated with Eq. (8.11) for different points of extraction. It is shown the position dependence from inside the moderator, but it is only applied for r>100.

Fixed *re*= 50 cm the optimal size of the system can be studied. FIG. 67 (right) shows the product ϕ(10 cm + X_M + X_{NS} + 25 cm – 50 cm + 8 cm, 10 cm +X_M, 20 cm, 50 cm) × ε(20 cm) in a contour plot with a fixed radius of the tube, *rs*= 20 cm. The geometry can be observed on the left of the same figure, the sample is placed at 8 cm outside the facility. The optimal size is the same as the internal one, except that the highest value here is $\phi\varepsilon = 2.7 \times 10^4$ n · cm^{-2} · s^{-1}.

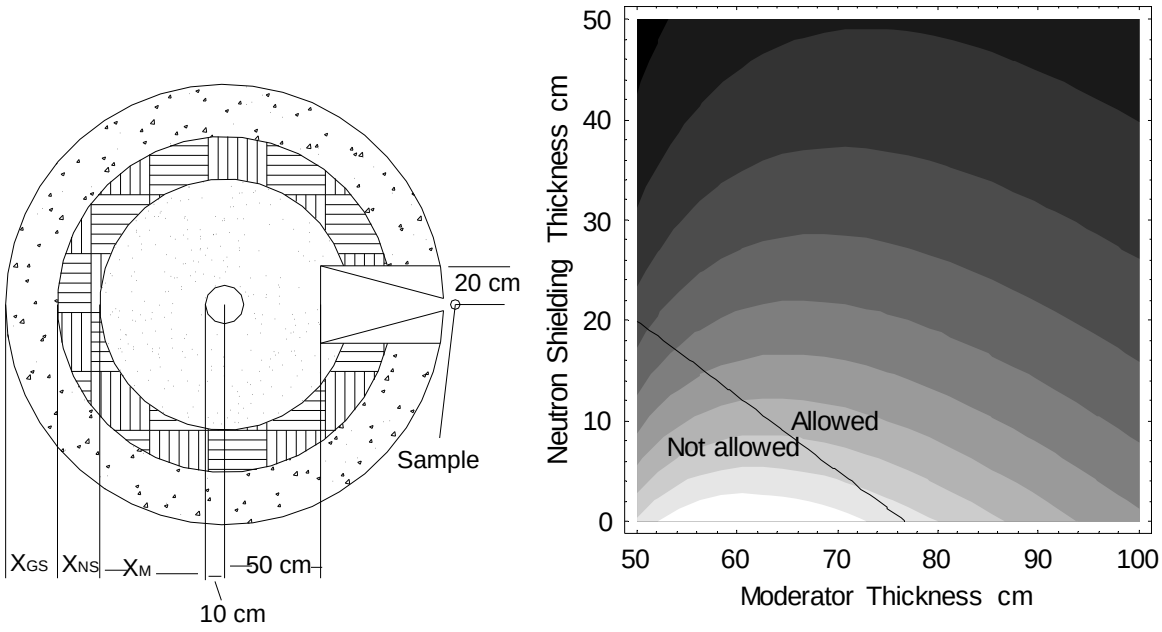

FIG. 67. Contour plot of the product $\phi\varepsilon$ for an internal configuration. Each colour level rise a value of 2.5 × 10^3, from 5 × 10^3 to 3 × 10^4.(X_{GS}=25 cm).

By enlarging the radius of the inner end of the tube this value can be increased, but the increase is not proportional to the area because the flux depends on the position inside the moderator. The centre of the inner end has the highest flux and the positions around it have lower flux. In addition to that, a wider tube weakens the fast neutron and gamma shielding around the beam, and it obliges to put the detector further away. This problem links the detector–sample distance with the radius of the tube, and it could be studied exactly only by MCNP simulations.

Although a first analysis of it is presented as follows. A fact is that the fast neutrons and photons scatter at the collimator exit. This scattering produces a dispersion of the uncollimated radiation. Three hypotheses can be considered in order to link the radius of the inner end of the extraction tube with the detector–sample distance. The detector can be placed at:

(1) A distance equal to the middle of the radius of the tube.
(2) The same radius
(3) The nearest point that the line from the source to the sample does not pass through any void place.

Each one of those situations can be seen in FIG. 68, left; and the performance of each one is calculated with the simplified model on the right. It can be seen that the three curves share a

"plateau" between 20 and 40 cm. This means that a source radius between 20 and 40 cm gives the optimal size for any of the three hypotheses.

The last variable to analyze is the alignment of the tube relative to the neutron source; it could be radial or tangential. If the point of extraction is at a fixed *r*, the tangential lines from this position to outside the facility are longer than a radial line (see FIG. 69 left). So, it can be expected lower fluxes in the tangential positions.

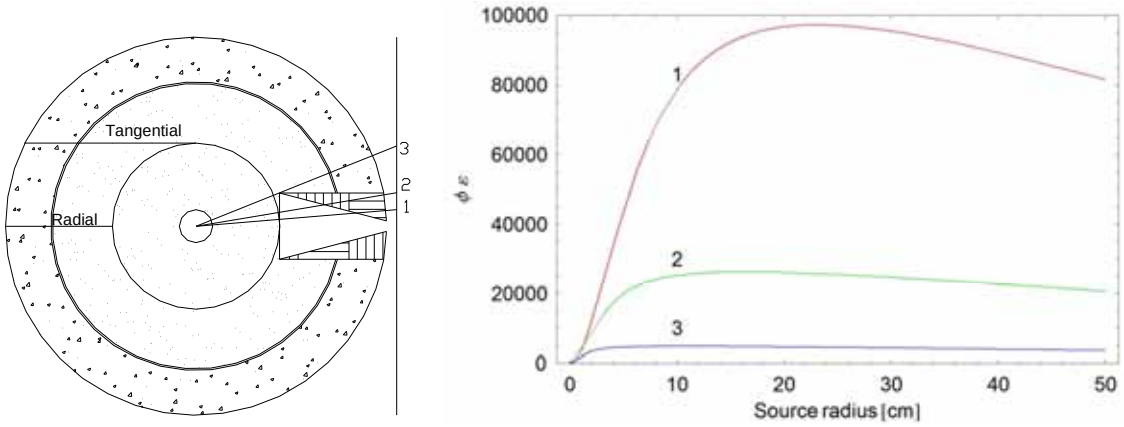

FIG. 68. Dependence of the performance an external configuration with the radius of the inner end of the tube of extraction.

9.3.2.3. Enhancement of reactions with a cold neutron source

Most, if not all, cold neutron sources (CNS) in the world are used for long wavelength neutrons extraction through neutron guides. But, could it be used for in situ enhancing the number of absorption reactions on a sample?

The expected increase of the number of reactions is given by the factor $\sqrt{(T_0 / T)}\ \phi / \phi_0$, where the subindex "0" indicates the room temperature. For a boiling H or D, the maximum increase is about $\sqrt{(293 / 20)} = 3.8$, but it could be lower due to the absorption of the moderators.

The work of Matsuo [199] shows that the maximum flux for LH_2 is $\phi/\phi_0 \approx 0.3$ for an optimum moderator radius of 3 cm and for LD_2, $\phi/\phi_0 \approx 1$ for a radius of 50 cm. This means that with LH_2 there is not any important improvement in the reaction rate, and with LD_2 a spherical cold vessel of 1 m of diameter is needed in order to gain a maximum factor of 3.8.

Up to this part of the work the best moderator radius is about 86 cm, which is not enough for placing a CNS vessel of 100 cm of diameter. Although a system with a LD_2 in a two NGs configuration is presented to evaluate how higher the flux could be in a system of these characteristics.

9.3.3. Test of the selected designs with MCNP

In the previous section the theoretical optimal performance of the internal and external configurations was presented considering that the introduction of tubes does not perturb neither the flux nor the shielding. These designs are tested with MCNP introducing the

needed empty tubes for beam extraction. The product $\phi\varepsilon$, the fast neutron flux at the detector position and ϕ_T / ϕ_E ratio are evaluated in order to select the best design. The photon transport calculation is left at the end for testing the best of them because it demands much more computing time.

9.3.3.1. Internal configuration

The optimal design of a gamma detection system should measure mainly capture photons from the sample rather than other source. For this reason the detector should only look at sample, and no other surface emitting photons. FIG. 69 shows a proposed irradiation chamber: It is an empty tube made of a neutronic transparent material, such as aluminium, where the sample is placed inside and two detectors can look at it through collimators made of lead. Those collimators are lined with a Li-6 shielding material in order to prevent any more photons generated inside it.

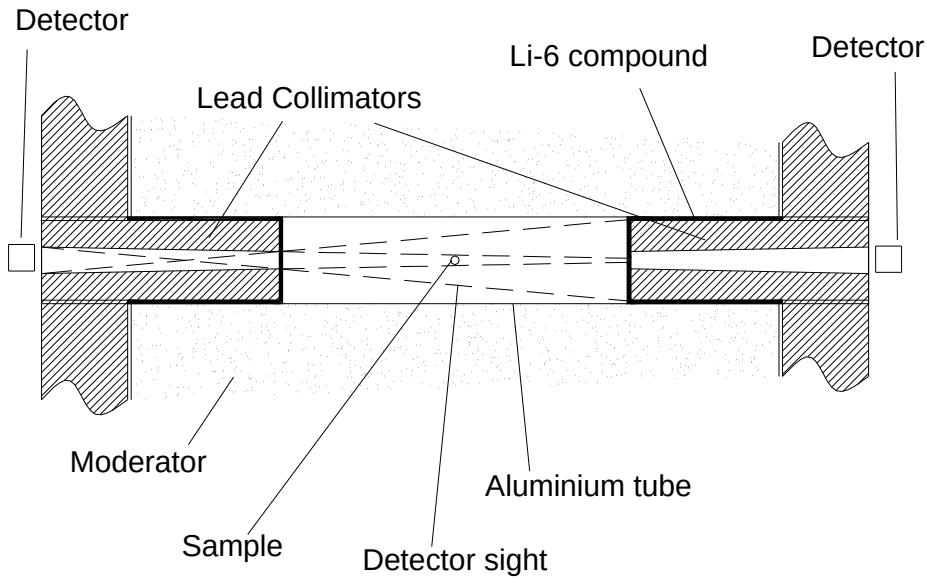

FIG. 69. Irradiation chamber for internal configuration.

A model of the system with two irradiation chambers is shown in FIG. 70 (left) the maximum sample size is about 5 cm^3. A comparison between this system and the same without tubes is shown in TABLE 9. It can be seen that the product $\phi_{TH}\,\varepsilon$ is 5.9×10^4 for the system without tubes (calculated with MCNP), and with the simplified model is 5.7×10^4 (item 9.3.2.1). This agreement between both results backs the previous optimization.

The thermal flux in the system with tubes is 70% lower, the ϕ_T / ϕ_E ratio is about half and the fast neutrons flux at the surface is much higher than the system without tubes. In FIG. 70 at the right, some places where the fast neutrons scatter are shown by using the program MCNP5 Vised. This powerful graphical tool helps discovering of leaks in the shielding. It can be observed that an important number of fast neutrons reach the lead, where they can scatter without a significant energy loss.

TABLE 9. INTERNAL CONFIGURATION PERFORMANCE CALCULATED WITH MCNP

Configuration	Fast Neutrons ($n \cdot cm^{-2} \cdot s^{-1}$)	Gamma photons ($p \cdot cm^{-2} \cdot s^{-1}$)	ϕ_{TH} at sample ($n \cdot cm^{-2} \cdot s^{-1}$)	ϕ_{TH} / ϕ_E	$\phi_{TH}\, \varepsilon$ ($n \cdot cm^{-2} \cdot s^{-1}$)
Without tubes	2.1	0.3	8.0×10^7	1320	5.9×10^4
With tubes	88	–	5.7×10^7	435	4.2×10^4

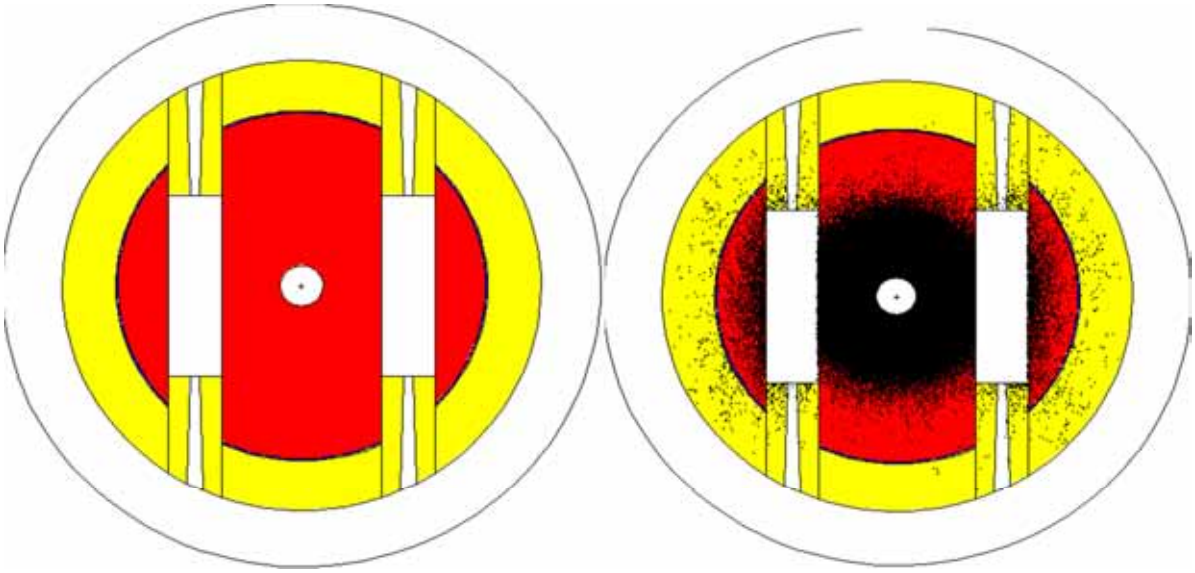

FIG. 70. Left: Model of an internal configuration PGNAA with two irradiation chambers. Right: MCNP Vised shielding test with fast neutrons Each point represent a collision of a neutron. It can be seen that at each side of the figure are much more scatterings than in the top and bottom.

In order to reduce the number of fast neutrons at the facility surface and increase the ϕ_T / ϕ_E ratio, the value of "H" (FIG. 65) should be greater. The only way to do this without affecting the geometrical efficiency is breaking the spherical symmetry of the system and enlarging it in one direction. This design is calculated in the next section.

9.3.3.2. External configuration

The proposed design for an external type PGNAA is shown in FIG. 71 on the right. The beam is extracted by a 20 cm inner radius radial tube placed at 50 cm away from of the NG. The size of the moderator and shielding are the same of the internal configuration deduced in the previous section. The collimator is a cone of borated polyethylene, which limits the radius of the beam and protects the detector against the fast neutrons. The sample is placed at 8 cm outside the facility surface.

A fast neutron flux calculation around the beam is shown on the left of FIG. 71. A big attenuation behind shielding (yellow zone) can be seen. But the detector should be placed not

closer than 60 cm from the sample. In this position the fast neutron flux is below the maximum dose rate.

The flux calculation with and without the perturbation of the extraction tubes is shown in TABLE 10. In the latter case, the flux at the sample position is calculated with Eq. (8.12) with $\phi_{TH}(re,R)$ calculated with the MCNP in place of Eq. (8.11). In the former case, the flux at sample is calculated "exactly" with a tally "4". The difference between them is a factor 2, which is produced by an overestimation of the flux calculated at the inner end of the extraction tube. To improve the simplified model for the external configuration a detailed study on the neutron source at the extraction tube is needed, but this is beyond this work. Although this evaluation has demonstrated that the external configuration has a lower performance of the internal one.

TABLE 10. EXTERNAL CONFIGURATION PERFORMANCE CALCULATED WITH MCNP

Configuration	Fast Neutrons ($n \cdot cm^{-2} \cdot s^{-1}$)	ϕ_{TH} at sample ($n \cdot cm^{-2} \cdot s^{-1}$)	ϕ_{TH} / ϕ_E	$\phi_{TH}\,\varepsilon$ (20 cm) ($n \cdot cm^{-2} \cdot s^{-1}$)
Without tubes	2.1	1.5×10^6	1320	2.7×10^4
With tubes	10	7.6×10^5	275	1.3×10^4

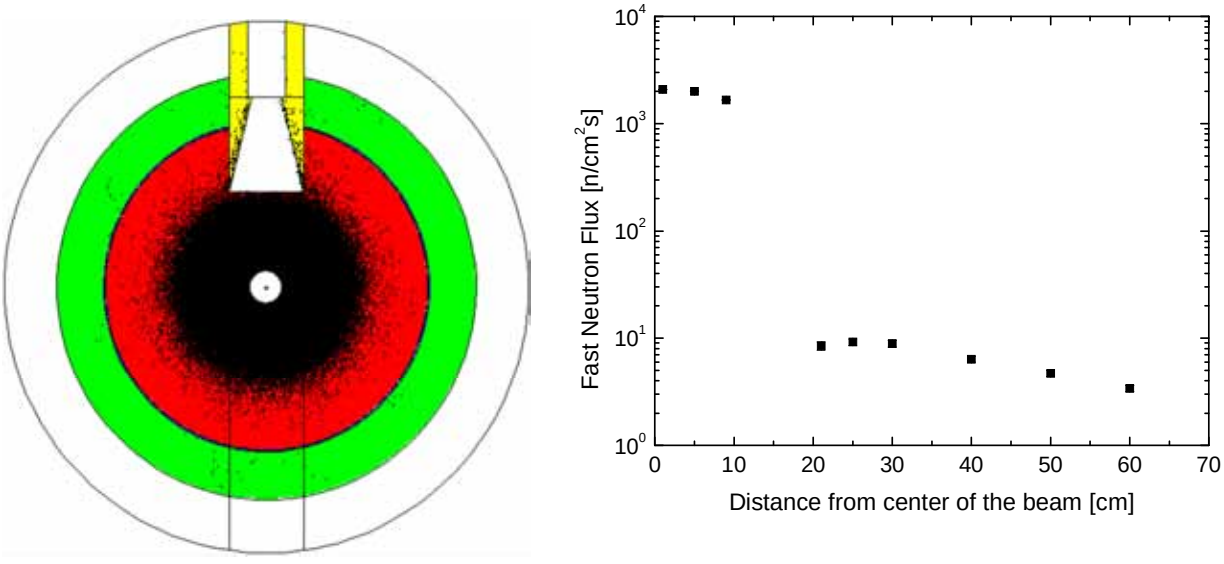

FIG. 71. Left: Model of an external PGNAA facility with one external irradiation port. It has been plotted the fast neutrons collisions in order to check the shielding around the beam. Right: A calculation of the fast flux around the beam.

9.3.3.3. Cold source with two neutron generators

The design presented in FIG. 72 shows a system with a cold source cell of 50 cm of radius. Two NGs with an intensity of 10^{11} are placed at each side of the cold cell in order to have the highest thermal flux. The selected materials are the same as the previous designs except for the cold moderator that is LD_2 at 19K with a density of 0.052 atoms/cm^3. The sample is placed inside a tube passing through the cold source (internal configuration).

Two calculations are shown in TABLE 11. The first, the NGs are placed at 75 cm from the centre of the system, and the other at 85 cm. This increase is done in order to reduce the neutron dose at the surface of the facility. The neutron flux distribution of the cold source can be observed in FIG. 73 for the "85 cm" system. A non-pure maxwellian cold distribution can be seen, although the most probable energy is 2 meV giving a gain factor in the performance of 3.5.

This double NG system with a CNS is 3 times better than the presented one without a CNS (see TABLE 9 and TABLE 11). If the cost is considered, the economic balance does not present an interesting gain because it is at least the double and it has only one irradiation position.

TABLE 11. PERFORMANCE OF A PGNAA WITH A CNS

	75 cm	85 cm
Thermal neutron flux ($n \cdot cm^{-2} \cdot s^{-1}$)	9.1×10^7	6.71×10^7
Epithermal neutron constant ($n \cdot cm^{-2} \cdot s^{-1}$)	4.2×10^4	9.2×10^3
Fast neutron flux ($n \cdot cm^{-2} \cdot s^{-1}$)	1.5×10^4	2600
Thermal + Epithermal Fast	6000	26000
Thermal Epithermal Constant	2175	7200
Most probable energy (meV)	2	2
Performance ($n \cdot cm^{-2} \cdot s^{-1}$)	1.75×10^5	1.3×10^5
Fast Neutrons at detector ($n \cdot cm^{-2} \cdot s^{-1}$)	4	0.5
Max. neutron dose at surface (μSv/h)	17	10

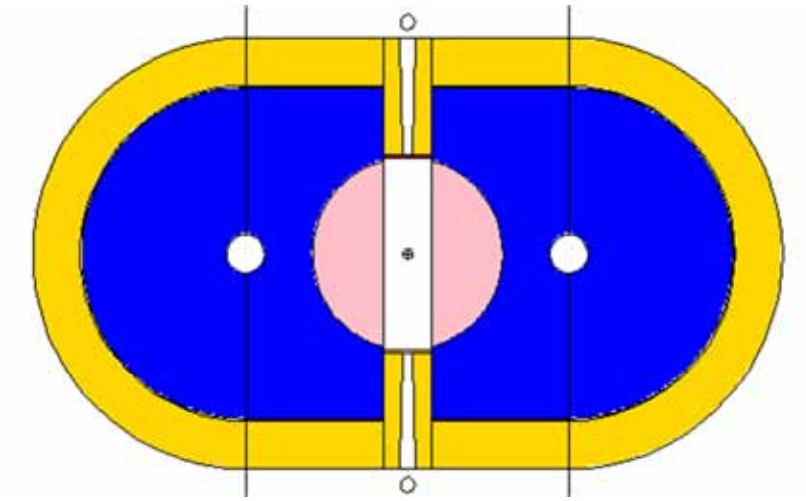

FIG. 72. Cut view of the model of a PGNAA facility with a CNS of LD_2 (pink circle at the centre) and two NG at each side. The 3 D figure is a revolution of this figure around the horizontal axis, with the exception of the irradiation chamber.

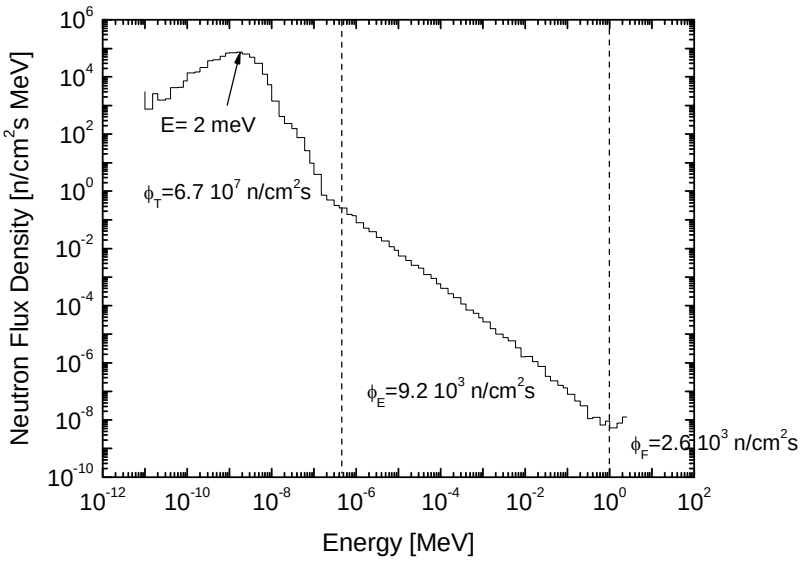

FIG. 73. Neutron flux energy distribution of the recommended design at sample position.

9.3.4. Recommended design

A model of an improved PGNAA internal configuration design with two irradiation positions is shown in FIG. 74. The difference with the previous one (section 9.3.3.1) is an added extension between the two hemispheres that shields better both irradiation chambers. The performance is presented in TABLE 12. A lower thermal flux can be seen, but the ϕ_T / ϕ_E and the $(\phi_T + \phi_E) / \phi_F$ are higher.

The design fulfils almost all the proposed radiological requirements, except for the number of gamma photons at the detector position. Two runs for photon transportation have been done: in the first about 100 $p \cdot cm^{-2} \cdot s^{-1}$ reach the detector; most of them have low energy. For this reason, in a second calculation a low energy shielding made of 1 cm of lead is added closing the exit of the collimator. This improvement reduces the photon background below 10 $p \cdot cm^{-2} \cdot s^{-1}$, but it reduces the low energy efficiency.

The performance of this system is about 7 times lower than the one with two NGs and a cold source, but it could analyze two, or even more, 3 or 4 samples per time (of course by adding more irradiations chambers). This possibility, which the other system does not have, could weight when evaluating costs.

TABLE 12. PERFORMANCE OF RECOMMENDED DESIGN FOR PGNAA

Thermal neutron flux ($n \cdot cm^{-2} \cdot s^{-1}$)	2.9×10^7
Epithermal neutron constant ($n \cdot cm^{-2} \cdot s^{-1}$)	1.4×10^4
Fast neutron flux ($n \cdot cm^{-2} \cdot s^{-1}$)	7.0×10^3
Thermal + Epithermal Fast	4.1×10^3
Thermal Epithermal Constant	2.1×10^3
Performance	1.9×10^4
Fast Neutrons at detector ($n \cdot cm^{-2} \cdot s^{-1}$)	2.5
Gamma Photons at detector ($p \cdot cm^{-2} \cdot s^{-1}$)	**7**
Neutron dose at surface (μSv/h)	<5
Gamma dose at surface (μSv/h)	<1

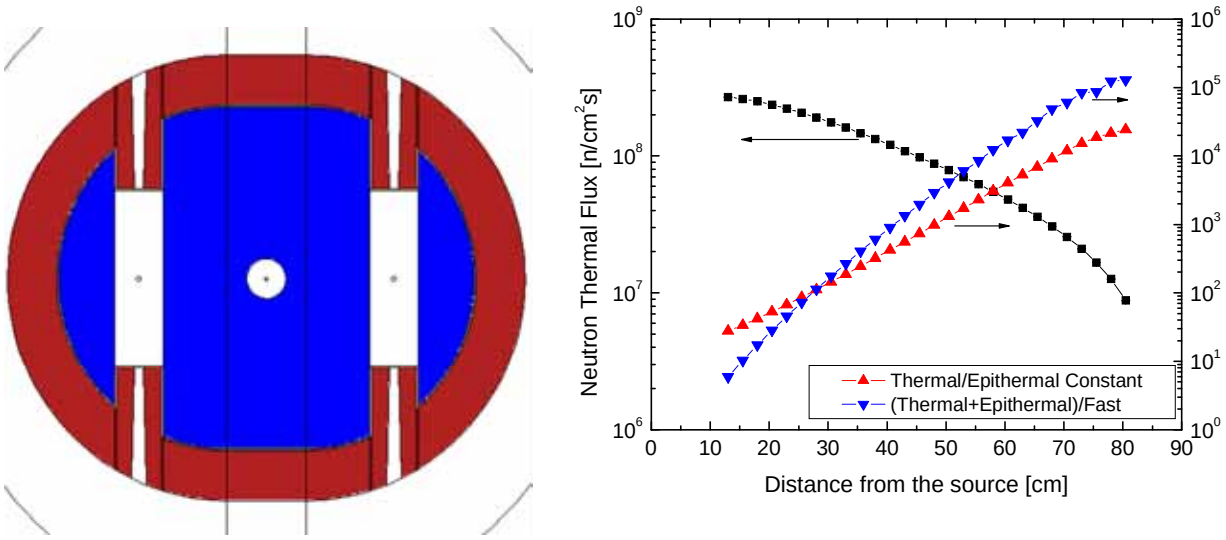

FIG. 74. Left: Recommended design for NAA/PGNAA. The 3 D figure is a revolution of this figure around the horizontal axis, with the exception of the irradiation tubes. Right: Thermal flux, Thermal to Epithermal and Thermal plus Epithermal to Fast ratios for NAA.

The ϕ_T, ϕ_T / ϕ_E and $(\phi_T + \phi_E) / \phi_F$ NAA´s parameters are shown in FIG. 74 (right). The calculation positions are the small circles drawn in the centre of the Figure on the left. For distances greater than 50 cm from the source, the samples have a $\phi_T / \phi_E > 1000$.

9.4. Conclusions

An optimal design facility for neutron activation in the mode PGNAA and NAA has been presented. This design has been obtained by analyzing the most important variables, which determine the performance of the system. It can be established for a 10^{11} n/s generator that:

(1) Heavy water is better than light water, polyethylene, beryllium, beryllium oxide and graphite.

(2) The optimal radius of it is about 86 cm.
(3) It needs a minimum lead thickness of 25 cm.
(4) It is better to use the moderator as a fast neutron shielding than adding a hydrogenous absorber.
(5) It is better for PGNAA to irradiate the sample inside the moderator in an internal configuration than outside of it in a beam.

An extreme system with two NGs with a cold neutron source has been tested. The performance of it is at maximum 7 times better than the recommended design for one generator, but the last one can analyze simultaneously several samples and it could cost not more than half. The best option of them has to be carefully analyzed from the economic point of view. Hence, the simpler option has been recommended in this work. The problem is not closed because there exist more variables that have not been analyzed such as structural materials, impurities in the moderator, etc. but the best performance that can be expected for those systems has been established.

REFERENCES

[1] HEVESY, G., Adventures in radioisotope research, Vol. 1, Pergamon Press, New York (1962) 47–62.

[2] MEUDERS, J.P., LELEUX, P., MACQ, P.C., PIRART, C., Fast neutron yields and spectra from targets of varying atomic number bombarded with deuterons from 16 to 50 MeV (for radiobiology and radiotherapy), Phys. Med. Biol. **20** (1975) 235–243.

[3] WREAN, P.R., BRUNE, C.R., KAVANAGH, K.W., Total cross sections and thermonuclear reaction rates for $^{9}Be(\alpha,n)^{12}C$, Phys. Rev. **49** (1994) 1205–1213.

[4] CSIKAI, J., CRC Handbook of Fast Neutron Generators, CRC Press, Boca Raton (1987).

[5] STEYERL, A., Very low energy neutrons, Springer Tracts Mod. Phys. **80** (1977) 57

[6] BELGYA, T., MOLNAR, G., YATES, S.W., Analysis of doppler-shift attenuation measurements performed with accelerator-produced monoenergetic neutrons, Nucl. Phys. A **607** (1996) 43.

[7] MARMIER, P., SHELDON, E., Physics of Nuclei and Particles, Vol. 1, Academic Press, New York (1969).

[8] MCLANE, V., DUNFORD, C.L., ROSE, P.F., "Neutron cross section curves", Neutron Cross Sections, Vol. 2, Academic Press, New York (1988).

[9] EHMANN, W.D., VANCE, D.E., Radiochemistry and nuclear methods of analysis, Wiley, New York (1991).

[10] PEPELNIK, R., Experience in 14-MeV neutron activation analysis using short lived nuclides, J. Trace Microprobe Tech. **6** (1988) 271.

[11] EHMANN, W.D., 14-MeV neutron activation analysis: Methodology, applications, and potential, J. Radioanal. Nucl. Chem. **167** (1993) 67.

[12] AMERICAN SOCIETY FOR TESTING AND MATERIALS, Standard Test Method for Oxygen Content Using a 14-MeV Neutron Activation and Direct-Counting Technique, E385-90, American Society for Testing and Materials, Philadelphia (1991).

[13] MITRA, S., SUTCLIFFE, J.F., HILL, G.L., A proposed three-phase counting system for the in vivo measurement of the major elements using pulsed 14 MeV neutrons , Biol. Trace. Elem. Res. **26/27** (1990) 423.

[14] MITRA, S., WOLFF, J.E., GARETT, R., Calibration of a prototype in vivo total body composition analyser using 14 MeV neutron activation and the associated particle technique, Appl. Radiat. Isot, Elsevier Science **49** 5/6 (1998) 537–539.

[15] COHN, S.H., DOMBROWSKI, C.S., Measurement of total-body calcium, sodium, chlorine, nitrogen, and phosphorus in man by in vitro neutron activation analysis, J. Nucl. Med. **12** 7 (1971) 499–505

[16] GORDON, C.M., PETERS, C.W., OLSON, T.K., A fast-neutron diagnostic probe, J. Res. Natl. Bur. Stand. US **93** (1988) 484.

[17] EVSENIN, A.V., GORSHOKOV, I.Y., KUZNETSOV, A.V., OSETROV, O.I., VAKHTIN, D.N., Detection of Explosives and other Illicit Materials by Nanosecond Neutron Analysis (Proc. Series CD, STI/PUB/1433, 2009), IAEA, Vienna (2010).

[18] LE TOURNEUR, P., SULIS: A Portable Neutron Device for Explosive and Chemical Detection (Proc. Series CD, STI/PUB/1433, 2009), IAEA, Vienna (2010).

[19] ILA, P., Determination of total oxygen in standard rocks by cyclic activation analysis using a 14 MeV neutron generator, J. Radioanal. Nucl. Chem. **148** (1991) 415.
[20] ANDERSON, N.E., Assay for oxygen in uranium in the 0.1–1.0 wt% range using 14-MeV neutron activation, J. Radioanal. Nucl. Chem. **100** (1986) 373.
[21] MAO, Y., EHMANN, W.D., MACKERSBY, W.R., Simultaneous determination of P and N in human tissue by 14 MeV neutron activation analysis, Nucl. Instrum. Methods Phys. Res. B **24/25** (1987) 1003.
[22] JAMES, W.D., 14 MeV fast neutron activation analysis in the year 2000, J. Radioanal. Nucl. Chem. **243** (2000) 119.
[23] SANG, H.F., WANG, F.L., LIU, L.M., SANG, H.J., Detection of element content in coal by pulsed neutron method based on an optimized back-propagation neural network, Nucl. Instrum. Methods Phys. Res. B **239** (2005) 202.
[24] JING, S.W., GU, D.S., QIAO, S., LIU, Y.R., LIU, L.M., Development of pulse neutron coal analyzer, Rev. Sci. Instrum. **76** (2005) 045110.
[25] NAT, A., ENE, A., LUPU, R., Rapid determination of gold in Romanian auriferous alluvial sands, concentrates and rocks by 14 MeV NAA, J. Radioanal. Nucl. Chem. **261** (2004) 179.
[26] LUPU, R., NAT, A., ENE, A., Determination of gold in Romanian auriferous alluvial sands and rocks by 14 MeV neutron activation analysis, Nucl. Instrum. Meth. B **217** (2004) 123.
[27] DULLOO, A.R., et al., Neutron fluence rate measurements in a PGNAA 208-liter drum assay system using silicon carbide detectors, Nucl. Instrum. Meth. B **213** (2004) 400.
[28] ADESANMI, C.A., ESSIETT, A.A., BALOGUN, F.A., Essential corrections of interference reactions in the determination of protein contents of Nigeria foodstuffs using fast neutron activation analysis, Nucl. Instrum. Methods Phys. Res. A **505** (2003) 521.
[29] GAUDRY, A., et al., Biomonitoring of the atmospheric pollution by heavy metals in Morocco, J. Phys. IV **107** (2003) 533.
[30] SENHOU, A., et al., Comparison of 14 MeV-NAA, k0-NAA and ED-XRF for air pollution bio-monitoring, J. Radioanal. Nucl. Chem. **253** (2002) 247.
[31] HANNAN, M.A., OLUWOLE, A.F., KEHINDE, L.O., BORISADE, A.B., Determination of oxygen, nitrogen, and silicon in Nigerian fossil fuels by 14 MeV neutron activation analysis, J. Radioanal. Nucl. Chem. **256** (2003) 61.
[32] JONAH, S.A., OKUNADE, I.O., JIMBA, B.W., UMAR, I.M., Application of a low-yield neutron generator for rapid evaluation of alumino-silicate ores from Nigeria by FNAA, Nucl. Instrum. Methods Phys. Res.A **463** (2001) 321.
[33] EWA, I.O.B., Determination of protein levels in Nigerian grains using 14 MeV neutron activation analysis, Spectroscopy Letters **29** (1996) 885.
[34] PANDA, S.P., KULKARNI, S.G., SAHU, S.K., BHORASKAR, V.N., DOKHALE, P.A., Fast neutron activation analysis of glycidyl azide polymers, Bul. Mat. Sci. **19** (1996) 1125.
[35] CUNHA, I.I.L., DE OLLIVEIRA, R.M., Phosphorus determination in milk and bone samples by neutron activation analysis, J. Radioanal. Nucl. Chem. **213** (1996) 185.
[36] KAFALA, S.I., BAHAL, B.M., GIDRAB, K.M., 14-MeV NAA of steel alloys by an absolute method, J. Radioanal. Nucl. Chem. **189** (1995) 15.
[37] JAMES, W.D., ZEISLER, R., Uptake of oxygen in a coal standard reference material® determined by fast (14-MeV) neutron activation analysis, J. Radioanal. Nucl. Chem. **248** (2001) 233.

[38] MA, J.L., MARIANI, A., First experimental attempts of ^{129}I direct measurements by neutron interrogation and gamma ray spectrometry, J. Radioanal. Nucl. Chem. **216** (1997) 129.
[39] WOMBLE, P.C., VOUVOPOULOS, G., PASCHAL, J., NOVIKOV, I., CHEN, G.Y., Optimizing the signal-to-noise ratio for the PELAN system, Nucl. Instrum. Methods Phys. Res. A **505** (2003) 470.
[40] GOZANI, T., ELSALIM, M., STRELLIS, D., BROWN, D., Fusion of time-dependent gamma production spectra from thermal neutron capture and fast neutron inelastic scattering to improve material detection, Nucl. Instrum. Methods Phys. Res. A **505** (2003) 486.
[41] POUMAREDE, B.A., CLUZEAU, S., LETOUTNEUR, P., BACH, P., Cross-sections measurements on fast neutron reactions leading to very short half-life nucleus, J. Trace Microprobe Tech **14** (1996) 19.
[42] BACH, P., CLUZEAU, S., LAMBERMONT, C., Application of nuclear analytical techniques using long-life sealed-tube neutron generators, Biol. Trace El. Res. **43** (1994) 131.
[43] IDIRI, Z., KHELIFI, R., TOBBECHE, S., A simple method to correct for pulse pile-up and dead time losses: Application to cyclic activation analysis with 14-MeV neutrons, Appl. Radiat. Isot. **45** (1994) 631.
[44] MITRA, S., WOLFF, J.E., GARRETT, R., PETERS, C.W., Application of the associated particle technique for the whole-body measurement of protein, fat and water by 14 MeV neutron activation analysis-a feasibility study, Phys. Med. Biol. **40** (1995) 1045.
[45] GRUIN, J.P. (Ed.), Modern Trends in Activation Analysis (Proc. Int. Conf. Texas, 1961), Activation Analysis Research Laboratory, Texas, (1961).
[46] GRUIN, J.P. (Ed.), Modern Trends in Activation Analysis (Proc. Conf. Texas, 1965), Activation Analysis Research Laboratory, Texas, (1965).
[47] DEVOE, J.R. (Ed.), Modern Trends in Activation Analysis (Proc. Int. Conf. Gaithersburg, 1968), National Bureau of Standards, Gaithersburg, (1968).
[48] NARGOLWALLA, S.S., PRZYBYLOWICZ, E.P., Activation Analysis with Neutron Generators, John Wiley and Sons, New York, (1973).
[49] VOLBORTH, A., BANTA, H.E., Oxygen determination in rocks, minerals, and water by neutron activation, Anal. Chem. **35** (1963) 2203.
[50] MARTIN, T.C., MATHUR, S.C., MORGAN, I.L., The application of nuclear techniques in coal analysis, Int. J. Appl. Radiat. Isot. **15** (1964) 331.
[51] VOGT, J.R., EHMANN, W.D., The Non-Destructive Determination of Silicon and Oxygen in Meteorites by Fast Neutron Activation Analaysis (Proc. Int. Conf. Texas, 1965), A&M University Consortium Press, Texas, (1966) 82–85
[52] JAMES, W.D., AKANNI, M.S., Application of on-line laboratory computer analysis to fast neutron activation oxygen determinations, IEEE Trans. Nucl. Sci. **30** 2 (1983) 1610–1613.
[53] BUTTERFIELD, D., LOVERING, J.F., Neutron activation analysis of rhenium and osmium in Apollo 11 lunar material (Proc. Conf. Houston, 1970), Geochim. Cosmochim. Ac. **2** (1970) 1351–1355.
[54] ENDRESS, M., HEUSCHKEL, S., KEYDEL, A., KNADEL, S., SOSNA, I., Automated cement plant quality control: in-situ versus extractive sampling and instrumentation, Cement Int. **2** (2004) 38.
[55] BELBOT, M.D., VOURVOPOULOS, G., WOMBLE, P.C., PASCHAL, J., Elemental on-line coal analysis using pulsed neutrons (Proc. Conf. Kentucky, 1999), SPIE **3769** (2000) 168.

[56] GRODZINS, L., Nuclear techniques for finding chemical explosives in airport luggage, Nucl. Instrum. Methods Phys. Res. B **56/57** (1991) 829.
[57] GOZANI, T., Advances in accelerator based explosives detection systems, Nucl. Instrum. Methods Phys. Res. B **79** (1993) 601.
[58] VOURVOPOULOS, G., SCHULTZ, F.J., A pulsed fast-thermal neutron system for the detection of hidden explosives, Nucl. Instrum. Methods Phys. Res. B **79** (1993) 585.
[59] SMITH, R.C., HURWITZ, M.J., TRAN, K.C., System to detect contraband in cargo containers using fast and slow neutron irradiation and collimated gamma detectors, Nucl. Instrum. Methods Phys. Res. B **99** (1995) 733.
[60] OVERLEY, J.C., CHMELIK, M.S., RASMUSSEN, R.J., SCHOFIELD, R.M.S., LEFEVRE, H.W., Explosives detection through fast-neutron time-of-flight attenuation measurements, Nucl. Instrum. Methods Phys. Res. B **99** (1995) 728.
[61] BACH, P., MA, J.L., FROMENT, D., JAUREGUY, J.C., Chemical weapons detection by fast neutron activation analysis techniques, Nucl. Instrum. Methods Phys. Res. B **93** (1993) 605.
[62] ROONEY, B.D., YORK, R.L., CLOSE, D.A., WILLIAMS III, H.E., Active neutron interrogation package monitor (Proc. Nucl. Sci. Symp. Toronto, 1998), Los Alamos Nat. Lab. **2** (1998) 1027–1030,
[63] YATES, S.W., FILO, A.J., CHENG, C.Y., COPE, D.F., Elemental analysis by gamma ray detection following inelastic neutron scattering, Radioanal. Chem. **46** 2 (1978) 343–355.
[64] INTERNATIONAL ATOMIC ENERGY AGENCY, Table of simple integral neutron cross section data from JEF-2.2, ENDF/B-VI, JENDL-3.2, BROND-2, and CENDL-2, JEF Report 14, OECD Nuclear Energy Agency, Paris, (1994).
[65] INTERNATIONAL ATOMIC ENERGY AGENCY, Thermal neutron cross-sections, resonance-parameters, resonance integrals, JEF 2.2 INTER, IAEA Nuclear Data Section.
[66] BODE, P., OVERWATER, R.M.W., Trace elements determinations in very large samples: a new challenge for neutron activation analysis, J. Radioanal. Nucl. Chem. **167** (1993) 169–176.
[67] OVERWATER, R.M.W., The physics of big sample INAA, PhD Dissertation, Delft University of Technology, (1994).
[68] OVERWATER, R.M.W., BODE, P., DE GOEIJ, J.J.M., Feasibility of elemental analysis of kilogram-size samples by instrumental neutron activation analysis, Anal Chem. **68** (1996) 341–348.
[69] BAAS, H.W., BLAAUW, M., BODE P., DE GOEIJ, J.J.M., Collimated scanning towards 3D-INAA of inhomogeneous large samples, Fres. J. Anal. Chem. **363** (1999) 753–759.
[70] NAKANISHI, T.M., DON-JIN, K., KITAMURA, T., ISHII, R., MATSUBAYASHI, M., Identification of water storage tissue in the stem of cowpea plant (Vigna unguliculata Walp) by neutron radiography, J. Radionanal. Nucl. Chem. **242** 2 (1999) 353–359.
[71] YAMADA, T., et al., Detection of wood discoloration in a canker fungus-inoculated Japanese cedar by neutron radiography, J. Radionanal. Nucl. Chem. **264** 2 (2005) 329–332.
[72] Neutron radiography: non destructive testing, CEA Saclay, Gif-sur-Yvette Cedex.
[73] MUMBA, N.K., VAS, L., BUCZKÓ, Cs.M., Uranium and thorium analyses by delayed fission neutron counting technique using a small neutron generator, J. Radioanal. Nucl. Chem. Letters **95** (1985) 311–322.

[74] FAKHI, S., PAULUS, J.M., BOUHLASSA, S., ABBE, J.C., Analysis of uranium using delayed neutron emission, J. Radioanal. Nucl. Chem. **249** 3 (2001) 565–567.
[75] SENFTLE, F.E., HOYTE, A.F., Mineral exploration and soil analysis using in situ neutron activation, Nucl. Instrum. Methods Phys. Res. **42** 1 (1966) 93–103.
[76] YULE, H.P., LUKENS, Jr. H.R., GUINN, V.P, Utilization of reactor fast neutrons for activation analysis, Nucl. Instrum. Methods Phys. Res. **33** 2 (1965) 277–282.
[77] GUINN, V.P., MILLER, D.A., Recent instrumental neutron activation analysis studies utilizing very short-lived activities, J. Radioanal. Chem. **37** 1 (1977) 313.
[78] ALFASSI, Z.B., LAVI, N., Epithermal neutron activation analysis using (n, n′) reaction, J. Radioanal. Chem. **76** (1983) 257.
[79] SCHRADER, C.D., STINNER, R.J., Remote analysis of surfaces by neutron gamma ray inelastic scattering technique, J. Geophys. Res. **66** (1961) 1951.
[80] WYLIE, A.W., Nuclear Assaying of Mining Boreholes, Elsevier, Amsterdam (1984) 344 pp.
[81] JIGGINS, A.H., HABBANI, F.I., Prompt gamma-ray analysis using 3.29 MeV neutron inelastic scattering, Int. J. Appl. Radiat. Isot. **27** (1976) 689.
[82] IM, H.J., et al., Noise reduction in prompt gamma spectra acquired in short times, Nucl. Instrum. Methods Phys. Res. A **574** (2007) 272.
[83] ABDEL-HALEEM, A.S., ABDEL-SAMAD, M.A., ZAGHLOUL, R.A., HASSAN, A.M., The uses of neutron capture γ-rays in environmental pollution measurements, Radiat. Phys. Chem. **47** (1996) 719.
[84] ALFASSI, Z.B., CHUNG, C., Prompt Gamma Neutron Activation Analysis, CRC Press, London (1995).
[85] CLIFFORD, E., ING, H., MCFEE, J., COUSINS, T., High rate counting electronics for a thermal neutron analysis land mine detector (Proc. Conf. Denver, 1999), SPIE **3769** (1999) 155–166.
[86] MARTIN, R.C., KNAUER, J.B., BALO, P.A., Production, distribution and applications of californium-252 neutron sources, Appl. Radiat. Isot. **53** (2000) 785.
[87] GOZANI, T., et al., Coal elemental analysis by prompt-neutron activation analysis, Trans. Am. Nucl. Soc. **28** (1978) 88.
[88] CLAYTON, C.G., WORMALD, M.R., Coal analysis by nuclear methods, Int. J. Appl. Radiat. Isot. **345** (1983) 3.
[89] CHARBUCINSKI, J., YOUL, S. F., EISLER, P. L., BORSARU, M., Prompt neutron gamma logging for coal ash in waterfilled boreholes, Geophysics **51** 5 (1986) 1110–1118.
[90] PINAULT, J.L., DAUDU, F., Borehole logging in a bauxite mine by use of prompt gamma neutron activation analysis (Proc. Symp. Vienna, 1990), IAEA, Vienna (1991) 203–214.
[91] SHUE, S.L., FAW, R.E., SHULTIS, J.K., Thermal-neutron intensities in soils irradiated by fast neutrons from point sources, Chem. Geol. **144** (1998) 47.
[92] PARK, Y.J., SONG, B.C., CHOWDHURY, M.I., JEE, K.Y., A neutron induced prompt gamma-ray spectroscopy system using a ^{252}Cf neutron source for quantitative analysis of aqueous samples, Radioanal. Nucl. Chem. **260** (2004) 585.
[93] JURNEY, E.T., CURTIS, D.B., GLADNEY, E.S., Determination of sulfur in environmental materials by thermal neutron capture prompt gamma-ray spectrometry, Anal. Chem. **49** (1977) 1741.
[94] SAVIO, D.L., MARISCOTTI, M.A.J., GUEVARA, S.R., Elemental analysis of a concrete sample by capture gamma rays with a radioisotope neutron source, Nucl. Instrum. Methods Phys. Res. B **95** (1995) 379.

[95] KHELIFI, R., IDIRI, Z., OMARI, L., SEGHIR, M., Prompt gamma neutron activation analysis of bulk concrete samples with an Am–Be neutron source, Appl. Radiat. Isot. **51** (1999) 9.
[96] IM, H.J., et al., Transparent solid-state lithiated neutron scintillators based on self-assembly of polystyrene-block-polyethylene oxide copolymer architectures**,** Adv. Mater. **16** (2004) 1757.
[97] BRUSCHINI, C., Commercial systems for the direct detection of explosives for explosive ordnance disposal tasks, Subsurface Sensing Technologies and Applications **2** 3 (2001) 299–336.
[98] NUNES, W.V., DA SILVA, A.X., CRISPIM, V.R., SCHIRRU, R., Explosives detection using prompt-gamma neutron activation and neural networks, Appl. Radiat. Isot. **56** (2002) 937.
[99] KUZNETSOV, A.V., EVSENIN, A.V., GORSHKOV, I.Y., OSETROV, O.I., VAKHTIN, D.N., Detection of buried explosives using portable neutron sources with nanosecond timing, Appl. Radiat. Isot. **61** (2004) 51.
[100] YINON, J., Forensic and Environmental Detection of Explosives, John Wiley & Sons, New York (1999).
[101] CHUNG, C., LIU, S.M., CHAO, J.H., CHAN, C.C., Feasibility study of explosive detection for airport security using a neutron source, Appl. Radiat. Isot. **44** (1993) 1425.
[102] YONEZAWA, C., Prompt gamma-ray analysis using cold and thermal guided neutron beams at JAERI, Biol. Trace. Elem. Res. **71–72** (1999) 407.
[103] BIGGIN, H.C., et al., Determination of nitrogen in living patients, J. Nature New Biol. **236** (1972) 187.
[104] DILMANIAN, F.A., et al., Improvement of the prompt-gamma neutron activation facility at Brookhaven National Laboratory, Phys. Med. Biol. **43** (1998) 339.
[105] GU, D.S., et al., Detection of low caloric power of coal by pulse fast-thermal neutron analysis, J. Radioanal. Nucl. Chem. **262** (2004) 493.
[106] LIU, Y., et al., Development and applications of an online thermal neutron prompt-gamma element analysis system, J. Radioanal. Nucl. Chem. **151** (1991) 83.
[107] REIJONEN. J., et al., First PGAA and NAA experimental results from a compact high intensity DD neutron generator, Nucl. Instrum. Methods Phys. Res. A **522** 3 (2004) 598–602.
[108] REIJONEN, J., et al., DD neutron generator development at LBNL, Appl. Radiat. Isot. **63** (2005) 757–763.
[109] REIJONEN, J., Compact neutron generators for medical, Homeland Security and planetary exploration, Nucl. Instrum. Methods Phys. Res. B **261** (2007) 272.
[110] LUDEWIGT B.A., WELLS, R.P., REIJONEN, J., High-yield D–T neutron generatorstar, Nucl. Instrum. Methods Phys. Res. B **261** (2007) 830.
[111] REIJONEN, J., et al., Compact Neutron Generator Development at LBNL (Proc. American Nucl. Soc. San Diego, 2003), Lawrence Berkeley National Laboratory, Berkely (2003).
[112] REIJONEN, J., LEUNG, K.N., JONES, G., RF ion source development for neutron generation and for material modification, Rev Sci. Instrum. **73** (2002) 934.
[113] FARNSWORTH, F.T., Electric Discharge Device for Producing Interactions Between Nuclei, U.S. Patent No. 3,358,402, issued June 28, 1966 after initial filing on May 5, 1956.
[114] HIRSCH, R., Inertial-electrostatic confinement of ionized fusion gases, J. Appl. Phys. **38** (1967) 4522.

[115] PARK, J., STRANGE, S.M., NEBEL, R.A., SUBRAMANIAN, K.M., Inertial-Electrostatic-Confinement Fusion Device, Los Alamos National Laboratory, LA-14202-PR.
[116] MILEY, G.H., Overview of IEC Research at the University of Illinois, US-Japan IEC Workshop, University of Wisconsin, Madison, Wisconsin (2002).
[117] HULL, R., "The Farnsworth/Hirsch Fusor, how a small vacuum system and a bit of basketweaving will get you a working inertial-electrostatic confinement neutron source", The Bell Jar, Vol. 6, No. 3–4, Chivers Press, (1997).
[118] SANTARIUS, J.F., et al., Overview of University of Wisconsin Inertial-Electrostatic Confinement Fusion Research (presented at the 16th ANS Topical Meeting on Fusion Energy, 14–16 September 2004), Madison WI (2004)
[119] MILEY, G.H., STUBBERS, R., YANG, Y., WEBBER, J., SHABAN, Y., Advances in IEC Technology for a Portable Neutron/Proton Source, 14th Pacific Basin Nuclear Conf., Mar (2004).
[120] MILEY, G.H., WU, L., KIM, H. J., IEC-based neutron generator for security inspection system, J. Radioanal. Nucl. Chem. **263** (2005) 159–164.
[121] PARK, J., NEBEL, R.A., RELLERGERT, W.G., SEKORA, M.D., Experimental studies of electrostatic confinement on the INS-e device, Physics of Plasmas **10** (2003) 3841–3849.
[122] PICKRELL, M.M., High Fluence Neutron Source for Nondestructive Characterization of Nuclear Materials, Midyear Progress Report, Los Alamos National Laboratory, LA-UR97-5196 (1997).
[123] NEBEL, R.A., BARNES, D.C., The periodically oscillating plasma sphere, Fusion Technology **38** (1998) 28.
[124] MARSHALL SPACE FLIGHT CENTER, Inertial Electrostatic Confinement research may lead to a new space propulsion system, Marshall Star, July 5, (2001) 7–9.
[125] YOSHIKAWA, K., R&D of Technology for Humanitarian Landmine Detection by a Compact IEC Fusion Neutron Source, 5th US-Japan Workshop on Inertial Electrostatic Confinement Fusion, U. of Wisconsin, Madison, Oct. 10–11, (2002).
[126] KHACHAN, J., MOORE, D., BOSI, S., Spatial distribution of ion energies in an inertial electrostatic confinement device, Physics of Plasmas **10** 3 (2003) 596–599.
[127] DUNCAN, M., "Should Google Go Nuclear?" Inertial Electrostatic Confinement Fusion provides a potential breakthrough in designing and implementing practical fusion plants, Google Tech Talks, Nov. 9, (2006).
[128] KRALL, N.A., The polywell: A spherically convergent ion focus concept, Fusion Technology **22** (1992) 42.
[129] BRUSSARD, R.W., Method and Apparatus for Creating and Controlling Nuclear Fusion, US Patent Number 5,160,695, issued Nov. 3, (1992).
[130] INTERNATIONAL ATOMIC ENERGY AGENCY, Handbook of Nuclear Data for Borehole Logging and Mineral Analysis, Technical Reports Series No. 357, Vienna, (1993).
[131] NATURAL RESOURCES EXPLORATION, Cf-252 Progress, NRE, No. 4 (1970) 13 and No. 5 (1970) 32
[132] HALL, A.W., MARTIN, J.W., STEWART, R.F., POSTON, A.M., Precision Tests of Neutron Sulphur Meter in Coal Preparation Plant, US Bureau of Mines Report 8038 (1975).
[133] WORMALD, M.R., CLAYTON, C.G., In-situ analysis of coal by measurement of neutron-induced prompt γ-rays, Int. J. Appl. Radiat. Isot. **34** 1 (1983) 83.

[134] CUNNINGHAM, J.B., SOWERBY, B.D., RAFTER, P.T., GREENWOOD-SMITH, R., Bulk analysis of sulphur, lead, zinc and iron in lead sinter feed using neutron inelastic scatter gamma rays, Int. J. Appl. Radiat. Isot. **35** (1984) 635.

[135] LIM, C.S., Recent developments in neutron-induced gamma activation for on-line multielemental analysis in industry, J. Radioanal. Nucl. Chem. **262** 2 (2004) 525–532.

[136] INTERNATIONAL ATOMIC ENERGY AGENCY, Use of research reactors for neutron activation analysis, IAEA-TECDOC-1215, IAEA, Vienna (2001).

[137] WESTPHAL, G.P., GRASS, F., LEMMEL, H., STERBA, J., A low-cost system for rapid automatic neutron activation analysis at small research reactors, J. Radioanal. Nucl. Chem. **272** (2007) 267–271.

[138] WESTPHAL, G. P., et al., Automatic activation analysis, J. Radioanal. Nucl. Chem. **271** (2007) 145–150.

[139] PEPELNIK, R., WESTPHAL, G.P., ANDERS, B., Application of the virtual pulse generator method to real-time correction of counting losses in high-rate gamma spectroscopy, Nucl. Instrum. Methods Phys. Res. **226** (1984) 411–417.

[140] TULLE, P.A., "Recent works with sealed tube neutron generators", Use of Accelerator Based Neutron Sources, IAEA-TECDOC-1153, IAEA, Vienna (2000) 59–63.

[141] HAMM, R.W., "Multipurpose neutron generators based on the radiofrequency quadrupole linear accelerator", Penetrating Radiation Systems and Applications II, (Proc. of SPIE, 2000), Vol. 4142, (DOTY, F.P., BRADFORD BARBER, H., ROEHRIG, H., MORTON, E.J., Eds), SPIE (2000) 39–47.

[142] SZTARICSKAI, T., "Problems related to the optimal use of accelerator based neutron generators", Use of Accelerator Based Neutron Sources, IAEA-TECDOC-1153, IAEA, Vienna (2000) 53–58.

[143] JONAH, S.A., "Utilization of a sealed-tube neutron generator for training and research", Use of Accelerator Based Neutron Sources, IAEA-TECDOC-1153, IAEA, Vienna (2000) 45–51.

[144] FOOD AND AGRICULTURE ORGANIZATION OF THE UNITED NATIONS, INTERNATIONAL ATOMIC ENERGY AGENCY, INTERNATIONAL LABOUR ORGANISATION, OECD NUCLEAR ENERGY AGENCY, PAN AMERICAN HEALTH ORGANIZATION, WORLD HEALTH ORGANIZATION, International Basic Safety Standards for Protection against Ionizing Radiation and for the Safety of Radiation Sources, Safety Series No. 115, IAEA, Vienna (1996).

[145] GILMORE, G., HEMMINGWAY, J., Practical Gamma-Ray Spectrometry, John Wiley and Sons, Chichester (1995).

[146] www.canberra.com

[147] www.detectors.saint-gobain.com

[148] www.ortec-online.com/Solutions/index.aspx

[149] www.scionix.nl

[150] RAUDORF, T.W., TRAMMELL, R.C., WAGNER, S., PEHL, R.H., Performance of reverse electrode HPGe coaxial detector after light damage by fast neutrons, IEEE Trans. on Nucl. Sci. **31** 1 (1984) 253-257.

[151] www.bsi.lv

[152] www.greenstar.ru

[153] www.elsevier.com

[154] WESTPHAL, G.P., High-rate gamma spectroscopy and related problems, J. Radioanal. Nucl. Chem. **61** (1981) 111–119.

[155] KEYSER, R.M., TWOMEY, T.R., BINGHAM, R.D., Improved performance in germanium detector gamma spectrometers based on digital signal processing, J. Radioanal. Nucl. Chem. **276** 3 (2008) 567–575.

[156] GEDCKE, D., KEYSER, R., TWOMEY, T., A New Method for Counting Loss Correction with Uncertainty in Gamma Spectroscopy Applications (Proc. INMM 42nd Annual Meeting Indian wells, 2001), Institute of Nuclear Materials Management, Oak Ridge (2001).

[157] WESTPHAL, G.P., JÖSTL, K., SCHRÖDER, P., WINKELBAUER, W., Adaptive digital filter for high-rate, high-resolution gamma spectrometry, IEEE Trans. Nucl. Sci. **48** (2001) 461–465.

[158] WESTPHAL, G.P., Real-time correction of counting losses in nuclear pulse spectroscopy, J. Rad. Chem. **70** (1982) 387–410.

[159] WESTPHAL, G.P., Method of, and system for, determining a spectrum of radiation characteristics with full counting-loss compensation, US Patent 4.476.384 (1984).

[160] DEBERTIN, K., HELMER, R.G., Gamma- and X-ray spectrometry with semiconductor detectors, North-Holland Publishing Company, Amsterdam (1988).

[161] ARNOLD, D., BLAAUW, M., FAZINIC, S., KOLOTOV, V.P., The 2002 IAEA intercomparison of software for low-level γ-ray spectrometry, Nucl. Instr. Meth. A **536** (2005) 196–210.

[162] BLAAUW, M., et al., The 1995 IAEA intercomparison of commercially available γ-ray spectrum analysis software, Nucl. Instrum. Meth. A **387** (1997) 416–432.

[163] SIMONITS, A., DE CORTE, F., HOSTE, J., Single comparator methods in reactor neutron activation analysis, J. Radioanal. Chem. **24** (1975) 31–46.

[164] DE CORTE, F., The k_0 Standardization Method - a Move to the Optimization of NAA, thesis, Rijksuniversiteit Ghent (1987).

[165] LANDSBERGER, S., PESHEV, S., Compton suppression neutron activation analysis: past, present and future, J. Radioanal. Nucl. Chem. **202** (1996) 201–224.

[166] WESTPHAL, G.P., Real-time correction of chance coincidence losses in high-rate Compton suppression spectrometry, Nucl. Instrum. Methods Phys. Res. A **416** (1998) 536–538.

[167] WESTPHAL, G.P., Correction of counting losses of the preloaded filter pulse processor, J. Radioanal. Nucl. Chem. **179** (1994) 55–59.

[168] WESTPHAL, G.P., JÖSTL, K., SCHRÖDER, P., LAUSTER, R., HAUSCH, E., Quantitative Compton suppression spectrometry at elevated counting rates, Nucl. Instrum. Methods Phys. Res. A **422** (1999) 347–351.

[169] EMBER, P.P.; BELGYA, T., MOLNÁR, G. A practical test of a γ-γ coincidence measurement setup for PGAA, Nucl. Instrum. Methods Phys. Res. B **213** (2004) 406–409.

[170] WAPSTRA, A.H., Alpha-, Beta- and Gamma-ray Spectroscopy, 5th Edn, Vol. 1, North-Holland Publishing Company, Amsterdam and New York, (1979) 539–555.

[171] MEYER, G.J., Multiparameter coincidence spectrometry applied to the instrumental activation analysis of rocks and minerals. Radioanal. Nucl. Chem. **114** (1987) 223–230.

[172] MEYER, G., PICCOT, S., ROCCHIA, R., TOUTAIN, J.P.J., Simultaneous determination of Ir and Se in K–T boundary clays and volcanic sublimates, Radioanal. Nucl. Chem. **168** (1993) 125–131.

[173] JAKUBEK, J., et al., Coincidence gamma-gamma spectroscopy system for instrumental neutron activation analysis, Nucl. Instrum. Methods Phys. Res. A **414** (1998) 261–264.

[174] KOEBERL, Ch., HUBER, H., Optimalization of the multiparameter γ-γ coincidence spectrometry for the determination of iridium geological materials, J. Radioanal. Nucl. Chem **244** (2000) 655–660.

[175] KEHAYIAS, J.J., ZHUANG, H., Use of the Zetatron D-T neutron generator for the simultaneous measurement of carbon, oxygen, and hydrogen in vivo in humans, Nucl. Instrum. Methods Phys. Res. B **79** (1993) 555–559.

[176] VOURVOPOULOS, G., Industrial on-line bulk analysis using nuclear techniques, Nucl. Instrum. Methods Phys. Res. B **56/57** (1991) 917.

[177] LEE W.C., et. al., Thermal neutron analysis explosive detection based on electronic neutron generators, Nucl. Instrum. Methods Phys. Res. B **99** (1995) 739.

[178] www.thermo.com

[179] www.sodern.fr

[180] www.slb.com

[181] vniia.ru/eng/index.html

[182] www.sciner.com

[183] www.adelphitech.com

[184] VELLA, M.C., et. al., Development of RF plasma generators for neutral beams, J. Vac. Sci. Technol. A **3** (1985) 3.

[185] LEUNG, K.N., et. al., RF driven multicusp H^- ion source, Rev. Sci. Instrum. **62** (1991) 100.

[186] HAHTO, S.K., et. al., Multicusp ion source with external RF antenna for production of protons, Rev. Sci. Instrum. **75** (2004) 355.

[187] JI, Q., LEUNG, K.N., KING, T.J., JIANG, X., APPLETON, B.R., Development of focused ion beam systems with various ion species Nucl. Instrum. Methods Phys. Res. B **241** (2005) 335.

[188] BECKER, R., HERRMANNSFELDT, W., IGUN−A program for the simulation of positive ion extraction including magnetic fields, Rev. Sci. Instrum. **63** (1992) 2756.

[189] BOERS, J.E., An interactive version of the PBGUNS program for the simulation of axisymmetric and 2D, electron and ion beams and guns (Proc. IEEE Particle Accelerator Conf. Dallas, 1995), American Physical Society, Dallas (1995) 2312.

[190] DAHL, D.A., DELMORE, J.E., APPELHANS, A.D., Simion PC/Ps2 electrostatic lens design program, Rev. Sci. Instrum. **61** (1990) 607–609.

[191] SPÄDTKE, P., MÜHLE, C., Simulation of ion extraction and beam transport, Rev. Sci. Instrum. **71** (2000) 820.

[192] U.S.NRC, Fact sheet on tritium exit signs, (2009) http://www.nrc.gov/reading-rm/doc-collections/fact-sheets/fs-tritium.html

[193] U.S.NRC, Backgrounder on tritium, radiation protection limits, and drinking water standards, (2011) http://www.nrc.gov/reading-rm/doc-collections/fact-sheets/tritium-radiation-fs.html
[194] BÉREST, P., BROUARD, B., Safety of salt caverns used for underground storage, Oil & Gas Sci. Technol. J. **58** 3 (2003) 361–384.
[195] NRC REGULATIONS, Units of radiation dose, 10CFR20.1004, (2011) http://www.nrc.gov/reading-rm/doc-collections/cfr/part020/part020-1004.html.
[196] BECKURTZ, K.H., WIRTZ, K., Neutron Physics, Springer Verlag, Berlin (1964).
[197] BREISMEISTER, J.F., MCNP-A general Monte Carlo N-Particle transport code, Version 5, LA-13709-M, LANL, Los Alamos, New Mexico (2000).
[198] LEUNG, K.N, Cylindrical Neutron Generator with Nested Option, IB-1764, available at: http://www.lbl.gov/tt/techs/lbnl1764.html
[199] MATSUO, Y., MORISHIMA, N., NAGAYA, Y., Neutronic study of spherical cold-neutron sources composed of liquid hydrogen and liquid deuterium, Nucl. Instrum. Methods in Phys. Res. A **486** (2003) 446–451.
[200] VOURVOPOULOS, G., Accelerator based techniques for contraband detection, Nucl. Instrum. Methods Phys. Res. B **89** (1994) 388.

ANNEX I
REACTION AND CROSS-SECTION FOR NAA WITH NEUTRON GENERATORS

I-1. DT Neutron Generators

Fast, 14.1 MeV neutrons can produce nuclear reactions on most isotopic targets. Typical (n,γ) cross-sections at these energies are typically less than 10 mb. Cross-sections up to 1 b are observed in (n,2n), (n,p), (n,n'γ) and (n,γ) at 14.1 MeV. TABLE 1 shows typical reactions for DT neutrons that produce radioactive products suitable for use in Fast Neutron Activation Analysis.

TABLE 1. USEFUL REACTIONS INDUCED BY 14.1 MEV NEUTRONS

Z	Element	Reaction	Cross-Section (mb)	Target Abundance (%)	Product	Half-life
5	B	^{10}B(n,p)	9	19.9	^{10}C	19.3 s
7	N	^{14}N(n,2n)	7.4	99.63	^{13}N	9.965 m
8	O	^{16}O(n.p)	5.9	99.76	^{16}N	7.13 s
9	F	^{19}F(n,p)	19	100	^{19}O	26.9 s
11	Na	^{23}Na(n,γ)	0.23	100	^{24}Na	14.95 h
12	Mg	^{26}Mg(n,γ)	0.2	11.01	^{27}Mg	9.46 m
13	Al	^{27}Al(n,γ)	56	100	^{24}Na	14.95 h
13	Al	^{27}Al(n,γ)	0.65	100	^{28}Al	2.24 m
13	Al	^{27}Al(n,p)	31	100	^{27}Mg	9.46 m
14	Si	^{30}Si(n,γ)	0.6	3.09	^{31}Si	157 m
19	K	^{41}K(n,γ)	112	6.73	^{38}Cl	37.2 m
19	K	^{41}K(n,γ)	3.5	6.73	^{42}K	12.32 h
21	Sc	^{45}Sc(n,γ)	44	100	^{42}K	12.3 h
22	Ti	^{50}Ti(n,γ)	3.5	5.18	^{51}Ti	5.76 m
22	Ti	^{50}Ti(n,p)	28	5.18	^{50}Sc	102.5 s
23	V	^{51}V(n,γ)	15	99.75	^{48}Sc	43.7 h
23	V	^{51}V(n,p)	29	99.75	^{51}Ti	5.76 m

TABLE 2. USEFUL REACTIONS INDUCED BY 14.1 MEV NEUTRONS (cont.)

Z	Element	Reaction	Cross-Section (mb)	Target Abundance (%)	Product	Half-life
24	Cr	^{50}Cr(n,2n)	20	4.34	^{49}Cr	42.3 m
24	Cr	^{50}Cr(n,γ)	1.3	4.34	^{51}Cr	46.2 m
24	Cr	^{52}Cr(n,2n)	350	83.79	^{51}Cr	46.2 m
25	Mn	^{55}Mn(n,γ)	29	100	^{52}V	3.74 m
25	Mn	^{55}Mn(n,γ)	0.65	100	^{56}Mn	2.58 h
26	Fe	^{54}Fe(n,2n)	18	5.84	^{53}Fe	8.51 m
28	Ni	^{58}Ni(n,n'p)	646	68.08	^{57}Co	271.7 d
29	Cu	^{63}Cu(n,2n)	500	69.17	^{62}Cu	9.67 m
29	Cu	^{63}Cu(n,γ)	2.6	69.17	^{64}Cu	12.7 h
29	Cu	^{65}Cu(n,2n)	950	30.83	^{64}Cu	12.7 h
29	Cu	^{65}Cu(n,γ)	0.45	30.83	^{66}Cu	5.12 m
29	Cu	^{65}Cu(n,n'γ)	1.0	30.83	^{61}Co	1.65 h
30	Zn	^{68}Zn(n,γ)	18	18.75	^{65}Ni	2.52 h
30	Zn	^{70}Zn(n,n'γ)	0.9	0.62	^{66}Ni	54.6 h
31	Ga	^{69}Ga(n,p)	20	60.11	^{69m}Zn	13.76 h
31	Ga	^{71}Ga(n,γ)	1.9	39.89	^{72}Ga	14.1 h
31	Ga	^{71}Ga(n,n'γ)	2.1	39.89	^{67}Cu	61.8 h
32	Ge	^{73}Ge(n,n'γ)		7.73	^{73m}Ge	0.499 s
33	As	^{75}As(n,γ)	93	100	^{72}Ga	14.1 h
33	As	^{75}As(n,n'γ)	13	100	^{75m}Ge	17.6 ms
34	Se	^{77}Se(n,n'γ)		7.63	^{77m}Se	17.4 s
34	Se	^{82}Se(n,γ)	1.4	8.73	^{83}Se	70.1 s

TABLE 3. USEFUL REACTIONS INDUCED BY 14.1 MEV NEUTRONS (cont.)

Z	Element	Reaction	Cross-Section (mb)	Target Abundance (%)	Product	Half-life
35	Br	^{79}Br(n,2n)	965	50.69	^{78}Br	6.46 m
35	Br	^{79}Br(n,γ)	9.2	50.69	^{76}As	1.09 d
35	Br	^{79}Br(n,γ)	1.7	50.69	^{80m}Br	17.7 m
35	Br	^{79}Br(n,n'γ)		50.69	^{78m}By	4.86 s
35	Br	^{81}Br(n,2n)	1130	49.31	^{80}Br	17.68 m
35	Br	^{81}Br(n,γ)	3.4	49.31	^{82m}Br	6.13 m
35	Br	^{81}Br(n,n'γ)		49.31	^{81m}Br	34.6 μs
36	Kr	^{80}Kr(n,γ)	1.5	2.28	^{81}Kr	4.57 h
37	Rb	^{87}Rb(n,γ)	4.5	27.83	^{84}Br	31.8 m
38	Sr	^{87}Sr(n,n'γ)		7.00	^{87m}Sr	2.82 h
39	Y	^{89}Y(n,γ)	2.2	100	^{90m}Y	3.19 h
39	Y	^{89}Y(n,n'γ)	393	100	^{89m}Y	15.3 s
40	Zr	^{90}Zr(n,2n)	120	51.45	^{89m}Zr	4.16 m
40	Zr	^{90}Zr(n,n'γ)	64	51.45	^{90m}Zr	0.809 s
40	Zr	^{90}Zr(n,n'p)	40	51.45	^{89m}Y	15.3 s
40	Zr	^{90}Zy(n.p)	43	51.45	^{90}Y	64.05 h
40	Zr	^{96}Zr(n,γ)	0.05	2.80	^{97}Zr	16.7 h
41	Nb	^{93}Nb(n,γ)	8.8	100	^{90m}Y	3.19 h
41	Nb	^{93}Nb(n,n'γ)	2.5	100	^{89m}Y	15.3 s
41	Nb	^{93}Nb(n,n'γ)	49	100	^{93m}Nb	16.13 y
42	Mo	^{92}Mo(n,2n)	17	14.84	^{91m}Mo	64.6 s
42	Mo	^{92}Mo(n,2n)	191	14.84	^{91}Mo	15.5 m

TABLE 4. USEFUL REACTIONS INDUCED BY 14.1 MEV NEUTRONS (cont.)

Z	Element	Reaction	Cross-Section (mb)	Target Abundance (%)	Product	Half-life
44	Ru	^{104}Ru(n,γ)	0.89	18.62	^{105}Ru	4.44 h
46	Pd	^{105}Pd(n,n'γ)		22.33	^{105m}Pd	36.1 μs
46	Pd	^{110}Pd(n,γ)	0.79	12.49	^{111}Pd	23.4 m
47	Ag	^{107}Ag(n,n'γ)		51.84	^{107m}Pd	44.5 s
47	Ag	^{109}Ag(n,γ)	2.4	48.16	^{106}Rh	29.8 s
47	Ag	^{109}Ag(n,n'γ)		48.16	^{109m}Pd	38.0 s
48	Cd	^{111}Cd(n,n'γ)		12.80	^{111m}Cd	48.5 m
48	Cd	^{113}Cd(n,n'γ)		12.22	^{113m}Cd	14.1 y
49	In	^{113}In(n,n'γ)		4.29	^{113m}In	99.5 m
49	In	^{115}In(n,γ)	2.7	95.71	^{112}Ag	3.13 h
49	In	^{115}In(n,n'γ)	81	95.71	^{115m}In	4.49 h
50	Sn	^{115}Sn(n,n'γ)		0.34	^{115m}Sn	159 μs
53	I	^{127}I(n,γ)	0.99	100	^{128}I	25.0 m
55	Cs	^{133}Cs(n,γ)		100	^{132}I	2.295 h
56	Ba	^{135}Ba(n,n'γ)		71.70	^{135m}Ba	28.7 h
56	Ba	^{138}Ba(n,γ)	0.8	6.59	^{139}Ba	12.8 d
57	La	^{139}La(n,γ)	1.9	99.91	^{138}Cs	33.4 m
57	La	^{139}La(n,γ)	0.96	99.91	^{140}La	1.68 d
58	Ce	^{142}Ce(n,γ)	1.8	11.11	^{143}Ce	33.0 h
59	Pr	^{141}Pr(n,γ)	1.3	100	^{142}Pr	19.1 h
63	Eu	^{151}Eu(n,γ)	9.6	47.81	^{152m}Eu	9.31 h
63	Eu	^{151}Eu(n,γ)	9.6	47.81	^{152m2}Eu	96 m

TABLE 5. USEFUL REACTIONS INDUCED BY 14.1 MEV NEUTRONS (cont.)

Z	Element	Reaction	Cross-Section (mb)	Target Abundance (%)	Product	Half-life
63	Eu	^{151}Eu(n,n'γ)		47.81	^{151m}Eu	58.9 μs
63	Eu	^{153}Eu(n,2n)	733	52.19	^{152m}Eu	9.31 h
63	Eu	^{153}Eu(n,2n)	733	52.19	^{152m2}Eu	96 m
64	Gd	^{160}Gd(n,γ)	1.6	21.86	^{161}Gd	3.66 m
65	Tb	^{159}Tb(n,p)	2.2	100	^{159}Gd	18.5 h
67	Ho	^{165}Ho(n,γ)	1.2	100	^{166}Ho	26.8 h
68	Er	^{167}Er(n,n'γ)		22.93	^{167m}Er	2.27 s
71	Lu	^{176}Lu(n,n'γ)	5.8	2.59	^{176m}Lu	3.66 h
72	Hf	^{178}Hf(n,n'γ)		27.28	^{178m}Hf	4.0 s
72	Hf	^{179}Hf(n,n'γ)		13.63	^{179m}Hf	18.7 s
72	Hf	^{180}Hf(n,n'γ)	12.4	35.08	^{180m}Hf	5.47 h
73	Ta	^{180}Ta(n,n'γ)	3.3	0.012	^{180m}Ta	8.15 h
74	W	^{180}W(n,n'γ)		0.12	^{180m}W	5.47 ms
74	W	^{183}W(n,n'γ)		14.31	^{183m}W	5.2 s
74	W	^{186}W(n,γ)	0.6	28.42	^{187}W	23.7 h
77	Ir	^{191}Ir(n,2n)	647	37.3	^{190m}2Ir	3.09 h
77	Ir	^{191}Ir(n,2n)	866	37.3	^{190m}Ir	1.12 h
77	Ir	^{191}Ir(n,γ)	1.0	37.3	^{192m}Ir	1.45 m
77	Ir	^{191}Ir(n,n'γ)	117	37.3	^{191m}Ir	4.94 s
77	Ir	^{193}Ir(n,2n)	397	62.7	^{192m}Ir	1.45 m
77	Ir	^{193}Ir(n,γ)	4.0	62.7	^{194}Ir	19.3 h
77	Ir	^{193}Ir(n,n'γ)	159	62.7	^{193m}Ir	10.5 d

TABLE 6. USEFUL REACTIONS INDUCED BY 14.1 MEV NEUTRONS (cont.)

Z	Element	Reaction	Cross-Section (mb)	Target Abundance (%)	Product	Half-life
78	Pt	^{198}Pt(n,γ)	1.7	7.16	^{199}Pt	30.8 m
79	Au	^{197}Au(n,γ)	0.25	100	^{194}Ir	19.3 h
79	Au	^{197}Au(n,γ)	10	100	^{198}Au	2.696 d
79	Au	^{197}Au(n,n'γ)	200	100	^{197m}Au	7.73 s
80	Hg	^{199}Hg(n,n'γ)		16.87	^{199m}Hg	42.7 m
80	Hg	^{201}Hg(n,n'γ)		13.18	^{201m}Hg	9.3 μs
81	Tl	^{203}Tl(n,2n)	1300	29.52	^{202}Tl	12.2 d
81	Tl	^{203}Tl(n,γ)	0.37	29.52	^{200}Au	48.4 m
81	Tl	^{205}Tl(n,γ)	0.75	70.48	^{202}Au	28.8 s
81	Tl	^{205}Tl(n,γ)	2.0	70.48	^{206}Tl	4.2 m
82	Pb	^{204}Pb(n,n'γ)		1.4	^{205m}Pb	1.14 h
82	Pb	^{207}Pb(n,n'γ)		22.1	^{207m}Pb	0.806 s
82	Pb	^{208}Pb(n,γ)	1.1	52.4	^{209}Pb	3.25 h
83	Bi	^{209}Bi(n,γ)	0.33	100	^{210}Bi	5.01 d
90	Th	^{232}Th(n,2n)	1290	100	^{231}Th	25.5 h
90	Th	^{232}Th(n,f)	380	100		
90	Th	^{232}Th(n,γ)	5.2	100	^{233}Th	21.8 m
92	U	^{235}U(n,f)	2075	0.72		
92	U	^{238}U(n,f)	1185	99.27		
92	U	^{238}U(n,γ)	0.95	99.27	^{239}U	23.4 m

I-2. DD Neutron Generators

Reactions suitable for Neutron Activation Analysis with 3 MeV neutrons from DD NG are shown in TABLE 7. Most elements can be analyzed by using (n,γ), (n,p), (n,γ) and (n,n'γ) reactions.

TABLE 8. USEFUL REACTIONS INDUCED BY 3 MEV NEUTRONS

Z	Element	Reaction	Cross-Section (mb)	Target Abundance (%)	Product	Half-life
4	Be	^{9}Be(n,γ)	105	100	^{6}He	807 ms
9	F	^{19}F(n,γ)	0.08	100	^{20}F	11.07 s
11	Na	^{23}Na(n,γ)	0.17	100	^{24}Na	14.95 h
13	Al	^{27}Al(n,γ)	0.42	100	^{28}Al	2.24 m
13	Al	^{27}Al(n,p)	1.1	100	^{27}Mg	9.46 m
14	Si	^{30}Si(n,γ)	0.65	3.09	^{31}Si	157 m
15	P	^{31}P(n,γ)	0.70	100	^{32}P	14.26 d
15	P	^{31}P(n,p)	60	100	^{31}Si	157 m
16	S	^{32}S(n,p)	120	94.93	^{32}P	14.26 d
17	Cl	^{37}Cl(n,γ)	0.6	75.78	^{38}Cl	37.2 m
19	K	^{41}K(n,p)	0.08	6.73	^{41}Ar	109.6 m
21	Sc	^{45}Sc(n,γ)		100	^{46m}Sc	18.75 s
22	Ti	^{50}Ti(n,γ)		5.18	^{51}Ti	5.76 m
22	Ti	^{47}Ti(n,p)	37	7.44	^{47}Sc	3.35 d
23	V	^{51}V(n,γ)	1.0	99.75	^{52}V	3.74 m
24	Cr	^{54}Cr(n,γ)	0.88	2.36	^{55}Cr	3.50 m
25	Mn	^{55}Mn(n,γ)	1.5	100	^{56}Mn	2.58 h
27	Co	^{59}Co(n,γ)		100	^{60m}Co	10.5 m
28	Ni	^{64}Ni(n,γ)	3.7	0.93	^{65}Ni	2.52 h
28	Ni	^{60}Ni(n,p)		26.22	^{60m}Co	10.5 m
29	Cu	^{63}Cu(n,γ)	5.6	69.17	^{64}Cu	12.7 h
29	Cu	^{65}Cu(n,γ)	4	30.83	^{66}Cu	5.12 m
30	Zn	^{68}Zn(n,γ)		18.75	^{69}Zn	56.4 m

TABLE 9. USEFUL REACTIONS INDUCED BY 3 MEV NEUTRONS (cont.)

Z	Element	Reaction	Cross-Section (mb)	Target Abundance (%)	Product	Half-life
30	Zn	^{64}Zn(n,p)		48.63	^{64}Cu	12.7 h
31	Ga	^{71}Ga(n,γ)		39.89	^{72}Ga	14.1 h
32	Ge	^{74}Ge(n,γ)	2.5	36.28	^{75}Ge	82.8 m
32	Ge	^{76}Ge(n,γ)	1.4	9.37	^{77m}Ge	52.9 s
33	As	^{75}As(n,γ)	38	100	^{76}As	1.09 d
34	Se	^{76}Se(n,γ)		9.37	^{77m}Se	17.4 s
34	Se	^{77}Se(n,n'γ)	67	7.63	^{77m}Se	17.4 s
34	Se	^{78}Se(n,γ)		23.77	^{79m}Se	3.92 m
34	Se	^{80}Se(n,γ)	8.3	49.61	^{81}Se	18.45 m
35	Br	^{79}Br(n,γ)	21	50.69	^{80}Br	17.68 m
35	Br	^{81}Br(n,γ)	6.0	49.31	^{82m}Br	6.13 m
37	Rb	^{85}Rb(n,γ)		72.17	^{86m}Rb	1.02 m
37	Rb	^{87}Rb(n,γ)	2.3	27.83	^{88}Rb	17.8 m
38	Sr	^{86}Sr(n,γ)	12	9.86	^{87m}Sr	2.82 h
38	Sr	^{87}Sr(n,n'γ)	21	7.00	^{87m}Sr	2.82 h
39	Y	^{89}Y(n,n'γ)	191	100	^{89m}Y	15.3 s
39	Y	^{89}Y(n,γ)	3.5	100	^{90m}Y	3.19 h
40	Zr	^{90}Zr(n,n'γ)	173	51.45	^{90m}Zr	809 ms
41	Nb	^{93}Nb(n,γ)	6.3	100	^{94m}Nb	6.26 m
42	Mo	^{100}Mo(n,γ)	6.5	9.63	^{101}Mo	14.6 m
44	Ru	^{104}Ru(n,γ)	21	18.62	^{105}Ru	4.44 h
45	Rh	^{103}Rh(n,γ)	21	100	^{104}Rh	42.3 s

TABLE 10. USEFUL REACTIONS INDUCED BY 3 MEV NEUTRONS (cont.)

Z	Element	Reaction	Cross-Section (mb)	Target Abundance (%)	Product	Half-life
46	Pd	^{108}Pd(n,γ)		26.46	^{109m}Pd	4.70 m
47	Ag	^{107}Ag(n,n'γ)	67	51.84	^{107m}Ag	44.5 s
47	Ag	^{109}Ag(n,n'γ)	13	48.16	^{109m}Ag	39.6 s
47	Ag	^{107}Ag(n,γ)	80	51.84	^{108}Ag	2.37 m
47	Ag	^{109}Ag(n,γ)	18	48.16	^{110}Ag	24.6 s
48	Cd	^{110}Cd(n,γ)		12.49	^{111m}Cd	48.5 m
48	Cd	^{111}Cd(n,n'γ)	8	12.80	^{111m}Cd	48.5 m
49	In	^{115}In(n,γ)	70	95.71	^{116m}In	54.3 m
49	In	^{113}In(n,n'γ)	5.4	4.29	^{113m}In	99.5 m
49	In	^{115}In(n,n'γ)	4.5	95.71	^{115m}In	4.49 h
50	Sn	^{116}Sn(n,γ)		14.54	^{117m}Sn	13.76 d
50	Sn	^{122}Sn(n,γ)	9	4.63	^{123m}Sn	40.06 m
50	Sn	^{124}Sn(n,γ)	13	5.79	^{125m}Sn	9.52 m
50	Sn	^{117}Sn(n,n'γ)	15	7.68	^{117m}Sn	13.76 d
51	Sb	^{123}Sb(n,γ)		42.79	^{124m}Sb	93 s
52	Te	^{130}Te(n,γ)	2.5	34.08	^{131}Te	25.0 m
53	I	^{127}I(n,γ)	22	100	^{128}I	24.99 m
55	Cs	^{133}Cs(n,γ)		100	^{134m}Cs	2.91 h
56	Ba	^{136}Ba(n,γ)		7.85	^{137m}Ba	2.55 m
56	Ba	^{137}Ba(n,n'γ)	43	11.23	^{137m}Ba	2.55 m
57	La	^{139}La(n,γ)	4	99.91	^{140}La	1.678 d
58	Ce	^{142}Ce(n,γ)	13	11.11	^{143}Ce	33.04 h

TABLE 11. USEFUL REACTIONS INDUCED BY 3 MEV NEUTRONS (cont.)

Z	Element	Reaction	Cross-Section (mb)	Target Abundance (%)	Product	Half-life
59	Pr	^{141}Pr(n,γ)	8	100	^{142}Pr	19.12 h
60	Nd	^{150}Nd(n,γ)	18	5.6	^{151}Nd	12.44 m
62	Sm	^{154}Sm(n,γ)	52	22.75	^{155}Sm	22.3 m
63	Eu	^{151}Eu(n,γ)	56	47.81	^{152m}Eu	9.312 h
63	Eu	^{151}Eu(n,γ)	56	47.81	^{152m2}Eu	96 m
63	Eu	^{153}Eu(n,γ)	94	52.19	^{154m}Eu	46.3 m
64	Gd	^{158}Gd(n,γ)	45	24.84	^{159}Gd	18.48 h
64	Gd	^{160}Gd(n,γ)	55	21.86	^{161}Gd	3.66 m
66	Dy	^{164}Dy(n,γ)	23	28.18	^{165m}Dy	1.257 m
67	Ho	^{165}Ho(n,γ)	25	100	^{166}Ho	26.83 h
68	Er	^{166}Er(n,γ)	150	33.61	^{167m}Er	2.269 s
68	Er	^{170}Er(n,γ)		14.93	^{171}Er	7.516 h
68	Er	^{167}Er(n,n'γ)	0.8	22.93	^{167m}Er	2.269 s
70	Yb	^{176}Yb(n,γ)		12.76	^{177}Yb	1.911 h
71	Lu	^{175}Lu(n,γ)	17	97.41	^{176m}Lu	3.664 h
71	Lu	^{176}Lu(n,n'γ)	770	2.59	^{176m}Lu	3.664 h
72	Hf	^{178}Hf(n,γ)	47	27.28	^{179m}Hf	18.67 s
72	Hf	^{179}Hf(n,n'γ)		13.63	^{179m}Hf	18.67 s
73	Ta	^{181}Ta(n,γ)	28	99.988	^{182m}Ta	283 ms
74	W	^{182}W(n,γ)		26.50	^{183m}W	5.2 s
74	W	^{186}W(n,γ)	14	28.42	^{187}W	23.72 h
75	Re	^{185}Re(n,γ)	60	37.40	^{186}Re	3.72 d

TABLE 12. USEFUL REACTIONS INDUCED BY 3 MEV NEUTRONS (cont.)

Z	Element	Reaction	Cross-Section (mb)	Target Abundance (%)	Product	Half-life
75	Re	^{187}Re(n,γ)	31	62.60	^{188}Re	17.00 h
75	Re	^{187}Re(n,γ)		62.60	^{188m}Re	18.59 m
77	Ir	^{191}Ir(n,n'γ)	527	37.3	^{191m}Ir	4.94 s
78	Pt	^{196}Pt(n,γ)		25.14	^{197}Pt	19.89 h
78	Pt	^{196}Pt(n,γ)		25.14	^{197m}Pt	95.41 m
78	Pt	^{198}Pt(n,γ)		7.16	^{199}Pt	30.80 m
78	Pt	^{198}Pt(n,γ)		7.16	^{199m}Pt	13.6 s
79	Au	^{197}Au(n,γ)	29	100	^{198}Au	2.696 d
79	Au	^{197}Au(n,n'γ)		100	^{198m}Au	2.27 d
80	Hg	^{198}Hg(n,γ)		9.97	^{199m}Hg	42.67 m
80	Hg	^{199}Hg(n,n'γ)		16.87	^{199m}Hg	42.67 m
81	Tl	^{205}Tl(n,γ)		70.48	^{206}Tl	4.20 m
82	Pb	^{206}Pb(n,γ)		24.1	^{207m}Pb	806 ms
82	Pb	^{204}Pb(n,n'γ)		1.4	^{204m}Pb	1.14 h
82	Pb	^{207}Pb(n,n'γ)	107	22.1	^{207m}Pb	806 ms
83	Bi	^{209}Bi(n,γ)	3	100	^{210}Bi	5.01 d

ANNEX II
LIST OF ABBREVIATIONS

Abbreviations	**Definition**
ADC	Analog to Digital Converter
API	Associated Particle Imaging
ASTM	American Society for Testing and Materials
BGO	Bismuth Germanate
BNL	Brookhaven National Laboratory
CCLC	Coincidence Loss Correction
CNS	Cold Neutron Sources
DD	Deuterium–Deuterium
DT	Deuterium–Tritium
ENAA	Epithermal Neutron Activation Analysis
FNAA	Fast Neutron Activation Analysis
FNA	Fast Neutron Analysis
HPGe	High Purity Germanium
ICP-MS	Inductively Coupled Plasma Mass Spectroscopy
ICRP	International Commission on Radiological Protection
IEC	Inertial Electrostatic Confinement
INAA	Instrumental Neutron Activation Analysis
KAERI	Korea Atomic Energy Research Institute
LD_2	Liquid Deuterium
LFC	Loss Free Counting
LH_2	Liquid Hydrogen
LNBL	Lawrence Berkeley National Laboratory
MCNP	Monte Carlo N-Particle Transport Code

NAA	Neutron Activation Analysis
NaI(Tl)	Sodium Iodide
NCT	Neutron Capture Therapy
NG	Neutron Generator
NIST	National Institute of Standards and Technology
OHSE	Occupational, Health, Safety & Environment
PELAN	Pulsed Elemental Analysis with Neutrons
PFNA	Pulsed Fast Neutron Analysis
PFTNA	Pulsed Fast Thermal Neutron Analysis
PGNAA	Prompt Gamma Neutron Activation Analysis
P&IST	Plasma and Ion Source Technology Group
PLDF	Preloaded Digital Filter
PTNA	Pulsed Thermal Neutron Analysis
RF	Radio Frequency
RFI	Radio Frequency Induction
RFQ	Radio Frequency Quadrupoles
TNA	Thermal Neutron Analysis
TBN	Total Body Nitrogen
TBH	Total Body Hydrogen
VHV	Very High Voltage

CONTRIBUTORS TO DRAFTING AND REVIEW

Firestone R.B.
Lawrence Berkeley National Laboratory
1 Cyclotron Rd.
MS 5R0121
Berkeley, CA, 94720
USA

James W.D.
Elemental Analysis Laboratory
Texas A&M University
College Station, TX 77843-3144
USA

Jee K.Y.
Korea Atomic Energy Research Institute
Nuclear Chemistry Research Team
150 Dukjin-dong
P.O. Box 105, Yusong
South Korea

Koster A.M.J.J.
Delft University of Technology
Reactor Institute Delft (RID)
Mekelweg 15,
NL-2629 JB Delft
Netherlands

Landsberger S.
University of Texas at Austin
Nuclear Engineering Teaching Lab
Pickle Research Campus, R-900
Austin, TX 78712
USA

Le Tourneur P.
EADS SODERN
20 Avenue Descartes
F-94451 Limeil Brevannes
France

Leung K.N.
Lawrence Berkeley National Laboratory
1 Cyclotron Rd.
MS 5R0121
Berkeley, CA, 94720
USA

Lim C.
CSIRO Minerals
Lucas Heights Science & Technology Centre
New Illawara Road
Lucas Heights, NSW
Australia

Mulhauser F.
International Atomic Energy Agency
Vienna International Centre
A-1400 Vienna
Austria

Nebbia G.
INFN
Padova University
Via Marzolo 8
I-35131 Padova
Italy

Ni B.
China Institute of Atomic Energy
P.O. Box 275-50
Beijing 102413
China

Piestrup M.A.
Adelphi Technology Inc.
981-B Industrial Road
San Carlos, CA 94070
USA

Reguigui N.
Centre National de Sciences et Technologies Nucléaires
Technopole de Sidi Thabet
2020 Route de Tunis
BP 72 Sidi Thabet
Tunisia

Reijonen J.
Lawrence Berkeley National Laboratory
1 Cyclotron Rd.
MS 5R0121
Berkeley, CA, 94720
USA

Revay Z.
Institute of Isotopes
Department of Nuclear Research
P.O. Box 77
Budapest H-1525
Hungary

Rossbach M.
International Atomic Energy Agency
Vienna International Centre
A-1400 Vienna
Austria

Sajo-Bohus L.
Universidad Simón Bólivar
Nuclear Physics Lab
Edificio Energética, Plante Baja
Sartenejas, Edo. Miranda
Baruta, Caracas
Venezuela

Sánchez F.A.
Div. Fisica de Reactores Avanzados
Centro Atómico Bariloche
Av. Ezequiel Bustillo km 9,75
R8402AGS San Carlos de Bariloche
Argentina

Simpson J.
Thermo Electron
Marketing & Sales Manager - Neutron Generators
5074 List Drive
Colorado Springs, CO 80919
USA

Soto L.
Comision Chilena de Energia Nuclear
Plasma and TC
Casilla 188 -D
Santiago
Chile

Sudarshan K.
Radiochemistry Division
B.A.R.C.
Trombay, Mumbai 400 085
India

Twomey T.
ORTEC Products,
Advanced Measurement Technology
Spectrum House
1, Millars Business Centre
Fishponds Close
Wokingham, Berkshire RG41 2TZ
United Kingdom

Van Bueren, J.E.P.
International Atomic Energy Agency
Vienna International Centre
A-1400 Vienna
Austria

Westphal G.
Atominstitut der Österreichischen Universitäten
Stadionallee 2
A-1020 Vienna
Austria

IAEA
International Atomic Energy Agency

Where to order IAEA publications

In the following countries IAEA publications may be purchased from the sources listed below, or from major local booksellers. Payment may be made in local currency or with UNESCO coupons.

AUSTRALIA
DA Information Services, 648 Whitehorse Road, MITCHAM 3132
Telephone: +61 3 9210 7777 • Fax: +61 3 9210 7788
Email: service@dadirect.com.au • Web site: http://www.dadirect.com.au

BELGIUM
Jean de Lannoy, avenue du Roi 202, B-1190 Brussels
Telephone: +32 2 538 43 08 • Fax: +32 2 538 08 41
Email: jean.de.lannoy@infoboard.be • Web site: http://www.jean-de-lannoy.be

CANADA
Bernan Associates, 4501 Forbes Blvd, Suite 200, Lanham, MD 20706-4346, USA
Telephone: 1-800-865-3457 • Fax: 1-800-865-3450
Email: customercare@bernan.com • Web site: http://www.bernan.com

Renouf Publishing Company Ltd., 1-5369 Canotek Rd., Ottawa, Ontario, K1J 9J3
Telephone: +613 745 2665 • Fax: +613 745 7660
Email: order.dept@renoufbooks.com • Web site: http://www.renoufbooks.com

CHINA
IAEA Publications in Chinese: China Nuclear Energy Industry Corporation, Translation Section, P.O. Box 2103, Beijing

CZECH REPUBLIC
Suweco CZ, S.R.O., Klecakova 347, 180 21 Praha 9
Telephone: +420 26603 5364 • Fax: +420 28482 1646
Email: nakup@suweco.cz • Web site: http://www.suweco.cz

FINLAND
Akateeminen Kirjakauppa, PO BOX 128 (Keskuskatu 1), FIN-00101 Helsinki
Telephone: +358 9 121 41 • Fax: +358 9 121 4450
Email: akatilaus@akateeminen.com • Web site: http://www.akateeminen.com

FRANCE
Form-Edit, 5, rue Janssen, P.O. Box 25, F-75921 Paris Cedex 19
Telephone: +33 1 42 01 49 49 • Fax: +33 1 42 01 90 90
Email: formedit@formedit.fr • Web site: http://www. formedit.fr

Lavoisier SAS, 145 rue de Provigny, 94236 Cachan Cedex
Telephone: + 33 1 47 40 67 02 • Fax +33 1 47 40 67 02
Email: romuald.verrier@lavoisier.fr • Web site: http://www.lavoisier.fr

GERMANY
UNO-Verlag, Vertriebs- und Verlags GmbH, Am Hofgarten 10, D-53113 Bonn
Telephone: + 49 228 94 90 20 • Fax: +49 228 94 90 20 or +49 228 94 90 222
Email: bestellung@uno-verlag.de • Web site: http://www.uno-verlag.de

HUNGARY
Librotrade Ltd., Book Import, P.O. Box 126, H-1656 Budapest
Telephone: +36 1 257 7777 • Fax: +36 1 257 7472 • Email: books@librotrade.hu

INDIA
Allied Publishers Group, 1st Floor, Dubash House, 15, J. N. Heredia Marg, Ballard Estate, Mumbai 400 001,
Telephone: +91 22 22617926/27 • Fax: +91 22 22617928
Email: alliedpl@vsnl.com • Web site: http://www.alliedpublishers.com

Bookwell, 2/72, Nirankari Colony, Delhi 110009
Telephone: +91 11 23268786, +91 11 23257264 • Fax: +91 11 23281315
Email: bookwell@vsnl.net

ITALY
Libreria Scientifica Dott. Lucio di Biasio “AEIOU”, Via Coronelli 6, I-20146 Milan
Telephone: +39 02 48 95 45 52 or 48 95 45 62 • Fax: +39 02 48 95 45 48
Email: info@libreriaaeiou.eu • Website: www.libreriaaeiou.eu

JAPAN
Maruzen Company, Ltd., 13-6 Nihonbashi, 3 chome, Chuo-ku, Tokyo 103-0027
Telephone: +81 3 3275 8582 • Fax: +81 3 3275 9072
Email: journal@maruzen.co.jp • Web site: http://www.maruzen.co.jp

REPUBLIC OF KOREA
KINS Inc., Information Business Dept. Samho Bldg. 2nd Floor, 275-1 Yang Jae-dong SeoCho-G, Seoul 137-130
Telephone: +02 589 1740 • Fax: +02 589 1746 • Web site: http://www.kins.re.kr

NETHERLANDS
De Lindeboom Internationale Publicaties B.V., M.A. de Ruyterstraat 20A, NL-7482 BZ Haaksbergen
Telephone: +31 (0) 53 5740004 • Fax: +31 (0) 53 5729296
Email: books@delindeboom.com • Web site: http://www.delindeboom.com

Martinus Nijhoff International, Koraalrood 50, P.O. Box 1853, 2700 CZ Zoetermeer
Telephone: +31 793 684 400 • Fax: +31 793 615 698
Email: info@nijhoff.nl • Web site: http://www.nijhoff.nl

Swets and Zeitlinger b.v., P.O. Box 830, 2160 SZ Lisse
Telephone: +31 252 435 111 • Fax: +31 252 415 888
Email: infoho@swets.nl • Web site: http://www.swets.nl

NEW ZEALAND
DA Information Services, 648 Whitehorse Road, MITCHAM 3132, Australia
Telephone: +61 3 9210 7777 • Fax: +61 3 9210 7788
Email: service@dadirect.com.au • Web site: http://www.dadirect.com.au

SLOVENIA
Cankarjeva Zalozba d.d., Kopitarjeva 2, SI-1512 Ljubljana
Telephone: +386 1 432 31 44 • Fax: +386 1 230 14 35
Email: import.books@cankarjeva-z.si • Web site: http://www.cankarjeva-z.si/uvoz

SPAIN
Díaz de Santos, S.A., c/ Juan Bravo, 3A, E-28006 Madrid
Telephone: +34 91 781 94 80 • Fax: +34 91 575 55 63
Email: compras@diazdesantos.es, carmela@diazdesantos.es, barcelona@diazdesantos.es, julio@diazdesantos.es
Web site: http://www.diazdesantos.es

UNITED KINGDOM
The Stationery Office Ltd, International Sales Agency, PO Box 29, Norwich, NR3 1 GN
Telephone (orders): +44 870 600 5552 • (enquiries): +44 207 873 8372 • Fax: +44 207 873 8203
Email (orders): book.orders@tso.co.uk • (enquiries): book.enquiries@tso.co.uk • Web site: http://www.tso.co.uk

On-line orders
DELTA Int. Book Wholesalers Ltd., 39 Alexandra Road, Addlestone, Surrey, KT15 2PQ
Email: info@profbooks.com • Web site: http://www.profbooks.com

Books on the Environment
Earthprint Ltd., P.O. Box 119, Stevenage SG1 4TP
Telephone: +44 1438748111 • Fax: +44 1438748844
Email: orders@earthprint.com • Web site: http://www.earthprint.com

UNITED NATIONS
Dept. I004, Room DC2-0853, First Avenue at 46th Street, New York, N.Y. 10017, USA
(UN) Telephone: +800 253-9646 or +212 963-8302 • Fax: +212 963-3489
Email: publications@un.org • Web site: http://www.un.org

UNITED STATES OF AMERICA
Bernan Associates, 4501 Forbes Blvd., Suite 200, Lanham, MD 20706-4346
Telephone: 1-800-865-3457 • Fax: 1-800-865-3450
Email: customercare@bernan.com · Web site: http://www.bernan.com

Renouf Publishing Company Ltd., 812 Proctor Ave., Ogdensburg, NY, 13669
Telephone: +888 551 7470 (toll-free) • Fax: +888 568 8546 (toll-free)
Email: order.dept@renoufbooks.com • Web site: http://www.renoufbooks.com

Orders and requests for information may also be addressed directly to:

Marketing and Sales Unit, International Atomic Energy Agency
Vienna International Centre, PO Box 100, 1400 Vienna, Austria
Telephone: +43 1 2600 22529 (or 22530) • Fax: +43 1 2600 29302
Email: sales.publications@iaea.org • Web site: http://www.iaea.org/books

This publication addresses recent developments in neutron generator (NG) technology. It presents information on compact instruments with high neutron yield to be used for neutron activation analysis (NAA) and prompt gamma neutron activation analysis in combination with high count rate spectrometers. Traditional NGs have been shown to be effective for applications including borehole logging, homeland security, nuclear medicine and on-line analysis of aluminium, coal and cement. Pulsed fast thermal neutron analysis, as well as tagged and timed neutron analysis, are additional techniques that can be applied using NG technology. NGs can be used effectively for elemental analysis and for analysis of hidden materials by neutron radiography. Useful guidelines for developing NG based research laboratories are provided in this report.

INTERNATIONAL ATOMIC ENERGY AGENCY
VIENNA
ISBN 978–92–0–125110–7
ISSN 2225–8833